

TRANSCRIPTIONAL AND TRANSLATIONAL REGULATION OF
LEAF POLARITY

By

TENGBO HUANG

A Dissertation submitted to the
Graduate School-New Brunswick
Rutgers, The State University of New Jersey
in partial fulfillment of the requirements

for the degree of

Doctor of Philosophy

Graduate Program in Plant Biology

written under the direction of

Dr. Randall A. Kerstetter

and approved by

New Brunswick, New Jersey

January, 2009

ABSTRACT OF THE DISSERTATION

Transcriptional and Translational Regulation of Leaf Polarity

By Tengbo Huang

Dissertation Director:

Dr. Randall Kerstetter

Normal biological functions of leaves such as intercepting light and exchanging gases during photosynthesis rely on proper differentiation of adaxial (dorsal)-abaxial (ventral) identity. Although several families of transcriptional and translational regulators have been identified in leaf polarity, their targets and the molecular basis for the regulatory circuitry are largely unknown. *KANADII* (*KAN1*), a member of the GARP family of transcription factors, is a key regulator of adaxial identity in leaf morphogenesis. The goal of my thesis study is to discover novel players and mechanisms associated with *KAN* to better elucidate the establishment of leaf polarity. My dissertation investigated the DNA binding specificity of *KAN1* both *in vitro* and *in vivo*. In the *in vitro* assay, I identified the 6 base pair motif GNATA (A/T) that the *Myb-like* domain in *KAN1* recognizes. I also found that *KAN1* acts as a transcriptional repressor *in vivo* and directly regulates several genes implicated in auxin responses and one in gibberellin (GA) metabolism. In addition, I studied in detail a specific target *ASYMMETRIC LEAVES2* (*AS2*), a key promoter of

adaxial leaf fate. I demonstrated that KAN1 directly interacts with *AS2* and represses its transcription in abaxial cells. Mutation of a single nucleotide in a KAN1 binding motif in the *AS2* promoter abolishes KAN1 targeting leading to ectopic expression of *AS2* in abaxial cells and conferring a dominant, adaxialized phenotype. These results suggest the significant role of *KAN1* in determining abaxial fate and provide novel insights in dissecting the transcriptional network of leaf morphogenesis.

In addition to the transcriptional regulation, I also gave my focus to the translational regulation of leaf polarity by characterizing an enhancer of *KAN*, *ARROW1* (*ARO1*). *aro1-1* mutant shows pleiotropic defects in development with significantly reduced overall growth rate that is due to the impaired proliferation of division competent cells in both leaves and roots. It also interacts with mutants of important leaf polarity genes probably by altering their expression timing, which suggests that *ARO1* plays significant roles in dorsiventral patterning. I cloned *ARO1* and it encodes a protein with a Pumilio/PUF RNA-binding domain. PUF domains have been shown to function in sequence-specific RNA binding and translational inhibition in various organisms. I also found that *ARO1* functions specifically in 18S rRNA biosynthesis, a critical step for translational regulation in eukaryotes. These results indicate the importance of the translational network in controlling leaf polarity and provide a novel view for understanding the relationship of growth and leaf patterning, two essential factors responsible for leaf morphogenesis.

Table of Contents

Abstract	ii
List of Tables	vii
List of Figures	viii
 Introduction	 1
References	4
 Chapter 1. KANADI1 acts as a transcriptional repressor in adaxial –abaxial polarity and regulates genes involved in auxin responses.....	 6
Introduction	6
Results	6
Discussion	19
Materials and Methods.....	24
Tables	31
Supplementary Figures	32
References	35
 Chapter 2. <i>ARROW1</i> , a translational regulator that links leaf growth with pattern formation	 38

Introduction	38
Results	39
Discussion	57
Materials and Methods.....	60
References	66
 Chapter 3. A novel selected and amplified binding-sequence (SAAB) approach identified the DNA-binding motif of KANADI1 in <i>Arabidopsis</i>	 70
References	77
 Appendices	 78
Introduction	78
 Appendix 1. KANADI1 acts as a transcriptional repressor of genes involved in auxin responses	 79
Methods Summary.....	86
References	91
Tables	94
Figures	95
Supplementary Information	97

Appendix 2. KANADI1 regulates abaxial-abaxial polarity in <i>Arabidopsis</i> by repressing the transcription of <i>ASYMMETRIC LEAVES2</i>	107
Introduction	107
Results and Discussion	109
Methods and Materials	117
References	123
Figures	125
Supplementary Figures	130
Curriculum Vitae	131

List of Tables

Table 1-1 Primers for Oligonucleotide Selection and EMSA.....	31
Table 1-2 Primers for Chromatin Immunoprecipitation	31
Table 3-1 Alignment of oligonucleotides identified in SAAB.....	75
Table A1 Enrichment of KBX sites in KAN-responsive promoters.....	94
Suppl. Table A1-2: Primers for Oligonucleotide Selection and EMSA	99
Suppl. Table A1-3: Primers for RT-PCR	99
Suppl. Table A1-4: Primers for Chromatin Immunoprecipitation.....	100

List of Figures

Figure 1-1. EMSA reveals KAN1 DNA-binding characteristics <i>in vitro</i>	8
Figure 1-2. Post-translational activation of KAN-GR produces defects in leaf polarity and meristem function.....	9
Figure 1-3: DEX and mock-treated <i>KAN-GR</i> plants display defects in root development.....	10
Figure 1-4. Chromatin immunoprecipitation confirms DEX-dependent association of KAN-GR with the promoters of <i>KANT</i> genes.....	12
Figure 1-5. <i>as2-5D</i> has an adaxialized phenotype.....	14
Figure 1-6. KAN1 binding site determines the spatial expression pattern of <i>AS2</i>	15
Figure 1-7. KAN1-GR represses <i>AS2</i> directly.....	17
Figure 1-8. <i>AS2</i> represses <i>KAN1</i> and <i>KAN2</i>	18
Supplementary Figure 1-1. Alignment of 50 sequences obtained from PCR-assisted binding site selection.....	32
Supplementary Figure 1-2. Phenotypes in loss of function mutants and post-translationally activated <i>KAN-GR</i> plants.....	33
Supplementary Figure 1-3: ChIP on mock- and DEX-treated Col seedlings revealed no enrichment.....	34
Figure 2-1. <i>aro1-1</i> enhances <i>kan1 kan2</i> double mutant phenotype.....	41
Figure 2-2. <i>aro1-1</i> plays pleiotropic roles in plant development.....	43

Figure 2-3. <i>aro1-1</i> interacts with adaxial polarity mutants.....	46
Figure 2-4. <i>aro1-1</i> enhances the inflorescence phenotype of <i>rev</i>	47
Figure 2-5. Vascular phenotype of leaf petioles in genetic combination of <i>aro1-1</i> and adaxial polarity mutants.....	48
Figure 2-6. Molecular identification <i>ARO1</i>	49
Figure 2-7. <i>ARO1</i> functions in 18S rRNA biosynthesis.....	52
Figure 2-8. Cell division pattern is impaired in <i>aro1-1</i> mutant.....	53
Figure 2-9. Expression pattern of <i>ARO1</i> in plants.....	54
Figure 2-10. <i>aro1-1</i> affects temporal expression pattern of <i>KAN1</i> and <i>AS2</i>	56
Figure 3-1. EMSA in the oligonucleotide selection step of SAAB.....	76
Figure A1-1. EMSA reveals KAN1 DNA-binding characteristics <i>in vitro</i>	95
Figure A1-2. Post-translational activation of KAN-GR produces defects in leaf polarity and meristem function.....	96
Figure A1-3. Chromatin immunoprecipitation confirms DEX-dependent association of KAN-GR with the promoters of <i>KANT</i> genes.....	96
Supplementary Figure A1-1. Alignment of 50 sequences obtained from PCR-assisted binding site selection.....	101
Supplementary Figure A1-2. Table of phenotypes in loss of function mutants and post-translationally activated <i>KAN-GR</i> plants.....	102
Supplementary Figure A1-3. DEX and mock-treated <i>KAN-GR</i> plants display defects in root development.....	103

Supplementary Figure A1-4. Expression of candidate KAN1 target genes was confirmed using semi-quantitative PCR.....	104
Supplementary Figure A1-5. <i>IAA2</i> expression is up-regulated in loss-of-function <i>kan</i> mutants and down-regulated in posttranslationally activated <i>KAN-GR</i>	105
Supplementary Figure A1-6. Chromatin immunoprecipitation experiments on mock- and DEX-treated Col seedlings reveal no enrichment.....	106
Figure A2-1. <i>as2-5D</i> affects a predicted KAN1 binding site.....	125
Figure A2-2. <i>as2-5D</i> has an adaxialized phenotype.....	126
Figure A2-3. KAN1 and KAN2 determine the spatial expression pattern of <i>AS2</i>	127
Figure A2-4. KAN1-GR represses <i>AS2</i> directly.....	128
Figure A2-5. Transgenic plants expressing <i>AS2</i> under the regulation of the <i>KAN1</i> promoter resemble <i>as2-5D</i>	128
Figure A2-6 <i>AS2</i> represses <i>KAN1</i> and <i>KAN2</i>	129
Supplementary Figure A2-1. <i>as2-d</i> suppresses the effects of DEX on <i>35S:KAN-GR</i> seedlings.....	130
Supplmentary Figure A2-2. <i>as2-1</i> does not rescue the mutant phenotype of <i>kan1 kan2</i>	130

Introduction

The leaves of most plants exhibit differences between their adaxial (dorsal) and abaxial (ventral) surfaces[1]. In *Arabidopsis thaliana*, the adaxial side of the leaf is usually dark green and trichome-rich, while the abaxial side is pale green with fewer trichomes. Moreover, the internal tissues of the leaf blade are polarized along this adaxial-abaxial axis[1]. Mesophyll cells adjacent to the adaxial surface are densely packed and contain plenty of chloroplasts for photosynthesis. On the abaxial side, mesophyll cells have more air spaces specialized for gas exchange.

Proper specification of adaxial and abaxial identity is required for the formation and function of leaves. This process is regulated by interactions between genes that individually promote either adaxial or abaxial identity[2, 3]. In *Arabidopsis*, adaxial identity is specified by the class III homeodomain-leucine zipper (HD-ZIP III) genes, Myb and LOB domain transcription factors *ASYMMETRIC LEAVES1 (AS1)* and *AS2*, and the trans-acting short-interfering RNA (ta-siRNA), whereas in the abaxial region, four *KANADI* genes, the *AUXIN RESPONSE FACTORS (ARF) ETTIN (ETT/ARF3)* and *ARF4*, four *YABBY* genes, and microRNA165/166 are essential promoters. The HD-ZIP III family consists of members such as *REVOLUTA (REV)*, *PHABULOSA (PHB)*, and *PHAVOLUTA (PHV)*. These genes are expressed adaxially and encode proteins with partially redundant functions. Gain-of-function mutations in a single gene result in adaxialized radial leaves [4, 5] and simultaneous knock-out of all three genes results in plants with abaxialized radial cotyledons [4]. Similar to HD-ZIP III

family, *KANADI* genes also have overlapping functions. Mutations in any single gene have relatively mild defects in leaf polarity [6-8]. However, if several of these genes are lacking or down-regulated, plants exhibit prominent defects associated with the loss of abaxial identity. For instance, *kan1 kan2* double mutant has reduced leaf blade expansion and develops ectopic outgrowths on the abaxial side of the leaf [9]. And even more dramatically, in the *kan1 kan2 kan3* triple mutant, leaves are almost fully radialized and adaxialized, and the ectopic outgrowths observed in double mutants are greatly reduced [9]. *ETT/ARF3* and *ARF4* are mediators of the auxin signaling pathway. The *arf3 arf4* double mutant has a phenotype similar to *kan1 kan2*, suggesting their function in promoting abaxial identity and a potential role of auxin in leaf polarity [10]. Compared to the other genes, single or even double mutants in *YABBY* gene family members don't render striking defects in leaf polarity. However, when the activity of *KANADI* is also compromised, the function of *YABBY* genes becomes more obvious. In the *kan1 kan2 fil yab3* quadruple mutant, leaves are narrow and short, showing dramatic loss of abaxial identity [11].

These mutant phenotypes imply a mutually antagonistic relationship between adaxial- and abaxial- promoting genes. Furthermore, genetic studies demonstrated that these morphological defects caused by the malfunction of genes specifying one side of the leaf are usually accompanied with impaired expression pattern of genes specifying the other side, such as abaxial expression of *PHB* in *kan1 kan2 kan3* triple mutants [11] and loss of *YABBY* activity in the *PHB* and *PHV* gain-of function alleles [12]. More direct evidence for this antagonism is the functions of small regulatory RNAs.

MicroRNA165/166 are expressed on the abaxial side and may repress HD-ZIPIII genes to promote abaxial identity by direct targeting and post-transcriptional gene silencing [13-16]. Conversely, ta-siRNA targets *ETT/ARF3* and *ARF4* to specify adaxial cell fate [17-19]. These antagonistic interactions constitute the basis for establishing a complex network for leaf initiation and blade expansion.

Among this network of regulatory genes, my dissertation research mainly focuses on the *KANADI (KAN)* family. In the following chapters, I will discuss my two projects, (1) Analysis of the DNA binding properties and downstream targets of *KAN1*, (2) Identification and characterization of *ARROW1*, an enhancer of *KAN*. These two projects investigated transcriptional and translational regulatory mechanisms associated with *KAN* in leaf polarity. I hope the result of this study can aid us in further understanding the process of leaf patterning and development.

References

1. Telfer, A., and Poethig, R.S. (1994). Leaf Development in Arabidopsis. In Arabidopsis, E.M. Meyerowitz and C.R. Somerville, eds. (Plainview: Cold Spring Harbor Laboratory Press), pp. 379-401.
2. Bowman, J.L., Eshed, Y., and Baum, S.F. (2002). Establishment of polarity in angiosperm lateral organs. *Trends in Genetics* 18, 134-141.
3. Kidner, C.A., and Timmermans, M.C. (2007). Mixing and matching pathways in leaf polarity. *Curr Opin Plant Biol* 10, 13-20.
4. Emery, J.F., Floyd, S.K., Alvarez, J., Eshed, Y., Hawker, N.P., Izhaki, A., Baum, S.F., and Bowman, J.L. (2003). Radial patterning of Arabidopsis shoots by class III HD-ZIP and KANADI genes. *Curr Biol* 13, 1768-1774.
5. McConnell, J.R., and Barton, M.K. (1998). Leaf polarity and meristem formation in Arabidopsis. *Development* 125, 2935-2942.
6. Kerstetter, R.A., Bollman, K., Taylor, R.A., Bomblies, K., and Poethig, R.S. (2001). KANADI regulates organ polarity in Arabidopsis. *Nature* 411, 706-709.
7. Eshed, Y., Baum, S.F., and Bowman, J.L. (1999). Distinct mechanisms promote polarity establishment in carpels of Arabidopsis. *Cell* 99, 199-209.
8. McAbee, J.M., Hill, T.A., Skinner, D.J., Izhaki, A., Hauser, B.A., Meister, R.J., Venugopala Reddy, G., Meyerowitz, E.M., Bowman, J.L., and Gasser, C.S. (2006). ABERRANT TESTA SHAPE encodes a KANADI family member, linking polarity determination to separation and growth of Arabidopsis ovule integuments. *Plant J* 46, 522-531.
9. Eshed, Y., Baum, S.F., Perea, J.V., and Bowman, J.L. (2001). Establishment of polarity in lateral organs of plants. *Curr Biol* 11, 1251-1260.
10. Pekker, I., Alvarez, J.P., and Eshed, Y. (2005). Auxin response factors mediate Arabidopsis organ asymmetry via modulation of KANADI activity. *Plant Cell* 17, 2899-2910.
11. Eshed, Y., Izhaki, A., Baum, S.F., Floyd, S.K., and Bowman, J.L. (2004). Asymmetric leaf development and blade expansion in Arabidopsis are mediated by KANADI and YABBY activities. *Development* 131, 2997-3006.
12. Siegfried, K.R., Eshed, Y., Baum, S.F., Otsuga, D., Drews, G.N., and Bowman, J.L. (1999). Members of the YABBY gene family specify abaxial cell fate in Arabidopsis. *Development* 126, 4117-4128.
13. Bao, N., Lye, K.W., and Barton, M.K. (2004). MicroRNA binding sites in Arabidopsis class III HD-ZIP mRNAs are required for methylation of the template chromosome. *Dev Cell* 7, 653-662.
14. Juarez, M.T., Kui, J.S., Thomas, J., Heller, B.A., and Timmermans, M.C. (2004). microRNA-mediated repression of rolled leaf1 specifies maize leaf polarity. *Nature* 428, 84-88.
15. Kidner, C.A., and Martienssen, R.A. (2004). Spatially restricted microRNA directs leaf polarity through ARGONAUTE1. *Nature* 428, 81-84.
16. Mallory, A.C., Reinhart, B.J., Jones-Rhoades, M.W., Tang, G., Zamore, P.D., Barton, M.K., and Bartel, D.P. (2004). MicroRNA control of PHABULOSA in leaf development:

- importance of pairing to the microRNA 5' region. *Embo J* 23, 3356-3364.
17. Allen, E., Xie, Z., Gustafson, A.M., and Carrington, J.C. (2005). microRNA-directed phasing during trans-acting siRNA biogenesis in plants. *Cell* 121, 207-221.
 18. Hunter, C., Willmann, M.R., Wu, G., Yoshikawa, M., de la Luz Gutierrez-Nava, M., and Poethig, S.R. (2006). Trans-acting siRNA-mediated repression of ETTIN and ARF4 regulates heteroblasty in Arabidopsis. *Development* 133, 2973-2981.
 19. Williams, L., Carles, C.C., Osmont, K.S., and Fletcher, J.C. (2005). A database analysis method identifies an endogenous trans-acting short-interfering RNA that targets the Arabidopsis ARF2, ARF3, and ARF4 genes. *Proc Natl Acad Sci U S A* 102, 9703-9708.

Chapter I

KANADI1 acts as a transcriptional repressor in adaxial –abaxial polarity and regulates genes involved in auxin responses

Introduction

KANADI encodes a protein with a conserved DNA-binding domain belonging to the Myb-related GARP family[1]. This gene family includes transcription factors such as *Arabidopsis* *RESPONSE REGULATORS (ARR)*[2]. The GARP domains of *ARR1* and *ARR2* have been shown to be multifunctional for both nuclear localization and sequence-specific DNA binding [3]. Similar to the *ARRs*, *KANI* also shows nuclear localization [4]. We postulate that *KANI* functions as a transcription factor for establishing abaxial leaf identity in *Arabidopsis*. To further characterize the DNA binding capacity and specificity of *KANI*, our lab has pursued the identification of the downstream targets of *KANI* both *in vitro* and *in vivo*.

Results

***KANI* protein recognizes a specific DNA sequence *in vitro*.**

To determine if KAN1 binds to a specific DNA sequence *in vitro*, I performed a PCR-assisted DNA binding site selection using purified KAN1 protein. The full-length KAN1 protein proved toxic when expressed in *E.coli* (data not shown), so I generated a truncated protein containing the predicted KAN1 DNA-binding domain

(KAN1bd) and fused it to a Glutathione S-Transferase (GST) tag. The recombinant protein KAN1bd-GST was affinity purified and applied to the oligonucleotide selection. After 6 cycles of selection, analysis of the final PCR products produced 50 non-redundant oligonucleotide sequences that contained one or more instances of the partly degenerate 6 bp motif GNATA(T/A), which we termed the KANADI box (KBX) (Fig. 1-1, Suppl. Fig. 1-1). To investigate the contribution of each base of KBX to KAN1 binding, I synthesized double-stranded oligonucleotides bearing point mutations in KBX (Table 1-1) and utilized EMSA to analyze the binding activity of KAN1 protein to these mutant variants. The result demonstrated that the nucleotides at the first, third, fourth and sixth positions were critical for effective binding by KAN1 *in vitro* (Fig. 1-1). I also tested an 8 bp palindrome, GAATATTC that appeared in six of the fifty selected sequences and the DNA binding site (AGATT) of the GARP protein ARR10 [3] (Fig. 1-1). KAN1 protein appeared to bind equally well to the palindrome and showed very little affinity to the binding motif of ARR10. These results suggest that KAN1bd selectively binds to a specific DNA sequence *in vitro* and define a novel binding site for this member of the GARP family.

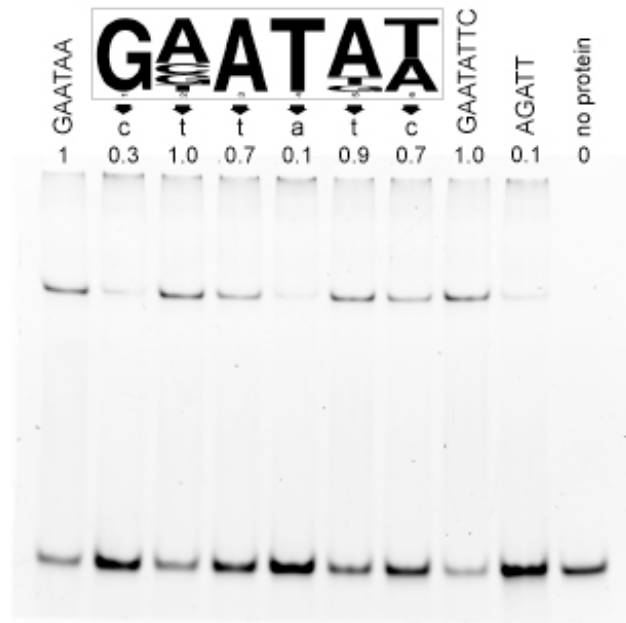


Figure 1-1. EMSA reveals KAN1 DNA-binding characteristics *in vitro*. The *in vitro* KAN1 DNA binding site (KBX, boxed) was identified using affinity purified KAN1db-GST protein in EMSA-based oligonucleotide selection (Suppl. Fig. 1-1). The height of each nucleotide letter is proportional to its representation. Effects of mutating individual sites within the consensus DNA binding site are shown immediately below each position in the consensus KBX site. The mean fraction of bound DNA in three independent replicates was calculated relative to the consensus (GAATAA, lane 1), which was arbitrarily set to 1.0. EMSA of KAN1db-GST bound to a perfect palindrome of KBX (GAATATTC, lane 8) was similar to that of that of a single site. The KAN1db-GST showed little affinity for the consensus binding site for the GARP protein ARR10 (AGATT, lane 9)[3].

KAN1 binds to specific target genes involved in plant development

In order to identify KAN1 target (*KANT*) genes *in vivo*, I applied Chromatin Immunoprecipitation (ChIP) in a system with inducible KAN1 overexpression. In this experiment, *KAN1* cDNA with a glucocorticoid receptor (GR) regulatory domain tag is uniformly expressed by the CaMV 35S promoter[5]. In the absence of the steroid inducer dexamethasone (DEX), KAN1-GR protein is sequestered in the cytosol and unable to regulate its targets in the nucleus, so transgenic plants bearing

35S:KAN1-GR (*KAN-GR*) were morphologically normal despite slightly slower growth than wild type (Fig. 1-2. Suppl. Fig. 1-2). However, *KAN-GR* seedlings grown on media containing 1 μ M DEX displayed dramatic defects due to the translocation of KAN1-GR into nuclei [6]. These plants have narrow cotyledons, the first two true leaves emerged as small, radialized, peg-like structures, and no subsequent leaves were formed (Fig. 1-2. Suppl. Fig. 1-2). These phenotypes were strikingly similar to *35S:KAN1* plants [4, 7, 8]. These plants also displayed defects in root gravitropism and root hair production (Fig. 1-3). In contrast, soil-grown seedlings treated with the same concentration of DEX every two days had relatively milder defects which resembled those observed in *as1* and *as2* mutants [9](Fig. 1-2 Suppl. Fig. 1-2).

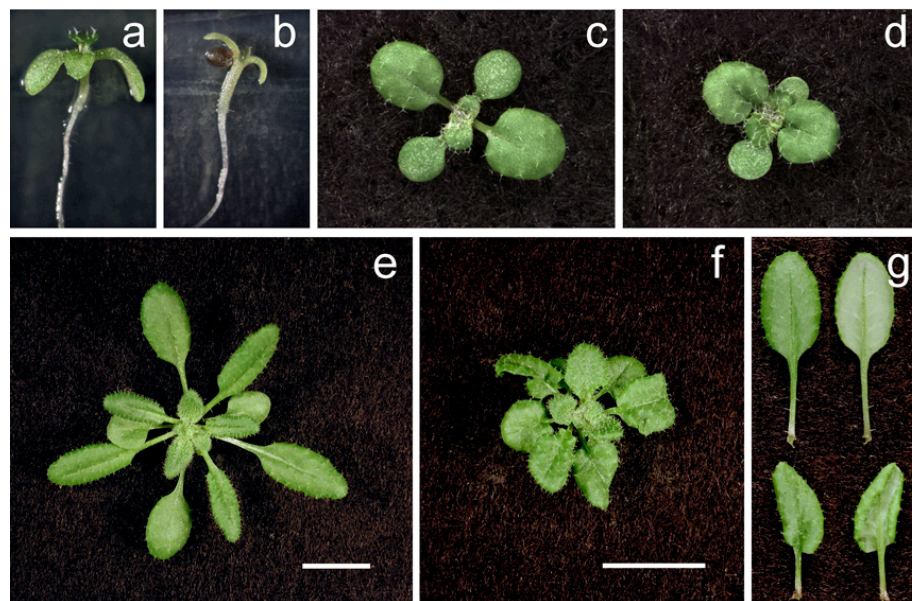


Figure 1-2. Post-translational activation of KAN-GR produces defects in leaf polarity and meristem function. Continuous exposure of *KAN-GR* seedlings to 10 mM DEX (b) on media for 9 days led to loss of cotyledon blade expansion, formation of partially radialized leaf primordia, and inhibition of further shoot meristem activity consistent with strong KAN1 overexpression. Mock-treated *KAN-GR* seedlings (a)

resembled mock- or DEX- treated Col seedlings (Suppl. Fig. 1-2). In contrast, soil grown *KAN-GR* seedlings exposed every other day to 10 mM DEX (d, and f) displayed reduced petiole and blade expansion with strong epinasty leading to leaves with an asymmetric appearance (g, bottom) that was not evident in mock-treated plants (c, e, and g top). Plants were photographed at 14 (c & d) and 29 days old (e, f, g). Bar=1cm

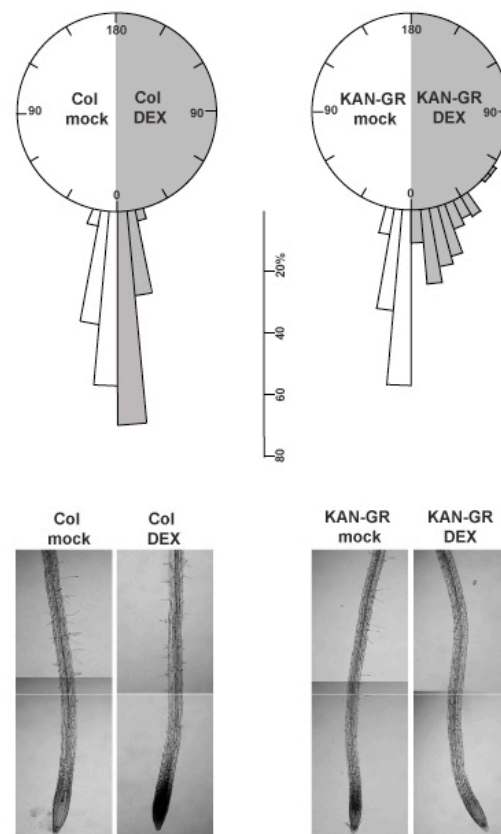


Figure 1-3: DEX and mock-treated *KAN-GR* plants display defects in root development. Roots were analyzed on 5 day old seedlings grown on vertically oriented media with DEX or mock supplementation. The angle of root growth relative to gravity was measured with Image J. Angles were allocated to 5° bins and with length of each bar indicating the fraction of plants within that bin (upper panel). Root angles diverged more in DEX-treated *KAN-GR* seedlings than mock-treated seedlings (upper panel right) indicating potential defects in sensing or responding to gravity. No differences were detected between mock- and DEX-treated Col roots. Root hair formation was also affected by DEX-treatment. DEX-treated *KAN-GR* seedlings failed to produce root hairs, which was not observed in mock-treated (lower right panels) or wild-type seedlings (lower left panels). Surprisingly, DEX influenced Col root hair formation; the number and length of hairs was slightly reduced in DEX-compared to mock-treated Col roots (lower left panels).

ChIP was performed on *KAN-GR* plants treated with DEX and mock and the enrichment of a particular gene promoter in the DEX-treated versus mock-treated samples serves as strong evidence for a direct interaction with the KAN1 protein. Our lab is particularly interested in genes involved in transcriptional regulation of leaf patterning and phytohormone signaling and biosynthesis. So I chose some candidates in these categories for ChIP based on previous microarray and RT-PCR results (Huang et al., 2008, submitted, Appendix 1). Quantitative assay of ChIP products has revealed 12 target gene promoters that are bound by KAN1 protein (Fig. 1-4). This list includes genes implicated in auxin response and signaling, such as *PIN-FORMED 4* (*PIN4*), an auxin efflux carrier[10], *IAA2*, a negative regulator of AUXIN RESPONSE FACTORS[11], *HAT2*, a homeobox gene that is rapidly and specifically induced by auxin and promotes auxin responses[12], and *FLS2*, a protein which mediates flagellin-induced expression of miR393a, a miRNA that targets the auxin receptor *TIR1*[13]. Other phytohormone-related *KANT* genes are identified as well, including the gibberellin catabolism gene *GIBBERELLIN-2 OXIDASE 6* (*GA2ox6*) [14] and *BRASSINOSTEROID ENHANCED EXPRESSION 1* (*BEE1*), a bHLH transcription factor that mediates early responses to brassinosteroids [15]. Another target of interest is *RADIALIS-LIKE 2* (*RL2*), a putative Myb transcription factor closely related to an *Antirrhinum* gene required for dorsal-ventral asymmetry during flower development [16]. ChIP applied with wild type plants did not reveal detectable differences between DEX- and mock-treated samples, confirming that the DEX-induced enrichment of promoter fragments in *KAN-GR* plants are solely attributed to KAN-GR (Suppl. Fig.

1-3).

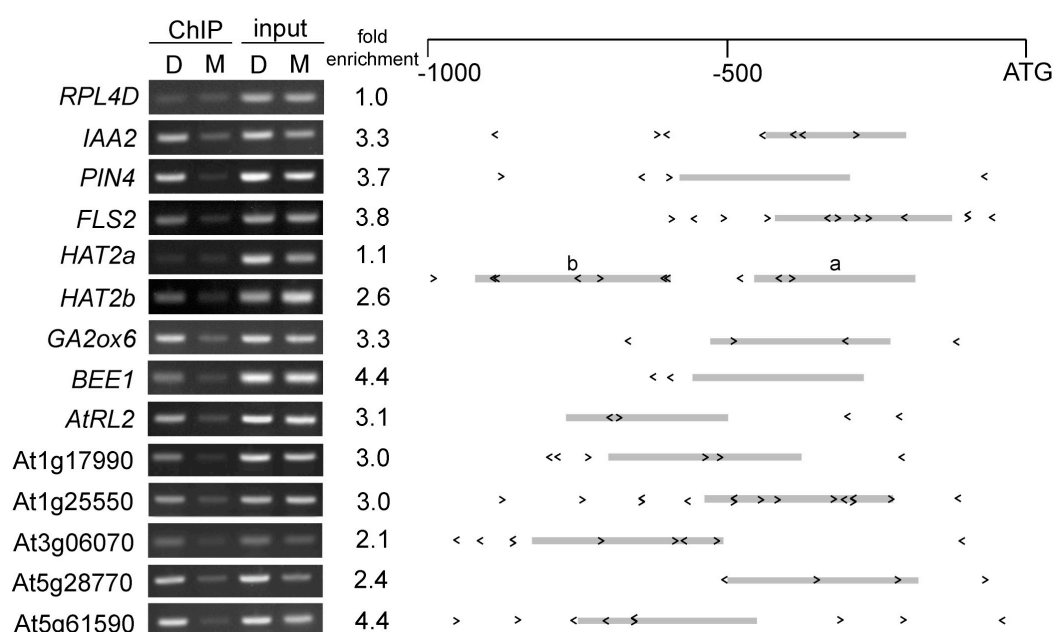


Figure 1-4. Chromatin immunoprecipitation confirms DEX-dependent association of KAN-GR with the promoters of *KANT* genes. Chromatin immunoprecipitation (ChIP) was performed on 9 day old transgenic Arabidopsis seedlings using antibodies specific for GR. Immunoprecipitated genomic DNA from mock (M) and DEX (D) treated KAN-GR and wild-type control seedlings was amplified with primers specific for the indicated promoters. Fold enrichment was calculated by normalizing PCR product intensities to a negative control, the *RIBOSOMAL PROTEIN L4D* (*RPL4D*) coding region, followed by calculating the ratio DEX IP/input to mock IP/input. The mean of at least two independent IP experiments with technical replicates is reported as fold-enrichment. Schematics of the gene promoters are shown with the positions and orientations of KBX sites indicated by < or > and the amplified region represented by a grey bar.

Along with the identification of *KANT* genes, another goal of ChIP is to evaluate the biological significance of KBX *in vivo*. The region I selected to represent an individual promoter in ChIP is always including or flanking a KBX. Although most tested regions appeared to be associated with KAN, there are some exceptions, such as in *HAT2* promoter, only one of the two KBX-containing regions (*HAT2b*) was

enriched in DEX (Fig. 1-4). This result indicates that KBX alone is not sufficient to render the binding of KAN to its targets.

KAN1 directly represses the transcription of *AS2*, a critical promoter of adaxial leaf fate

In order to further investigate the function of KAN in determining abaxial identity and more deeply understand the biological significance of KBX, we studied in detail a specific target of KAN, *ASYMMETRIC LEAVES2 (AS2)*. We first identified a mutant with a dominant, adaxialized phenotype. Plants homozygous or heterozygous for the mutation produced upwardly curled leaves and displayed impaired polarity in mesophyll cells (Fig. 1-5). The mutation was proved to be localized in the 5'-promoter region of *AS2*, a LOB domain transcription factor promoting adaxial cell fate [17, 18], so we dubbed this mutant as *as2-5D*. Sequencing the promoter of *as2-5D* revealed a G-to-A change in the first nucleotide of a tandem KBX repeat (GAATAAGAATAA). Existing ESTs and cDNAs (www.arabidopsis.org) and the results of 5' RACE (data not shown) indicate that *AS2* has multiple transcription start sites. The *as2-5D* mutation is located in the first intron of one of these transcripts, but is in the promoter of most of the transcripts produced from this locus (Fig. 1-5).

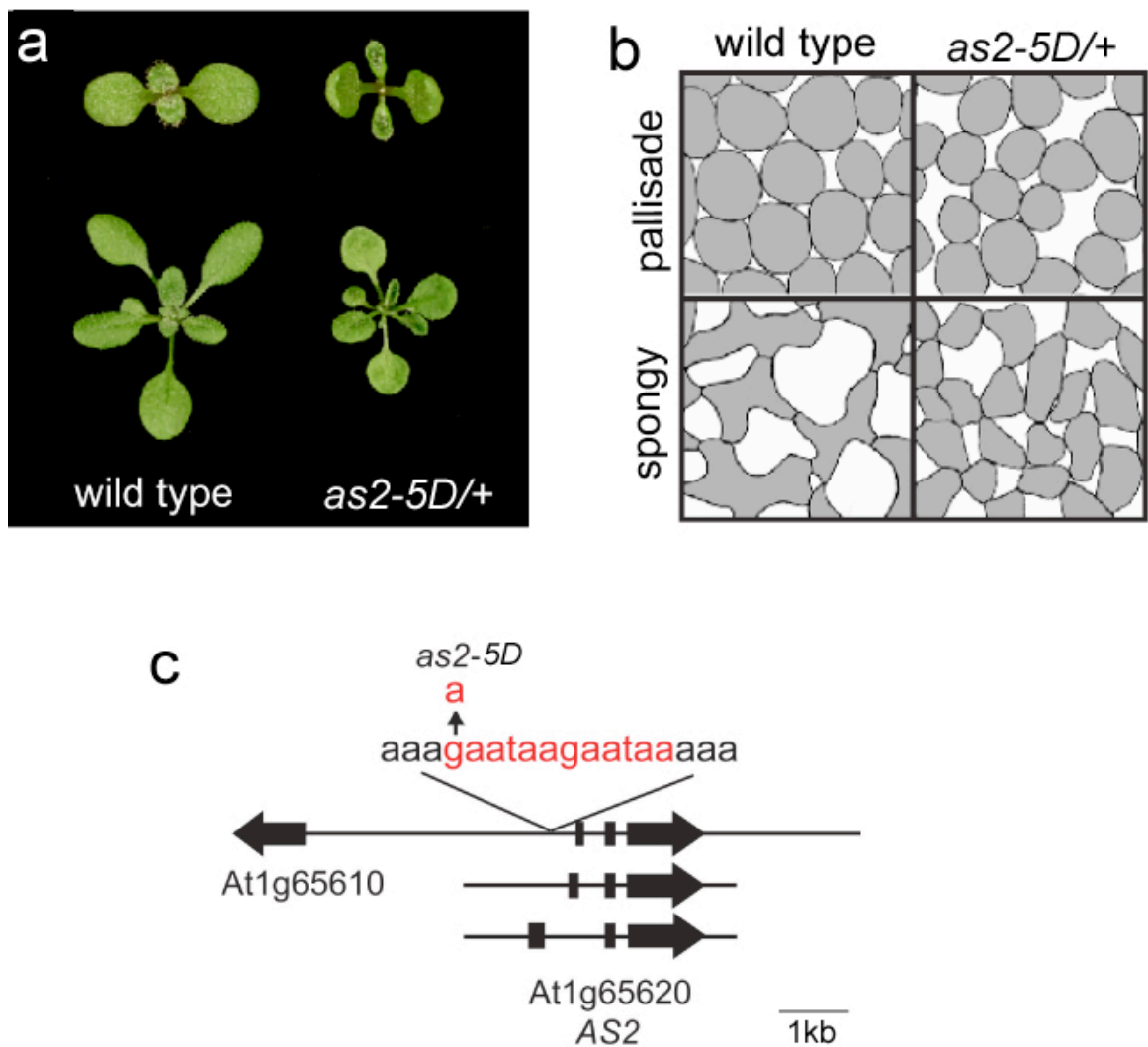


Figure 1-5. *as2-5D* has an adaxialized phenotype. (a) 8-day (top) and 21-day (bottom) old wild-type Columbia and *as2-5D/+* plants. *as2-5D* causes immature leaves and cotyledons to curl upwards, (b) Camera-lucida drawings of the adaxial and abaxial mesophyll of leaf 3 demonstrating the loss of tissue polarity in *as2-5D/+*. (c) *as2-5D* affects a predicted KAN1 binding site. *AS2* transcripts share exons 2 and 3, but have variable first exons. The location of the *as2-5D* mutation is indicated in red.

To examine the effect of the *as2-5D* mutation on the expression of *AS2*, we generated promoter-reporter lines containing wild type or mutated *AS2* regulatory sequences fused to β -glucuronidase (*GUS*). Transgenic plants bearing the following constructs,

pAS2:GUS (wild-type *AS2* promoter fused to GUS), *pAS2-5D:GUS* (*AS2-5D* promoter fused to GUS), and *pAS2-m:GUS* (*AS2* promoter in which the second G in the GAATAAGAATAA repeat was mutated and fused to GUS) were stained for GUS activity. Consistent with the expression pattern of *AS2* revealed by *in situ* hybridization [19, 20], GUS stain is distributed exclusively in the adaxial domain of cotyledons in *pAS2:GUS* embryos and seedlings (Fig. 1-6). In contrast, *pAS2-5D:GUS* plants expressed GUS throughout the cotyledons and the hypocotyl (Fig. 1-6), whereas *pAS2-m:GUS* embryos and seedlings exhibited the same expression pattern as the wild type construct (Fig. 1-6). These results proved that the *as2-5D* mutation caused ectopic expression of *AS2* and provided strong evidence that KAN1 repressed *AS2* through transcriptional regulation. They also further confirmed that the KBX sequence is necessary but not sufficient to confer KAN1-mediated repression on its target genes.

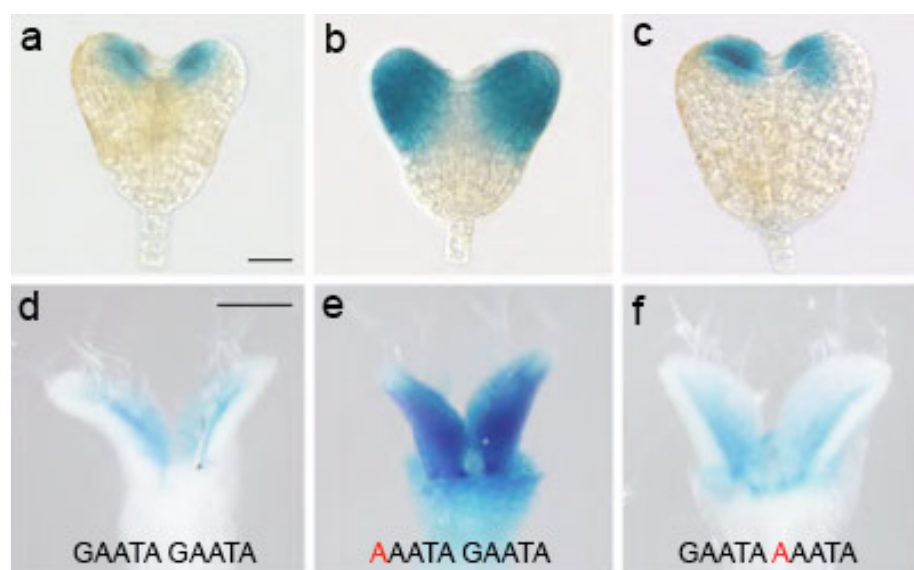


Figure 1-6. KAN1 binding site determines the spatial expression pattern of *AS2*. The expression pattern of *pAS2:GUS* (a,d), *pAS2-5D:GUS* (b,e) and *pAS2m:GUS* (c,f)

in embryos (upper row), and the leaf primordia of 8 day-old Columbia seedlings (lower row). The sequence of the KAN1 binding site in each construct is shown, with the mutated nucleotide shown in red. The *as2-5D* mutation causes *AS2* to be expressed in the abaxial domains of cotyledons and leaves, and in the hypocotyl. Bar = 20 μ m in a-c and 100 μ m in d-f.

In order to provide direct evidence that KAN1 binds to this sequence in the *AS2* promoter, I performed ChIP in *KAN1-GR* and *as2-5D KAN1-GR* seedlings. I tested three putative KBXs in the promoter of *AS2* and the enrichment in DEX was only detected on the site affected by the *as2-5D* mutation (Fig. 1-7). The ~3-fold enrichment is comparable to the enrichment observed in the previous identified target *IAA2*. No enrichment was observed in *KAN1-GR* plants homozygous for *as2-5D*, proving that the *as2-5D* mutation prevents or greatly reduces the binding of KAN1 to this site. Consistent with this result, in *as2-5D KAN1-GR* seedlings, DEX-dependent effects on cotyledon and leaf morphology, and root growth orientation are highly suppressed (Fig. 1-7). These results further confirmed that *AS2* is a direct target of KAN1 and suggested that the repression of *AS2* contributed to the phenotype of plants that ectopically express *KAN1*.

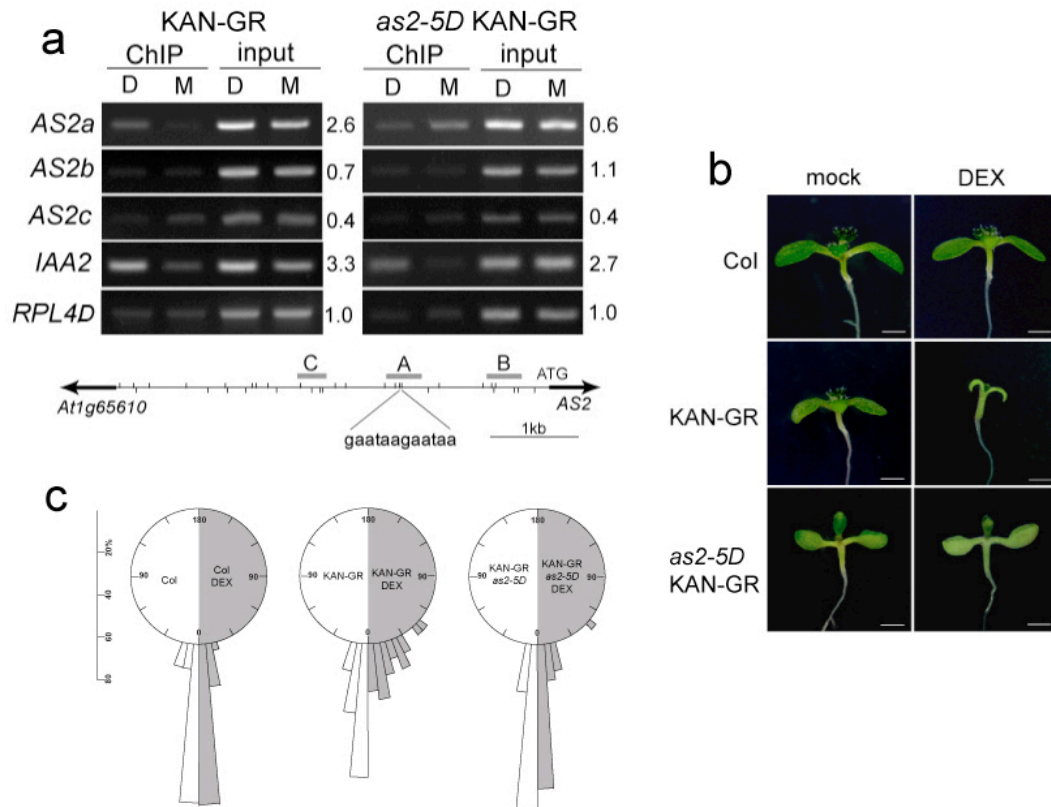


Figure 1-7. KAN1-GR represses *AS2* directly (a) Chromatin immunoprecipitation (ChIP) performed on DEX (D)- and mock (M)-treated *35S:KAN1-GR* and *35S:KAN1-GR as2-5D* seedlings (b). Chromatin from three different regions 5' of *AS2* (A, B, and C indicated by grey bars) were analyzed with semi-quantitative PCR prior to (input) and after ChIP. Fragment A contains the *as2-5D* point mutation. Average fold enrichment is indicated on the right of each image, and was calculated for three replicates in DEX versus mock samples after normalizing the band intensity to that of the control gene *RPL4D*. Note that *as2-5D* blocks the binding of KAN1-GR to the *AS2* promoter, as well as the effect of KAN-GR on seedling morphology (b) and root growth directions (c). Bar = 1 mm.

Plants constitutively expressing *AS2* have reduced levels of *KAN1* and *KAN2* mRNA and the leaf phenotype resembles *kan1 kan2* double mutant [17], whereas *as2-1* mutants have elevated levels of *KAN2*[20]. These observations suggest that *AS2* and *KAN* genes may mutually repress each other's transcription. To test this hypothesis, I investigated the expression of *pKAN1:GUS* in wild type, *as2-1* and *as2-5D*

background. In wild-type plants, *pKAN1:GUS* expressed in the abaxial side of very young leaf primordia and was restricted to the bottom of more mature leaves (Fig. 1-8). In *as2-1*, *pKAN1:GUS* expression extended to the adaxial side of young leaf primordia and persisted later in leaf development (Fig. 1-8). Conversely, in *as2-5D*, *pKAN1:GUS* expression was excluded from young leaves and restricted to a small region of the shoot apex (Fig. 1-8). This result implied that *AS2* directly or indirectly represses *KAN1* expression. Repression of *KAN* genes by *AS2* was further supported by the phenotype of *kan1-11 as2-5D* doubly mutant (Fig. 1-8). Double mutant leaves display abaxial outgrowths that are a characteristic feature of *kan1 kan2* but absent in either *kan1* or *as2-5D* single mutants (Fig. 1-8). A reasonable interpretation of this result is that *as2-5D* represses *KAN2* as well.

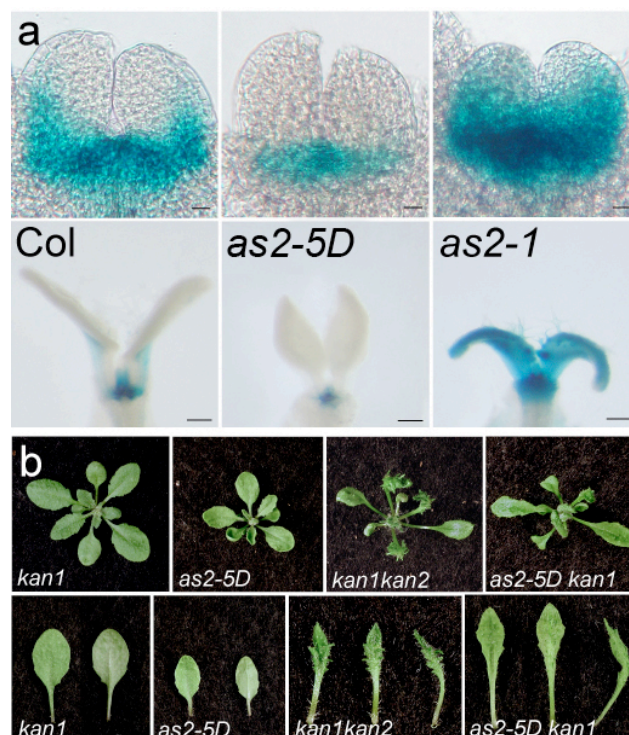


Figure 1-8. *AS2* represses *KAN1* and *KAN2*. (a) The expression of *pKAN1:GUS* in the leaf primordia of 3- (upper row) and 9-day-old (lower row) wild-type, *as2-5D* and *as2-1* seedlings. Cotyledons were removed to reveal the leaf primordia. Bar = 20 μ m in upper row and 200 μ m in lower row. The expression domain of *pKAN1:GUS* is

reduced in *as2-5D* and expanded in *as2-1*. **(b)** The rosette (top row) and leaf five (bottom row) of 18-day-old wild type, *kan1-11*, *as2-5D*, *kan1-11 as2-5D*, and *kan1-11 kan2-5* plants. Adaxial, abaxial, and side views of the leaf are shown from left to right. The phenotype of *kan1-11 as2-5D* resembles that of *kan1-11 kan2-5*.

Discussion

KANADI functions in leaf patterning by mediation of auxin action

The phytohormone auxin is implicated in various important processes in different developmental stages of plant growth. Three fundamental patterning events, establishment of apical–basal and central–peripheral axes, and differentiation of adaxial-abaxial symmetry, are all correlated with signaling and response of auxin. (reviewed in Krogan and Berleth, 2007). One unique feature of auxin is its polar-fashioned transport, which is directly relevant to most of its developmental roles [21]. Polar transport of auxin depends on a family of carrier proteins, *PINFORMED* (*PIN*), which controls auxin efflux in plant cells. Distribution of PIN proteins predicts auxin accumulation in different plant tissues. In embryogenesis, dynamic expression patterns of PIN directs initial accumulation of auxin in the apical cell, followed by a subsequent efflux of auxin to the basal domain, leading to the specification of hypophysis and defining the future root. Afterwards, the polar localization of PIN proteins in the late globular stage results in a focal point of auxin transport, marking the site of cotyledon initiation. The resulting cotyledon primodium acts as a sink to transport auxin basipetally to develop provascular strands and another auxin maxima will form distantly to become a new primodium, which contributes to the phyllotatic pattern of the mature plant.[22-24].

PIN proteins determine the spatial localization of auxin that leads to wide range of developmental events. The effectiveness of this process also relies on the factors perceiving the signal from the differentially distributed auxin and triggering the downstream gene expression. Members of two protein families, *Aux/IAA* and *AUXIN RESPONSE FACTORS (ARFs)* are key players among these factors. In the absence of auxin, IAA proteins interact with ARF proteins to repress their function in activating the gene responsible for auxin-dependent phenotypes. However, if auxin is applied, the IAA proteins are degraded and the de-repression of ARF proteins causes the activation of ARF-dependent genes and results in various auxin responses.[25]. Two members of ARF family, *ARF3/ETTIN* and *ARF4* have demonstrated roles in leaf polarity. Double mutant of *ARF3* and *ARF4* produces features reminiscent of *kan1 kan2* mutant, such as up-curling leaves and ectopic out-growths on the abaxial side of leaves[26]. These observations imply a possible correlation between adaxial-abaxial patterning and auxin response. Specifically, *KAN* genes are implicated in auxin distribution and response by the results that *PIN1* and *DR5* (a synthetic promoter whose expression indicates the responsiveness to auxin [23]) expression patterns are markedly affected by the loss of *KAN* genes [27]. Based on these findings, our results further supported the relationship between *KAN* and auxin. About half of the targets we identified with ChIP are auxin-related genes. For instance, *PIN4* belongs to the PIN family involved in regulating auxin distribution and *IAA2* is a member of *Aux/IAA* family functioning in auxin signal transduction. And *FLS2* indirectly enhances *TIR1*, an auxin receptor that mediates the degradation of IAA by auxin through 26S

proteasome pathway[28]. Another target *HAT2* also plays a role in promoting auxin response [12].

The identity of these target genes strongly suggests the involvement of auxin in the function of *KAN* genes in leaf morphogenesis. This conclusion is also supported by the profound developmental defects observed in *KAN-GR* plants treated with DEX, such as reduced leaf initiation, impaired root hair formation and abnormal root growth direction. All these mutant phenotypes are associated with disrupted auxin response [29, 30] (reviewed in Krogan and Berleth, 2007). We propose that *KAN1* may function to enhance auxin accumulation, sensitivity, and signaling on the abaxial side of the initiating leaf primordium, resulting in asymmetric changes in gene expression and growth. In other words, the high concentration of auxin on the abaxial side of the early leaf primordium induced by *KAN* versus a lower concentration on the adaxial side leads to differential gene expression critical for establishing the asymmetry of the primordium. This model is consistent with observations that *PIN1* reverses its polarity on the adaxial side of a leaf primordium very early in leaf initiation, thereby depleting this region of auxin [31]. It is also a plausible explanation of the radial structure formed after the surgical separation of young leaf from the shoot apical meristem (SAM), which indicates establishment of leaf polarity depends on continuity between the leaf primordium and the SAM [32]. The traditional interpretation for this result is that a “signal” from the SAM is required for adaxial-abaxial differentiation.

According to our model, this “signal” is probably the auxin gradient in young leaf primodium. In this scenario, surgical ablation actually perturbs this gradient and

isolates auxin in adaxial side, which consequently causes disruption of leaf polarity.

In vivo* experiments interpreted the importance of *in vitro* KBX in the actual circumstance *in planta

In vivo identification of KAN1 targets not only revealed the central role of *KAN* in transcriptional regulation of leaf polarity, but also evaluates the biological significance of *in vitro* binding motif that is the critical molecular basis for KAN1 function. Particularly in *as2-5D* plants, a single nucleotide change in KBX remarkably reduces binding of KAN1, which is consistent with the EMSA result (Fig. 1-1), indicating the key role of this base in the consensus binding motif and supporting that this motif is necessary for KAN1 targeting *in planta*. However, the same mutation in the adjacent KBX doesn't affect *AS2* expression (Fig. 1-6) suggesting this motif is not sufficient to confer KAN1-mediated interaction. This conclusion is also supported by the ChIP result with *HAT2* promoter (Fig. 1-3), in which only one of two KBXs is bound by KAN1 *in vivo*. This result is partly contributed to the technical barrier we encountered in purifying full-length KAN1 protein (as described in this chapter). The recombinant protein we used for *in vitro* selection contains only part of KAN1 protein. Although the essential DNA binding domain is included, other elements required for proper KAN1 action, such as other functional domains or correct secondary structures, are probably lost or not intact. Besides that, the experimental temperature is also a possible factor. I expressed KAN1 protein in *E. Coli* in 37°C and performed *in vitro* binding of protein with DNA in 4°C. Neither of these temperatures is optimal for protein biosynthesis and protein-DNA interaction in plants. Possible changes of

protein structure in these conditions may cause the discrepancy between *in vitro* and *in vivo* results. In addition, other cofactor proteins required for *in vivo* DNA binding by KAN1 and the accessibility of the specific motif within the context of chromatin are also plausible explanations. In order to define the target sequence of KAN1 *in vivo*, a ChIP-Seq strategy can be utilized which combines chromatin immunoprecipitation and subsequent sequencing of DNA fragments immunoprecipitated with KAN1 protein. Analyzing these sequences will provide the real consensus motif and facilitate the discovery of more KAN1 targets and better understanding of KAN1 function.

Direct repression of *AS2* by *KAN* contributes to the elucidation of antagonistic interaction between adaxial and abaxial identity genes

As described in the chapter of introduction, genes specifying adaxial and abaxial identity are mutually antagonizing each other. However, the molecular mechanism underlining this antagonistic relationship is still unclear. Based on the fact that most of the identified players in leaf polarity belong to protein families with transcription factors, the interactions between these genes are likely due to transcriptional regulation. Therefore, our investigations of *in vivo* targets of KAN, especially uncovering the direct interaction between KAN and a promoter element of *AS2*, established a platform to further demonstrate this regulatory network. Repression of *AS2* by KAN1 provides the first evidence for a direct interaction between transcription factors involved in leaf polarity. It also serves as a standard example for studying the mechanism of transcriptional regulation, although the situation is a bit extreme that a single nucleotide mutation can abolish the binding of a transcription

factor and cause profound change in gene expression. We are unaware of any other case like this in plant because multiple binding sites are usually required for regulation by a specific transcription factor.

Although *KAN* directly regulates *AS2* in specifying abaxial identity, the phenotypes associated with loss of *KAN* genes are not solely dependent on this interaction. The triple mutant *kan1 kan2 as2* displays a similar phenotype as *kan1 kan2*, despite that the vascular defect in *kan1 kan2* petioles are partially rescued by loss of *AS2* [33] and leaf blades of triple mutant are shorter and more irregular than the double mutant (Wu et al., 2008, submitted, Appendix 2). These observations suggest that *AS2* is not the only factor that *KAN* genes act on to determine abaxial cell fate. Consistent with our previous discussion about the interplay between *KAN* and auxin-related genes, we demonstrate that regulation of leaf morphogenesis by *KANADI* genes requires a complex network involving genes functioning in plant hormone metabolism, transport and response and important transcription factors. Elucidation these interactions will be our goal in the future and identification of new targets of *KAN*, as well as characterizing novel players in *KAN-AS2* pathway will be of special interest.

Materials and methods

Plant materials and treatments:

All plants used in this study were in the Columbia (Col) background and were grown at 22°C under long day (16 hour) illumination. The *KAN-GR* construct was produced as follows: the *p35S:KAN1-mGFP5* plasmid [4] was digested with *Bgl*II and partially

digested with *NheI* to remove the fragment encoding *mGFP5*. In its place, a DNA fragment was ligated that encoded amino acids 508-795 of the rat glucocorticoid receptor isolated from pBS-GR (a gift from Doris Wagner) by digestion with *BamHI* and *XbaI*. In order to generate *pKANI:GUS*, a 7.7 kb *BglIII* fragment from P1 clone MQK4 was ligated into the *BamHI* site of pCAMBIA2300 (www.cambia.org). A 3.5 kb *XbaI* fragment carrying the *KANI* promoter was subcloned into pBI101.2 to generate a translational fusion between the first 8 amino acids of the KAN1 coding region and GUS. The resulting constructs were sequenced to confirm their integrity and introduced into *Arabidopsis* plants using the floral dip method. Transformants were selected using hygromycin B. A line homozygous for the *KANGR* T-DNA that was phenotypically normal in the absence of DEX and showed a strong and consistent response on DEX containing media was selected for all subsequent experiments. For continuous DEX treatments, seeds homozygous for *KAN-GR* were germinated on media containing 1/2X MS salts and 0.8% agar supplemented either with 10 μ M DEX or 0.05% ethanol for mock treatment. For intermittent treatment, soil-grown seedlings were painted every second day either with 10 μ M DEX or mock (0.05% ethanol) plus 0.015% Silwet L-77. For chromatin immunoprecipitation, 9 day old seedlings were grown on 1/2X MS medium without sucrose before being submerged for 4 hours with gentle agitation in liquid 1/2X MS plus 1% sucrose containing 10 μ M DEX or 0.05% ethanol (mock).

Generation of *as2-5D* with ethylmethan sulphonate (EMS) and mapping the mutation in *as2-5D* is described in Appendix 2. To examine the effect of this mutation on gene

expression, the wild-type *AS2* promoter sequence was amplified from wild-type genomic DNA using primers pAS2-F: 5'-GGATCCTGGTAGCTAGCGTTGTTGACA-3' and pAS2-R: 5'-GGATCCGTGAACGTTTGCGAATTTTGTG-3', which contained introduced *Bam*HI sites, and the resulting PCR products were cloned into the binary vector pCB308 generating a translational fusion to the *GUS* gene in the pAS2:*GUS* construct. The pas2-5D:*GUS* and pAS2-m:*GUS* constructs were generated using site-directed mutagenesis, by amplification of the pAS2:*GUS* template with primers containing introduced mutations: pas2-d-F: 5'-CCCTAGACAAAAAAATAAGAATAAAAAGAGC-3' and pas2-d-R: 5'-GCTCTTTTTATTCTTATTTTTTTTGTCTAGGG-3' or pAS2-m-F: 5'-CCCTAGACAAAAGAATAAAAATAAAAAGAGC-3', and pAS2-m-R: 5'-GCTCTTTTTATTTTTTATTCTTTTTGTCTAGGG-3' with *PfuTurbo* DNA polymerase (Stratagene, La Jolla, CA). The PCR products were digested with *Dpn*I to restrict the parental DNA template. The resulting constructs were transformed into *Arabidopsis* as described above.

Plasmid Construction for expressing KAN1bd protein *in vitro*: The putative DNA binding domain of KAN1 was amplified from the cDNA clone [4] using the following primers and cycling conditions:

5'-ATTCggatCcAAGATGCCGACAAAGCGAAGC-3' and 5'-

AAGCgaattcCTTGTTAGTGGTCTTAACAGTTTCG-3' (lowercase letters represent

mismatched bases), 94°C for 20s, 54°C for 20s, 72°C for 15s for 34 cycles. Amplified

DNA and the vector pGEX-2TK (Amersham Biosciences, Piscataway, NJ) were digested with *Bam*HI and *Eco*RI and recombined such that the amino acids 210-280 of KAN1 were fused in-frame with glutathione S-transferase (GST) to form pGEX-KAN1bd.

Purification of KAN1bd protein: *E.coli* BL21 (DE3) cells carrying pGEX-KAN1bd were grown at 37°C in LB medium to OD600 between 0.6-0.8 and harvested 2.5 hours after protein expression was induced with 0.1 mM IPTG. Cell pellets were resuspended and lysed by sonication in 1X PBS at 4°C then centrifuged at 12,000xg for 30 minutes to pellet debris. Soluble recombinant protein was purified using MicroSpin GST Purification Modules (Amersham Biosciences, Piscataway, NJ) according to the manufacturer's instructions.

Purified KAN1bd protein was subsequently dialyzed against 20 mM Tris-HCl, pH 8.0 and 80 mM KCl to remove reduced glutathione. Proteins were prepared for EMSA by treating with 0.07 U/μl DNase I (Fermentas, Hanover, MD) on ice for 1 hour to remove contaminating *E. coli* DNA and DNase I was inactivated with 2 mM EDTA.

PCR-Assisted *in vitro* DNA binding site selection: KAN1bd DNA binding site selection was performed essentially as described [3]. A mixture of 54-base oligonucleotides was synthesized (IDT, Coralville, IA) with the central 16 bases consisting of random sequences (Table 1-1). Oligonucleotides were converted into dsDNA using Klenow fragment (Fermentas, Hanover, MD) and primer BSSr (Table 1-1). 2 nmol of dsDNA was incubated with 20 pmol of purified protein in dialysis buffer for 1 hour at 4°C. Sample buffer (2% SDS, 10% glycerol, 60 mM Tris, 5%

β -mercaptoethanol and 0.01% bromophenol blue, pH 6.8) was added and the protein/DNA mixture was separated on two identical 9% native polyacrylamide gels in 0.5X Tris-borate-EDTA (TBE) buffer at 4°C for 120 volt hours. One gel was stained with SYBR Safe™ (Invitrogen, Eugene, OR) to visualize DNA in the DNA-protein complex and the other gel was stained with E-Zinc™ reversible stain kit (Pierce, Rockford, IL) to visualize protein in the complex. A single band that was retarded relative to free DNA or free protein was excised from the gel and DNA was purified by phenol:chloroform extraction then amplified using primers BSSf and BSSr (Table 1-1). PCR products were precipitated and used in subsequent rounds of oligonucleotide selection. SYBR Safe™ and E-Zinc™ visualized EMSA selections were performed independently. After 6 cycles of selection, the resulting DNAs were cloned into pGEM-T Easy (Promega, Madison, WI) and sequenced. Sequence comparison and motif identification were performed using web implementations of MEME [34](<http://meme.nbcr.net/meme/intro.html>) and the Gibbs Motif Sampler [35](<http://bayesweb.wadsworth.org/gibbs/gibbs.html>).

Electrophoretic mobility shift assay (EMSA): Complementary 54-bp oligonucleotides (Table 1-1) containing a KBX or its variants were synthesized (IDT, Coralville, IA), annealed, and 2 pmol of DNA was incubated with 10 pmol of purified protein for 1 hour at 4°C. DNA-protein complexes were resolved on a 9% native polyacrylamide gels in TBE buffer at 4°C and stained with SYBR Safe™ (Invitrogen Corp., Eugene, OR). The fluorescence intensity of each DNA fragment was measured using KODAK Molecular Imaging Software 4.0 (Eastman KODAK

Company, Rochester, NY). Bands were normalized using Gaussian curve with background subtraction. Mean fluorescence intensities and standard errors were calculated from at least three independent EMSA experiments.

ChIP analysis: 9-day-old DEX- or mock-treated *KAN-GR* and wild-type seedlings were harvested, washed with deionized water and crosslinked with 1% formaldehyde. Crosslinking was quenched with 0.125M glycine. Procedures for nuclear extracts and immunoprecipitation were adapted [36] with following modifications: Conditions for sonication of nuclear extracts were empirically determined to obtain an average DNA fragment size of 600bp. Sonication was performed on ice with 4 pulses of 12 seconds with 1 minute pauses at power setting 6 (40% duty cycle, 20% input; Heat System-Ultrasonics, Farmingdale, NY). After chromatin shearing, 10µl anti-GR P-20 (Santa Cruz Biotechnology, Santa Cruz, CA) was added to each sample to immunoprecipitate KAN-GR proteins. After reversing crosslinks, DNA was purified by phenol:chloroform extraction, ethanol precipitated, and resuspended in 50 µl TE. 1µl of immunoprecipitated DNA was used in semi-quantitative ChIP PCR. Input DNA was diluted 120 times to achieve PCR product band intensities comparable to ChIP samples. Primers recognizing different regions in the promoters and the control gene *RPL4D* can be found in (Table 1-2) PCR conditions were as follows: 33 cycles, 94°C for 30s, 56°C for 30s, and 72°C for 30s. DNA band intensity was measured using the Gaussian Curve method with background subtraction with Molecular Imaging Software 4.0 (Eastman KODAK Company, Rochester, NY). The abundance ratio of promoter fragments in DEX- versus mock-treated ChIP and input samples

were normalized by dividing by the ratio of the negative-control gene *RPL4D* in DEX- or mock-treated samples. The enrichment of each gene in DEX- versus mock-treated samples results from dividing normalized DEX- to mock-treated ChIP ratios by the DEX- to mock-treated input ratios.

Histology: GUS staining was conducted according to the method of [37].

Specifically, siliques were opened along the valve margin with a needle and stained with GUS staining buffer. After staining, developing seeds were placed on a glass slide and the embryos were removed from the seed by applying gentle pressure with a needle.

Tables

Table1-1: Primers for Oligonucleotide Selection and EMSA

Oligo Name	Sequence (forward strand)
BSSlong	gctgagtctgaacaagcttgNNNNNNNNNNNNNNNNNNcctcgagtcagagcgctcg
BSSr	cgacgctctgactcgagg
BSSf	gctgagtctgaacaagcttg
GS13	gctgagtctgaacaagcttgGGAATAAAAACGTGCCcctcgagtcagagcgctcg
GS15	gctgagtctgaacaagcttgGcAATAAAAACGTGCCcctcgagtcagagcgctcg
GS17	gctgagtctgaacaagcttgGGtATAAAAACGTGCCcctcgagtcagagcgctcg
GS18	gctgagtctgaacaagcttgGGAAtATAAAAACGTGCCcctcgagtcagagcgctcg
GS19	gctgagtctgaacaagcttgGGAaAATAAAAACGTGCCcctcgagtcagagcgctcg
GS20	gctgagtctgaacaagcttgGGAATtAAAACGTGCCcctcgagtcagagcgctcg
GS28	gctgagtctgaacaagcttgGGAATAgAAACGTGCCcctcgagtcagagcgctcg
GS21	gctgagtctgaacaagcttgGGAATATTCACGTGCCcctcgagtcagagcgctcg
GS35 (ARR10 binding site)	gctgagtctgaacaagcttgCAATCTAAAACGTGCCcctcgagtcagagcgctcg
GS14	gctgagtctgaacaagcttgGtAATAAAAACGTGCCcctcgagtcagagcgctcg
GS16	gctgagtctgaacaagcttgGaAATAAAAACGTGCCcctcgagtcagagcgctcg
GS29	gctgagtctgaacaagcttgGGAATAcAAACGTGCCcctcgagtcagagcgctcg
GS32	gctgagtctgaacaagcttgGGAATcAAAACGTGCCcctcgagtcagagcgctcg
GS33	gctgagtctgaacaagcttgGGAATgAAAACGTGCCcctcgagtcagagcgctcg

Table1-2: Primers for Chromatin Immunoprecipitation

Gene	left primer	right primer
<i>RPL4D/At5g02870</i>	tgtgtttgtcattactgtgctatgc	ataaagctggcggttcgagt
<i>IAA2/At3g23030</i>	cgggtcggccgatagaat	tcggaagcatgaaaggcaag
<i>PIN4/At2g01420</i>	aacggtccaacagtggcttg	gttttctggaggggacgtgga
<i>FLS2/At5g46330</i>	cgtcaaaactaaatcgaaa	agggatcatgtcacggatgt
<i>HAT2a/At5g47370</i>	ttggccatcttatttgttttggga	tggtaatgaagaagagaggggatt
<i>HAT2b/At5g47370</i>	tgttttgtaccaaccactccaatta	tggataacgcaatttgcactactt
<i>GA2ox6/At1g02400</i>	ggttaggcaagaatgttgacaataaa	catcctacaaatcgcgtaaggtg
<i>BEE1/At1g18400</i>	gcattggccatttgggaagt	tggtcgtgggttcattagg
<i>AtRL2/At2g21650</i>	ttgatatggtttcatggcagaga	acgtgctcgcggaattac
<i>At1g17990</i>	gaaatggggtgagacagagatgat	aagacgtgcacaaatgcttaaggt
<i>At1g25550</i>	ttttctggttacatatcttgattccaa	cggattttacttgggaaagggtag
<i>At3g06070</i>	ttttaatggatgcgaatgcaaat	ggaattcctaactaccttatccaatga
<i>At5g28770</i>	cgttgtaactgtaggcgaatctca	taatggccccgacaagagtc
<i>At5g61590</i>	caagacaaccctacaagacaagca	cacaaacaaaacaaaaaagacttg

SUPPLEMENTARY FIGURES

```

s61 - gctgagtctgaacaagcttgACGGTGGGAATATTCcctcgagtcagagcgctcg
s11 +      cgacgctctgactcgaggGGAATATTCGCTAGCcaagcttggttcagactcagc
s51 -      gctgagtctgaacaagcttgAGGAATATTCGCTGCCcctcgagtcagagcgctcg
z41 +      gctgagtctgaacaagcttgGGAATATTCTCACAGCctcgagtcagagcgctcg
z32 -      gctgagtctgaacaagcttgGCGGAATATTCGTACCcctcgagtcagagcgctcg
s12 +      cgacgctctgactcgaggGGGGAATATTCGTGCGcaagcttggttcagactcagc
z40 +      cgacgctctgactcgaggGGAATATACCTGCCCTcaagcttggttcagactcagc
s62 -      gctgagtctgaacaagcttgGGGAGGAATATACGGCCcctcgagtcagagcgctcg
s59 +      cgacgctctgactcgaggGGCGAATATACCCTACcaagcttggttcagactcagc
z38 +      gctgagtctgaacaagcttgGAGTACC GAATATACcctcgagtcagagcgctcg
s16 +      cgacgctctgactcgaggGGGAATATGCGTACCcaagcttggttcagactcagc
z83 -      gctgagtctgaacaagcttgATTAGACGGAATATGcctcgagtcagagcgctcg
s20 +      gctgagtctgaacaagcttgCCCTCACGAATATGCCcctcgagtcagagcgctcg
s47 -      gctgagtctgaacaagcttgACGAATATGCCCTTCcctcgagtcagagcgctcg
z82 +      gctgagtctgaacaagcttgGGGAATATCCCATCGcctcgagtcagagcgctcg
z34 -      gctgagtctgaacaagcttgTTTAGCGGAATATCCCcctcgagtcagagcgctcg
s9 -      gctgagtctgaacaagcttgACCGCGAATATCCCcctcgagtcagagcgctcg
z27 -      gctgagtctgaacaagcttgGTAAGGAATAATCTGCGcctcgagtcagagcgctcg
z77 -      gctgagtctgaacaagcttgAGAATAATCCCGATAcctcgagtcagagcgctcg
z29 -      cgacgctctgactcgaggGGAATAATTATGCTGcaagcttggttcagactcagc
z24 -      cgacgctctgactcgaggGCACGAATAATTCTCTcaagcttggttcagactcagc
s58 +      gctgagtctgaacaagcttgGGGAATAATGAGTCCcctcgagtcagagcgctcg
z36 +      cgacgctctgactcgaggCGAATAATGCACTATGcaagcttggttcagactcagc
s14 -      gctgagtctgaacaagcttgCCAGAGAATAATGCCcctcgagtcagagcgctcg
s46 -      gctgagtctgaacaagcttgGAATAGGGAATAACCGcctcgagtcagagcgctcg
s3 -      gctgagtctgaacaagcttgAAGAATAACCCAGTGCcctcgagtcagagcgctcg
s17 -      gctgagtctgaacaagcttgGAATAAACGTAAACGCCcctcgagtcagagcgctcg
z42 -      cgacgctctgactcgaggGGAATAAACGTACTAaagcttggttcagactcagc
s6 -      gctgagtctgaacaagcttgAGGAATAAACACGGGCcctcgagtcagagcgctcg
s49 -      gctgagtctgaacaagcttgGGAATAAAAACGTGCCcctcgagtcagagcgctcg
z33 -      gctgagtctgaacaagcttgTGCGAGAATAAGTCGCcctcgagtcagagcgctcg
z39 +      gctgagtctgaacaagcttgAGAATATCAGCTGTACcctcgagtcagagcgctcg
s60 +      cgacgctctgactcgaggGGGATAATCCGTCCGTcaagcttggttcagactcagc
s52 -      cgacgctctgactcgaggGGGATAATCTGTGTACaagcttggttcagactcagc
s63 +      cgacgctctgactcgaggGGATATCCGTGGTGTcaagcttggttcagactcagc
s5 -      cgacgctctgactcgaggGGATAATTCGGACCCcaagcttggttcagactcagc
s44 +      cgacgctctgactcgaggCCGGATATCGGAATGTcaagcttggttcagactcagc
z81 -      gctgagtctgaacaagcttgGCGATAATACAGAATAcctcgagtcagagcgctcg
s22 -      cgacgctctgactcgaggGCGATAATTACCGTCCcaagcttggttcagactcagc
z26 +      tgacgctctgactcgaggCGCATATAATTTATACcaagcttggttcagactcagc
s21 -      gctgagtctgaacaagcttgACAACGCATAAAGGGCcctcgagtcagagcgctcg
z30 +      cgacgctctgactcgaggCAAGTATATTATGGTACaagcttggttcagactcagc
z75 -      cgacgctctgactcgaggGGAATGTCTTCCAGTcaagcttggttcagactcagc
s15 -      cgacgctctgactcgaggCGGAATGTCTTCTGCGcaagcttggttcagactcagc
s43 -      gctgagtctgaacaagcttgAAGAATGTCTCGGGCcctcgagtcagagcgctcg
z28 +      gctgagtctgaacaagcttgAAA GAATGTGCGCAGGCcctcgagtcagagcgctcg
s8 -      cgacgctctgactcgaggGGACAATCGAATGTGACaagcttggttcagactcagc
z25 -      cgacgctctgactcgaggGGAATGATATAGCGGACaagcttggttcagactcagc
z37 -      gctgagtctgaacaagcttgGGAATTAAATATGTCCGcctcgagtcagagcgctcg
s18 +      gctgagtctgaacaagcttgGTATTACTCAATTCCCcctcgagtcagagcgctcg
consensus      GNATdw

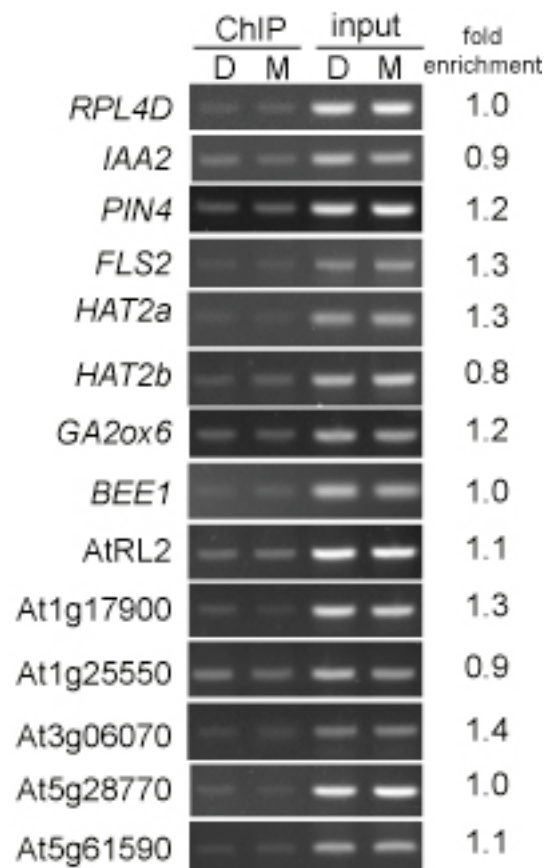
```

Supplementary Figure 1-1. Alignment of 50 sequences obtained from PCR-assisted binding site selection. The DNA sequences of fifty unique clones derived from two independent PCR-assisted binding site selection experiments were manually aligned to identify the consensus DNA binding site. Each oligonucleotide contained at least one instance of GNATDW (where N is any nucleotide, D is A, G, or

T, and W is A or T) and 28 oligonucleotides contained a second potential binding site. S indicates clones from DNA EMSA selection, Z indicates clones from protein EMSA selection; + & - the clone orientation. Consensus GAATAW sites are red and complementary (often overlapping) WTATTC sites are orange except where they overlap with red nucleotides.



Supplementary Figure 1-2: Phenotypes in loss of function mutants and post-translationally activated *KAN-GR* plants. Top row, *kan1-11*, *kan1-11 kan2-5*, wild-type (Col), and *KAN-GR* seeds were germinated and grown for 9 days on media containing mock or DEX supplementation (as indicated). Cotyledons (inset photos, first row) of *kan1-11 kan2-5* are strongly cupped and DEX-treated *KAN1-GR* cotyledons are narrow and pointed in contrast to Col or mock-treated *KAN-GR* seedlings that form normal cotyledons and first leaves. Intermittent DEX application has different effects on morphogenesis of soil-grown *KAN-GR* plants than continuous exposure in media. Whole 14-day old (second row) and 29-day old (third row) rosettes display effects of loss of *kan* function and ectopic expression of *KAN-GR*. Soil-grown DEX-treated *KAN-GR* plants formed leaves with short petioles and asymmetric leaf blades, which were not observed in mock-treated plants. (Bar = 1 cm)



Supplementary Figure 1-3: ChIP on mock- and DEX-treated Col seedlings revealed no enrichment. ChIP was performed on Col seedlings lacking the *KAN-GR* transgene as a control for potential non-specific immunoprecipitation effects. None of the promoter fragments tested showed enrichment in DEX- versus mock-treated Col samples indicating that enrichment depends on the *KAN-GR* transgene. Fold enrichment was calculated as in Fig. 1-4.

References

1. Riechmann, J.L., Heard, J., Martin, G., Reuber, L., Jiang, C., Keddie, J., Adam, L., Pineda, O., Ratcliffe, O.J., Samaha, R.R., et al. (2000). Arabidopsis transcription factors: genome-wide comparative analysis among eukaryotes. *Science* 290, 2105-2110.
2. Imamura, A., Hanaki, N., Nakamura, A., Suzuki, T., Taniguchi, M., Kiba, T., Ueguchi, C., Sugiyama, T., and Mizuno, T. (1999). Compilation and characterization of Arabidopsis thaliana response regulators implicated in His-Asp phosphorelay signal transduction. *Plant Cell Physiology* 40, 733-742.
3. Hosoda, K., Imamura, A., Katoh, E., Hatta, T., Tachiki, M., Yamada, H., Mizuno, T., and Yamazaki, T. (2002). Molecular structure of the GARP family of plant Myb-related DNA binding motifs of the Arabidopsis response regulators. *Plant Cell* 14, 2015-2029.
4. Kerstetter, R.A., Bollman, K., Taylor, R.A., Bomblied, K., and Poethig, R.S. (2001). KANADI regulates organ polarity in Arabidopsis. *Nature* 411, 706-709.
5. Wagner, D., Sablowski, R.W., and Meyerowitz, E.M. (1999). Transcriptional activation of APETALA1 by LEAFY. *Science* 285, 582-584.
6. Pratt, W.B., Galigniana, M.D., Morishima, Y., and Murphy, P.J. (2004). Role of molecular chaperones in steroid receptor action. *Essays Biochem* 40, 41-58.
7. Eshed, Y., Baum, S.F., Perea, J.V., and Bowman, J.L. (2001). Establishment of polarity in lateral organs of plants. *Curr Biol* 11, 1251-1260.
8. Hawker, N.P., and Bowman, J.L. (2004). Roles for Class III HD-Zip and KANADI genes in Arabidopsis root development. *Plant Physiol* 135, 2261-2270.
9. Serrano-Cartagena, J., Robles, P., Ponce, M.R., and Micol, J.L. (1999). Genetic analysis of leaf form mutants from the Arabidopsis Information Service collection. *Mol Gen Genet* 261, 725-739.
10. Friml, J., Benkova, E., Blilou, I., Wisniewska, J., Hamann, T., Ljung, K., Woody, S., Sandberg, G., Scheres, B., Jurgens, G., et al. (2002). AtPIN4 mediates sink-driven auxin gradients and root patterning in Arabidopsis. *Cell* 108, 661-673.
11. Rogg, L.E., and Bartel, B. (2001). Auxin signaling: derepression through regulated proteolysis. *Dev Cell* 1, 595-604.
12. Sawa, S., Ohgishi, M., Goda, H., Higuchi, K., Shimada, Y., Yoshida, S., and Koshida, T. (2002). The HAT2 gene, a member of the HD-Zip gene family, isolated as an auxin inducible gene by DNA microarray screening, affects auxin response in Arabidopsis. *Plant J* 32, 1011-1022.
13. Navarro, L., Zipfel, C., Rowland, O., Keller, I., Robatzek, S., Boller, T., and Jones, J.D. (2004). The transcriptional innate immune response to flg22. Interplay and overlap with Avr gene-dependent defense responses and bacterial pathogenesis. *Plant Physiol* 135, 1113-1128.
14. Wang, H., Caruso, L.V., Downie, A.B., and Perry, S.E. (2004). The embryo MADS domain protein AGAMOUS-Like 15 directly regulates expression of a gene encoding an enzyme involved in gibberellin metabolism. *Plant Cell* 16, 1206-1219.
15. Friedrichsen, D.M., Nemhauser, J., Muramitsu, T., Maloof, J.N., Alonso, J., Ecker, J.R., Furuya, M., and Chory, J. (2002). Three redundant brassinosteroid early response genes encode putative bHLH transcription factors required for normal growth. *Genetics* 162,

- 1445-1456.
16. Baxter, C.E., Costa, M.M., and Coen, E.S. (2007). Diversification and co-option of RAD-like genes in the evolution of floral asymmetry. *Plant J* 52, 105-113.
 17. Lin, W.C., Shuai, B., and Springer, P.S. (2003). The Arabidopsis LATERAL ORGAN BOUNDARIES-domain gene ASYMMETRIC LEAVES2 functions in the repression of KNOX gene expression and in adaxial-abaxial patterning. *Plant Cell* 15, 2241-2252.
 18. Xu, L., Xu, Y., Dong, A., Sun, Y., Pi, L., Xu, Y., and Huang, H. (2003). Novel as1 and as2 defects in leaf adaxial-abaxial polarity reveal the requirement for ASYMMETRIC LEAVES1 and 2 and ERECTA functions in specifying leaf adaxial identity. *Development* 130, 4097-4107.
 19. Iwakawa, H., Ueno, Y., Semiarti, E., Onouchi, H., Kojima, S., Tsukaya, H., Hasebe, M., Soma, T., Ikezaki, M., Machida, C., et al. (2002). The ASYMMETRIC LEAVES2 gene of Arabidopsis thaliana, required for formation of a symmetric flat leaf lamina, encodes a member of a novel family of proteins characterized by cysteine repeats and a leucine zipper. *Plant Cell Physiol* 43, 467-478.
 20. Iwakawa, H., Iwasaki, M., Kojima, S., Ueno, Y., Soma, T., Tanaka, H., Semiarti, E., Machida, Y., and Machida, C. (2007). Expression of the ASYMMETRIC LEAVES2 gene in the adaxial domain of Arabidopsis leaves represses cell proliferation in this domain and is critical for the development of properly expanded leaves. *Plant J* 51, 173-184.
 21. Friml, J. (2003). Auxin transport - shaping the plant. *Curr Opin Plant Biol* 6, 7-12.
 22. Benkova, E., Michniewicz, M., Sauer, M., Teichmann, T., Seifertova, D., Jurgens, G., and Friml, J. (2003). Local, efflux-dependent auxin gradients as a common module for plant organ formation. *Cell* 115, 591-602.
 23. Friml, J., Vieten, A., Sauer, M., Weijers, D., Schwarz, H., Hamann, T., Offringa, R., and Jurgens, G. (2003). Efflux-dependent auxin gradients establish the apical-basal axis of Arabidopsis. *Nature* 426, 147-153.
 24. Reinhardt, D., Pesce, E.R., Stieger, P., Mandel, T., Baltensperger, K., Bennett, M., Traas, J., Friml, J., and Kuhlemeier, C. (2003). Regulation of phyllotaxis by polar auxin transport. *Nature* 426, 255-260.
 25. Leyser, O. (2006). Dynamic integration of auxin transport and signalling. *Curr Biol* 16, R424-433.
 26. Pekker, I., Alvarez, J.P., and Eshed, Y. (2005). Auxin response factors mediate Arabidopsis organ asymmetry via modulation of KANADI activity. *Plant Cell* 17, 2899-2910.
 27. Izhaki, A., and Bowman, J.L. (2007). KANADI and Class III HD-Zip Gene Families Regulate Embryo Patterning and Modulate Auxin Flow during Embryogenesis in Arabidopsis. *Plant Cell* 19, 495-508.
 28. Gray, W.M., Kepinski, S., Rouse, D., Leyser, O., and Estelle, M. (2001). Auxin regulates SCF(TIR1)-dependent degradation of AUX/IAA proteins. *Nature* 414, 271-276.
 29. Rashotte, A.M., Brady, S.R., Reed, R.C., Ante, S.J., and Muday, G.K. (2000). Basipetal auxin transport is required for gravitropism in roots of Arabidopsis. *Plant Physiol* 122, 481-490.
 30. Pitts, R.J., Cernac, A., and Estelle, M. (1998). Auxin and ethylene promote root hair elongation in Arabidopsis. *Plant J* 16, 553-560.

31. Heisler, M.G., Ohno, C., Das, P., Sieber, P., Reddy, G.V., Long, J.A., and Meyerowitz, E.M. (2005). Patterns of auxin transport and gene expression during primordium development revealed by live imaging of the *Arabidopsis* inflorescence meristem. *Curr Biol* 15, 1899-1911.
32. Sussex, I.M. (1955). Morphogenesis in *Solanum tuberosum* L.: Experimental investigation of leaf dorsiventrality and orientation in the juvenile shoot. *Phytomorphology* 5, 286-300.
33. Ha, C.M., Jun, J.H., Nam, H.G., and Fletcher, J.C. (2007). BLADE-ON-PETIOLE 1 and 2 control *Arabidopsis* lateral organ fate through regulation of LOB domain and adaxial-abaxial polarity genes. *Plant Cell* 19, 1809-1825.
34. Bailey, T.L., Williams, N., Mischak, C., and Li, W.W. (2006). MEME: discovering and analyzing DNA and protein sequence motifs. *Nucleic Acids Res* 34, W369-373.
35. Thompson, W., Rouchka, E.C., and Lawrence, C.E. (2003). Gibbs Recursive Sampler: finding transcription factor binding sites. *Nucleic Acids Res* 31, 3580-3585.
36. Gendrel, A.V., Lippman, Z., Yordan, C., Colot, V., and Martienssen, R.A. (2002). Dependence of heterochromatic histone H3 methylation patterns on the *Arabidopsis* gene DDM1. *Science* 297, 1871-1873.
37. Senecoff, J.F., McKinney, E.C., and Meagher, R.B. (1996). De novo purine synthesis in *Arabidopsis thaliana*. II. The PUR7 gene encoding 5'-phosphoribosyl-4-(N-succinocarboxamide)-5-aminoimidazole synthetase is expressed in rapidly dividing tissues. *Plant Physiol* 112, 905-917.

Chapter 1 is based on the following two manuscripts:

1. Huang, T., Harrar, Y., Lin, C., and Kerstetter, R. A. (2008). KANADI1 acts as a transcriptional repressor of genes involved in auxin responses. submitted
2. Gang Wu, Wan-ching Lin, Tengbo Huang, R. S. Poethig, Patricia S. Springer, Randall A. Kerstetter (2008), KANDAI1 regulates adaxial-abaxial polarity in *Arabidopsis* by repressing the transcription of *ASYMMETRIC LEAVES2*. *Proc Natl Acad Sci U S A*. 105: 16392-7

Chapter 1 was written by integrating and reorganizing part of the results in both manuscripts. The original articles and author contributions are stated in the appendices.

Chapter 2

***ARROW1*, a translational regulator that links leaf growth with pattern formation**

Introduction

Growth and pattern formation are two fundamental processes in organogenesis of plants and animals. Proper coordination of growth and patterning determines essential aspects of development such as achieving the correct size and proportions of different functional compartments in an organ [1]. In plants, a typical example demonstrating the correlation between patterning and growth is the interplay of adaxial-abaxial polarity and leaf blade expansion. Leaf polarity is controlled by a complex network involving multiple gene families with mutually antagonistic functions [2]. Simultaneous loss of several members in a family or ectopic expression of an critical gene in this regulatory circuitry often results in reduced leaf blade expansion, sometimes producing a radialized structure, indicating that specification of adaxial-abaxial asymmetry is required for leaf lamina growth [3-7]. Another piece of evidence for this relationship is that several leaf polarity genes are directly implicated in modulating growth-related genes and processes. In *Antirrhinum*, mutations in an adaxial determinant *PHANTASTICA* (*PHAN*) [8, 9] caused upregulation of *CycD3a*, a member of *CycD* family functioning in cell division [10]. In *Arabidopsis*, *ASYMMETRIC LEAVES2* (*AS2*), a LOB domain transcription factor specifying adaxial identity, regulates cell proliferation in the adaxial domain for proper blade

expansion [11]. If we consider the connection between leaf patterning and growth as a two-way route, these instances will contribute to the build-up of one direction of the communication. However, construction of the other bound still lacks solid evidence. One breakthrough finding in this aspect was reported recently that several ribosomal large subunit proteins are influencing leaf polarity by interacting with important polarity genes [12, 13]. Ribosomes are critical translational regulators that play significant roles in cell growth and proliferation [14]. Discovering the specific effect of ribosome proteins in leaf polarity strongly indicates the “growth-to-pattern” direction is active. However, although these studies identified obvious polarity phenotypes when the ribosome subunit proteins were compromised in multiple polarity mutant backgrounds, they didn’t really commit a defined model for the function of ribosomes in leaf pattern formation. So it is still a mystery how this pathway winds up.

In this chapter, I will introduce a novel *Arabidopsis* mutant involved in both leaf polarity and growth. This mutant was dubbed as *ARROW1* (*ARO1*) according to its elliptical and serrated leaf phenotype. I will describe in detail its biological function and significance in connecting growth regulation with leaf pattern formation.

Results

***ARO1* enhances *kan1 kan2* and displays pleiotropic defects in plant development**

The *aro1-1* mutant was identified in a chemical mutagenesis screen of enhancers of *kan1 kan2* double mutant. *kan1 kan2* has up-curling leaves with ectopic outgrowths on the abaxial side [15] (Fig. 2-1). The *aro1-1 kan1 kan2* triple mutant enhances *kan1*

kan2 by producing rosette leaves with reduced blade expansion (Fig. 2-1). This defect becomes more severe as leaf number increases. Leaf 9 of the triple mutant is almost completely radialized indicating a dramatic loss of leaf polarity (Fig. 2-1j). Furthermore, the abaxial outgrowths of the *kan1 kan2* mutant are also repressed by the addition of *aro1-1*. In order to further characterize the triple mutant phenotype, we analyzed the internal structure of the leaf petioles. Transverse section of the midveins of *aro1-1* (Fig. 2-1l) displayed a vascular pattern similar to wild type (Fig. 2-1lk), while *kan1 kan2* had a vascular bundle with partial adaxialization (Fig. 2-1m). However, in the triple mutants, most sections showed a disorganized vascular pattern consisting of very few phloem cells. These cells are surrounded by adjacent xylem tissues, suggesting a remarkable loss of abaxial identity (Fig. 2-1n).

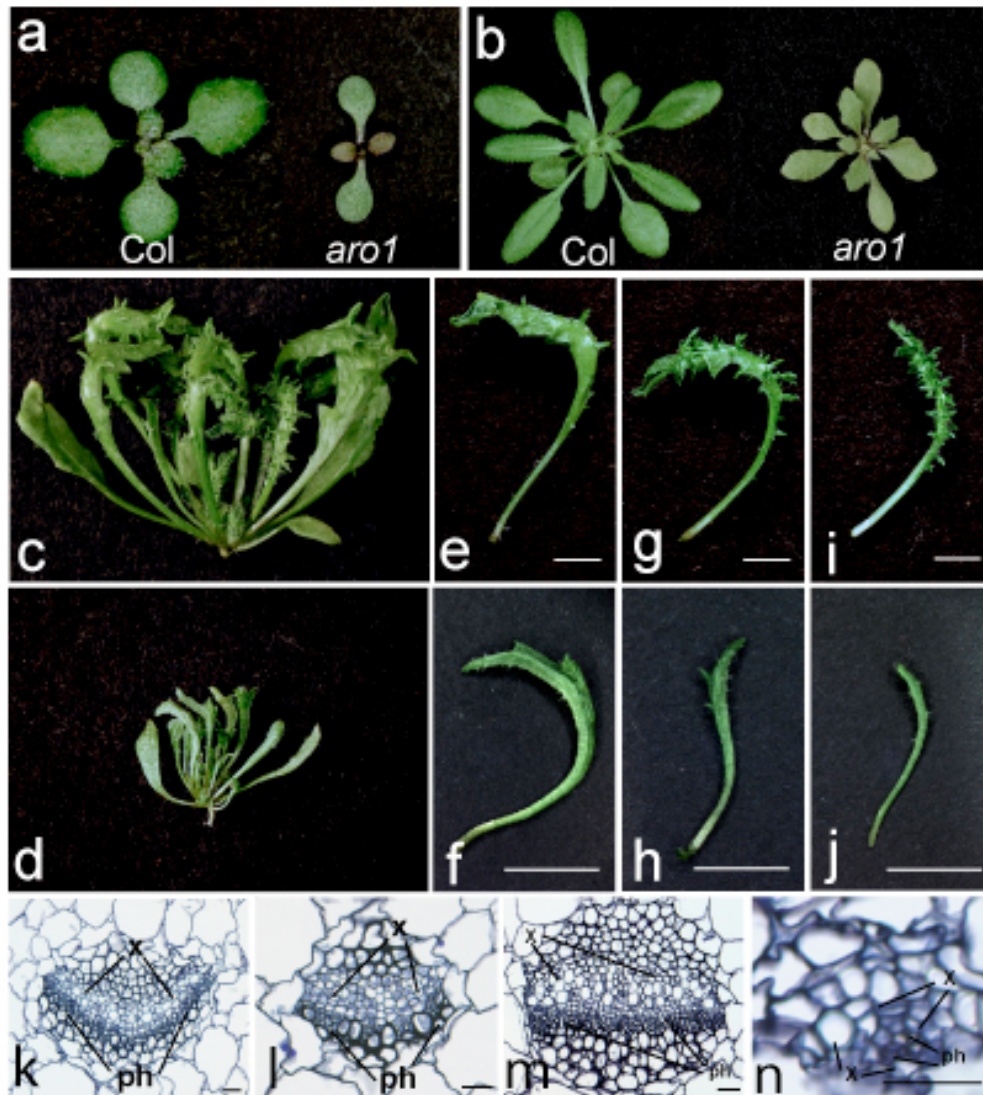


Figure 2-1 *aro1-1* enhances *kan1 kan2* double mutant phenotype. 10-day (a) and 21-day (b) old wild type Col and *aro1-1*, as well as 30-day old *kan1 kan2* (c) and *aro1-1 kan1 kan2* (d) were shown. The individual leaf 5, 7 and 9 of *kan1 kan2* (e,g,i) were compared with those of *aro1-1 kan1 kan2* (f,h,j). Note that the blade expansion and the abaxial outgrowths on *kan1kan2* are highly reduced in the triple mutant. The vascular structure of petiole was examined by paraffin section on Col (k), *aro1-1* (l), *kan1 kan2* (m) and *aro1-1 kan1 kan2* (n). *aro1-1* doesn't show defects in vascular development and *kan1 kan2* has partially adaxialized vein pattern. The adaxialization is more dramatic in the triple mutant indicated by the xylem-surrounding-phloem phenotype. ph, phloem; x, xylem; bar=5mm in e to j and 100μm in k to n.

Enhancement of the *kan1 kan2* phenotype implies the direct involvement of *ARO1* in leaf polarity. We then characterized the single mutant. The *aro1-1* single mutant has elliptical, flat and serrated leaves with a grayish green adaxial side (Fig. 2-1a,b; Fig.

2-2a). The mutant displayed diverse developmental defects including delayed leaf formation (2 days later than wild type, Fig. 2-2c), delayed phase transition from juvenile to adult measured by the appearance of the first abaxial trichomes (on leaf 17 in *aro1-1* versus leaf 5 in wild type Fig. 2-2b), reduced leaf venation complexity (Fig. 2-2e) and late flowering (34 ± 2 days after planting in *aro1-1* and 25 ± 1 days after planting in wild type). Moreover, impaired root growth is also observed in *aro1-1* (4.1 ± 0.1 cm in Col vs. 0.9 ± 0.1 cm in *aro1-1* on the 10th day after planting) and the root cell division zone is significantly shorter than in wild type (Fig. 2-2f). In addition, we investigated the morphology of sub-epidermal mesophylls in *aro1-1* and wild type (Fig. 2-2d). In wild type leaves, adaxial mesophyll cells are round and densely packed, whereas abaxial side consists of irregular cells with large air spaces. In *aro1-1*, both adaxial and abaxial mesophyll cells are fewer but slightly bigger than wild type and the abaxial cells are more regular in shape. Thus, *aro1-1* affected the differentiation of both adaxial and abaxial cells and decreased the dorsiventrality of leaf blade.

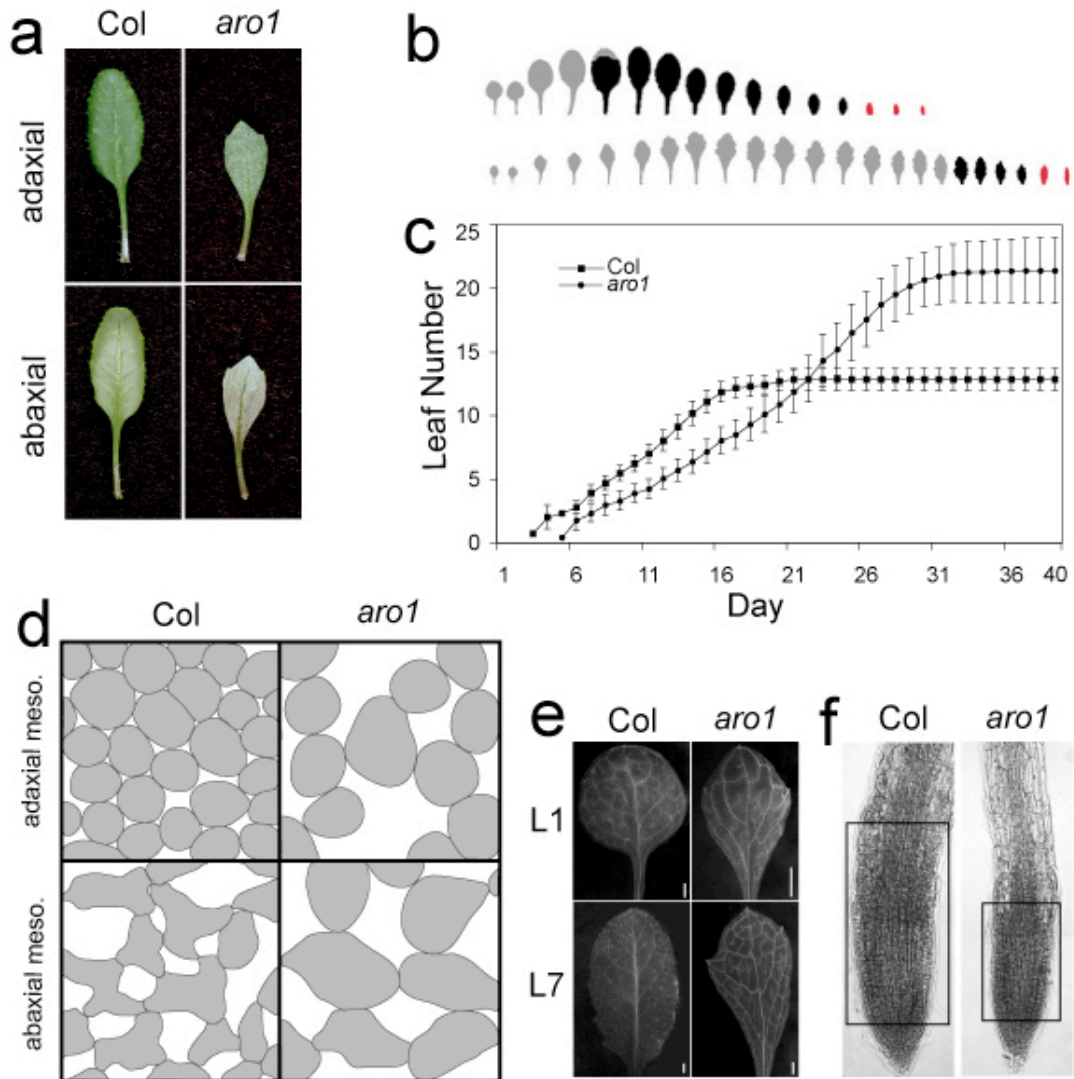


Figure 2-2 *aro1-1* plays pleiotropic roles in plant development. (a) adaxial and abaxial surfaces of leaf 5 of 21-day old Col and *aro1-1* plants. (b) Outline of leaves from Col (upper row) and *aro1-1* (lower row) indicates the delayed transition from juvenile to adult stage. Leaves lacking abaxial trichomes are shown in light gray, leaves with abaxial trichomes in dark gray. Bracts are in red. (c) The rate of leaf initiation in Col and *aro1-1*. The first visible leaf appears 2 days later in *aro1-1* but the leaf production persists longer resulting in more leaves. (d) Camera-lucida drawing of the adaxial and abaxial mesophyll layers of leaf 5 in Col and *aro1-1* illustrates the reduced cell number and polarity in *aro1-1*. (e) Chloral hydrate-cleared leaves of Col and *aro1-1* show reduced complexity of vascular strands in *aro1-1*. Bar=1mm (f) Compared to Col, *aro1-1* roots have shorter cell division zone marked by the black rectangle.

***ARO1* synergistically interacts with genes specifying adaxial identity**

In addition to *kan1 kan2*, we also combined *aro1-1* with other leaf polarity mutants.

Surprisingly, *aro1-1* showed synergistic interactions with mutants affecting adaxial fate, such as *revoluta (rev)*, *asymmetric leaves1 (as1)* and *asymmetric leaves2 (as2)*.

REV belongs to the HD-ZIP III family composed of transcription factors redundantly promoting adaxial identity [3]. Due to the overlapping roles of these genes, *rev* single mutant is not dramatically different from wild type in the vegetative stage (Fig. 2-3a).

However, loss of *ARO1* greatly modified the leaf formation in *rev*. *aro1-1 rev* double mutant produced pin-shaped structures in the center of the rosette after the emergence of several *aro1*-like, but more elongated and narrower leaves (Fig. 2-3b). Petiole sections also confirmed the effect of *aro1-1* on *rev*. Consistent with the morphological phenotype, vascular pattern of *rev* is similar to that of wild type (Fig. 2-5a), whereas in the *aro1-1 rev*, some degree of abaxialization was observed with phloem partially surrounding xylem (Fig. 2-5d). In addition to vegetative growth, *aro1-1* also enhanced the inflorescence defects of *rev*. In contrast to the relatively normal leaf phenotype, *rev* markedly impairs flower development. Inflorescence of *rev* contains both wild type flowers and filamentous structures due to the failure of flower formation [16, 17]. *aro1-1* mutant strongly magnified this defect by producing a completely sterile inflorescence with radial filamentous structures (Fig. 2-4f, g).

Besides HD-ZIP III genes, *ASI* and *AS2* are also critical regulators of adaxial fate. *ASI* is a MYB domain transcription factor closely related to *PHANTASTICA (PHAN)* [8, 9] mentioned above *AS2* interacts with *ASI* [18] and participates in leaf polarity by

antagonizing *KAN* genes (Wu et al., 2008, submitted, Appendix 2). *as1* and *as2* both produce asymmetric, rumpled leaves with ectopic leaflet-like structures on petioles[19-23] (Fig.2-3 d,g). *aro1-1* showed similar interactions with *as1* and *as2*. In contrast to the relatively subtle polarity defects in all 3 single mutants, both double mutants drastically altered the leaf morphology. In these plants, only the first 4-5 leaves are expanded and the subsequent leaves are replaced by radial pin-shaped or branched structures (Fig. 2-3f, i). The expanded leaves are also distinct from single mutants with occasional production of a “trumpet” shape (Fig. 2-3e, h). Internal vasculature of petioles was also analyzed in these mutants. *as1* and *as2* often have slightly abaxialized vein morphology [24](Fig. 2-5b, c). However, in both double mutants, the abaxialization is strikingly enhanced. Midveins of these plants were radialized with phloem surrounding xylem (Fig. 2-5e, f), a typical indication of the complete loss of adaxial identity.

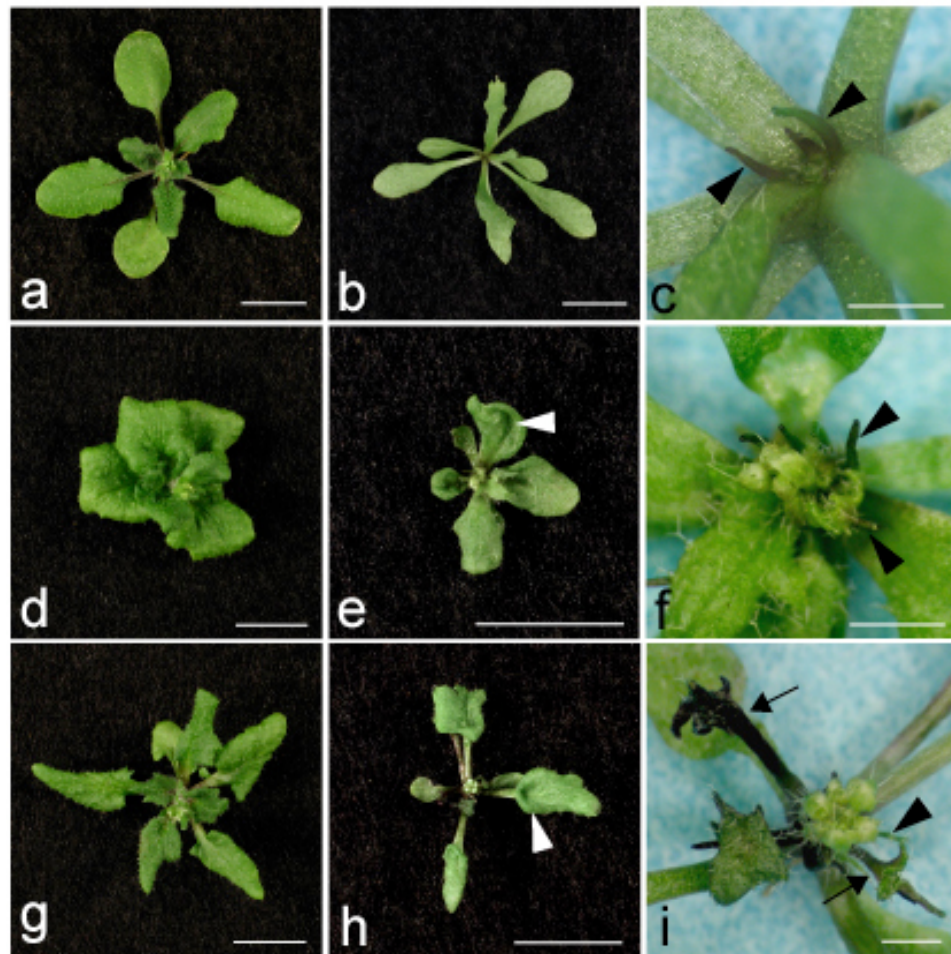


Figure 2-3 *aro1-1* interacts with adaxial polarity mutants. Pictures of 21-day old *rev* (a), *as1-1* (d), *as2-2* (g), *aro1-1 rev* (b), *aro1-1 as1-1* (e) and *aro1-1 as2-2* (h). (c), (f) and (i) are the higher magnification of (b), (e) and (h), respectively. White arrowheads in (e) and (h) indicate the trumpet-shaped leaves in *aro1-1 as1-1* and *aro1-1 as2-2* mutants. Black arrowheads in (c), (f) and (i) show the pin-shaped structures in the double mutants and the black arrows in (i) show the branched radialized structures in *aro1-1 as2-2*. Bar=1mm in (c), (f) and (h) and 1cm in the other pictures.

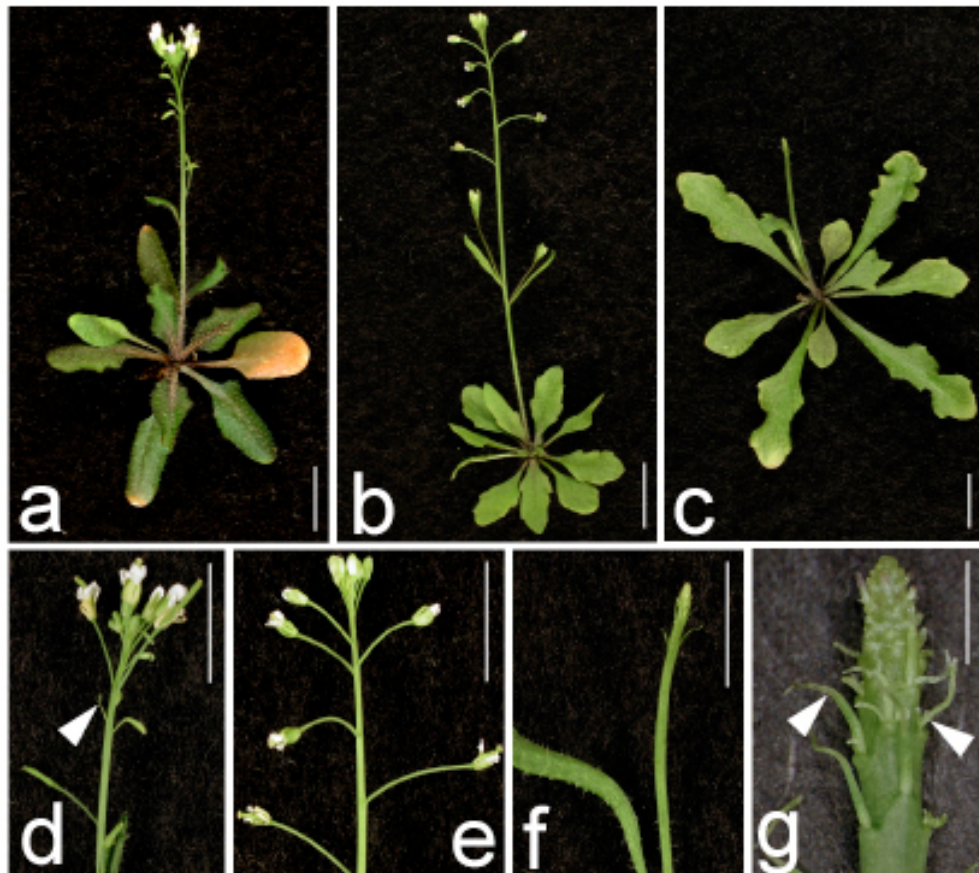


Figure 2-4 *aro1-1* enhances the inflorescence phenotype of *rev*. (a), (b) and (c) are 30-day old *rev aro1-1* and *aro1-1 rev* plants. The inflorescence of each plant is shown in (d), (e) and (f), respectively. (g) is the higher magnification of (f). The white arrowhead in (d) points out the degenerate flower in *rev*. The sterile and filamentous structures in *aro1-1 rev* are indicated by the white arrowheads in (g). Bar=1 cm in (a), (b) and (c); Bar=1 mm in (d), (e) and (f); Bar=100 μ m in (g).

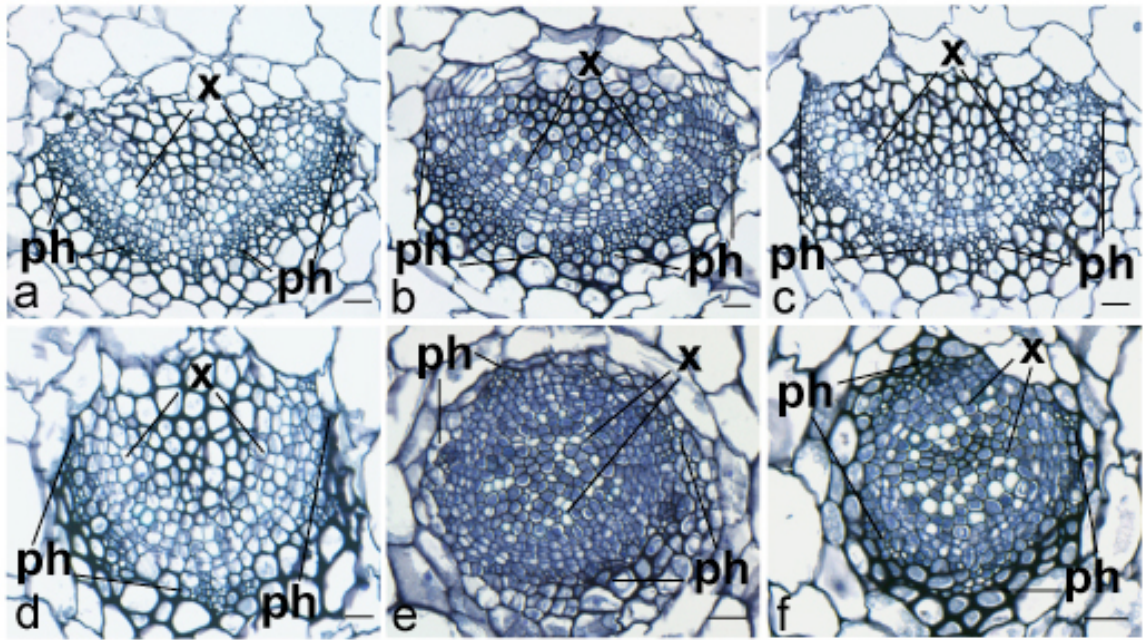


Figure 2-5 Vascular phenotype of leaf petioles in genetic combination of *aro1-1* and adaxial polarity mutants. Transverse sections of leaf petioles in 21-day old *rev* (a), *as1-1* (b), *as2-2* (c), *aro1-1 rev* (d), *aro1-1 as1-1* (e) and *aro1-1 as2-2* (f) display the vascular patterns of these mutants. *aro1-1* synergistically interacts with these adaxial mutants by producing partially or completely abaxialized vascular strands, which is characterized by the phloem-surrounding-xylem phenotype in the double mutants. ph, phloem; x, xylem; Bar=100 μ m

***ARO1* encodes a PUF domain containing protein**

ARO1 maps to a region containing 13 genes at the bottom of chromosome I in the overlap of bacterial artificial chromosome (BACs) T10D10 and T9N14. In the *aro1-1* background, sequencing 6 genes in this region revealed a single nucleotide mutation (G→A) in At1g72320 that disrupts the 3'-splice site of intron 5 in this gene (Fig. 2-6a), which suggests that this lesion may account for the *Aro1*⁻ phenotype. Moreover, we obtained a SAIL T-DNA line that resembled *aro1-1*. I verified that the T-DNA insertion in this line was in the exon 7 of this gene (Fig. 2-6a), which further confirmed that At1g72320 is *ARO1*. The molecular identity of *ARO1* was also proved by transgene complementation. A 6.7kb genomic DNA fragment including the wild

type At1g72320 gene was amplified and cloned into the binary vector pCAMBIA1300. *aro1-1* plants transformed with this plasmid showed wild type phenotype, while plants carrying the empty vector still looked *AroI*⁻ (Fig 2-6b).

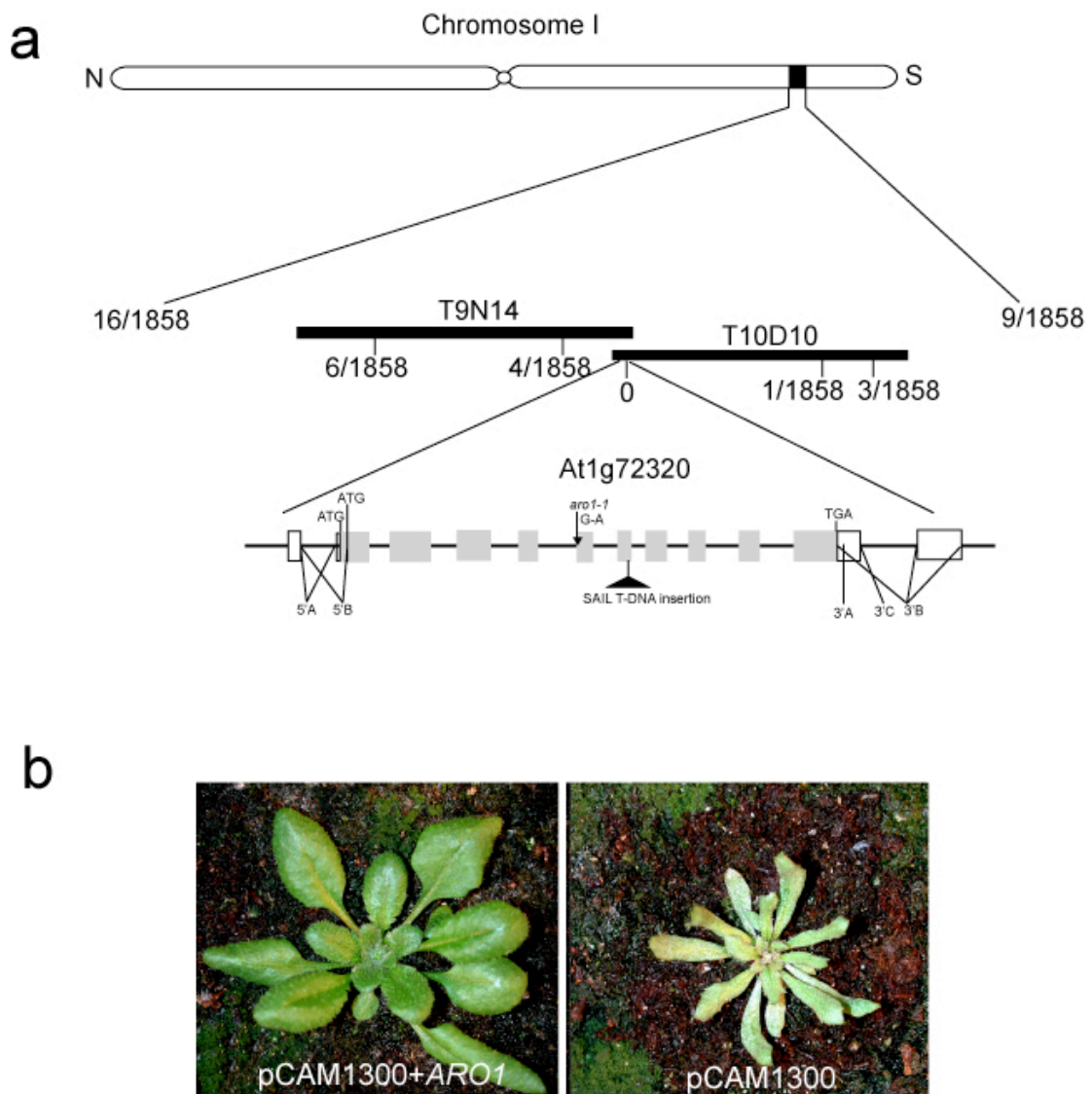


Figure 2-6 Molecular identification *ARO1*. (a) Positional cloning and gene structure of *ARO1*. Two solid black lines are two BACs containing the *ARO1* gene. The recombinant frequency at each molecular marker is shown as number recombination/number chromosome. The genomic structure of *ARO1* (At1g72320) is illustrated with grey solid bars representing exons and black lines representing introns. *ARO1* has 2 non-coding exons at each 5' and 3'-end, which are displayed by hollow bars. The alternative splicing variants at the 5'- and 3'-end are indicated with

5'A, 5'B, 3'A, 3'B and 3'C. The lesion of *aro1-1* and the SAIL T-DNA line that confirmed the molecular identity of *ARO1* are also shown in the graph. **(b)** *ARO1* genomic sequence transformed in *aro1* mutant completely rescued the *AroI*⁻ phenotype (left), whereas transgenic plants with the empty vector still showed *AroI*⁻ phenotype (right).

Gene annotation indicates that *ARO1* contains 10 coding and 2 non-coding exons (one in the 5'-UTR and the other in the 3'-UTR) and has alternative splicing at both 5' and 3' ends (Fig. 2-6a). To study the detailed genomic structure of *ARO1*, RACE (rapid amplification of cDNA ends) assay was performed at 5' and 3' ends of the gene. 5'-RACE revealed two major and 4 minor transcription start sites and two alternative splice sites in the 5' region (Fig. 2-6a). These two splice forms result in two different transcripts, each with a unique translation start site (ATG). 3'-RACE uncovered three distinct mRNA ends, suggesting a complex form of *ARO1* genomic sequence (Fig. 2-6a).

ARO1 (At1g72320) is annotated as a Pumilio/PUF RNA-binding domain containing protein. Computational analysis by PFAM identified 7 PUF repeats in *ARO1*, which proves it is a member of the PUF family [25]. *Drosophila Pumilio* is a founding member of this family and is required for establishment of anterior-posterior polarity[26] and stem cell maintenance[27, 28] through translation inhibition. PUF proteins specifically bind to sequences named nanos response elements (NREs) in the 3'-UTR of target mRNAs[29-31] and usually function in a complex with other RNA-binding proteins such as Nanos (NOS)[32] and Brat[33]. Presence of PUF domains in *ARO1* suggests that *ARO1* may function as a translational regulator in a manner similar to *Pumilio*. In *Arabidopsis*, 26 putative PUF genes have been

predicted by genome database (TAIR 8). However, none of these genes are characterized in detail in terms of their developmental functions. *ARO1* is probably the first functionally described PUF gene in *Arabidopsis*. It can serve as a reference for extensively investigating this gene family in the future.

***ARO1* functions in 18S rRNA biosynthesis by facilitating the cleavage of pre-rRNA**

In order to further study the molecular function of *ARO1*, we performed a comparative assay to search for genes similar to *ARO1* in other model organisms. Computational analysis revealed a unique yeast homolog named *NOP9*. *NOP9* also contains PUF repeats and functions as an essential component of pre-40S ribosomes that is required for the cleavage of 35S pre-rRNA, a critical step for 18S rRNA biosynthesis[34]. To test if *ARO1* functions through the same mechanism, we first performed a yeast complementation experiment. Because null *nop9* mutant is lethal, we employed a heterozygous diploid strain *nop9/+* and transformed it with the yeast *NOP9* genomic DNA and *Arabidopsis ARO1* full length cDNA that were cloned into yeast vector BG1805. We then utilized the Magic Marker technology [35] to select the *nop9* haploid cells carrying the above plasmids after sporulation. Growth test showed that *ARO1* can partially rescue *nop9* defects compared to the full complementation by native *NOP9* gene (Fig. 2-7a), which suggested some level of similarity between these two homologs. Based on the fact that the cleavage of 35S pre-rRNA is conserved in all eukaryotes[36], we directly focused on the function of *ARO1* in this aspect. In

addition, the cleavage site in *Arabidopsis* has been identified in previous studies [37, 38]. We then examined the accumulation of the pre-rRNA in *Arabidopsis* by amplifying this specific site. As we expected, the amount of unprocessed 35S rRNA was 2.1 ± 0.6 fold higher in the *aro1-1* than in wild type (Fig. 2-7b). This result strongly supported that *ARO1* functions in 18S rRNA biosynthesis by facilitating the cleavage of 35S pre-rRNA.

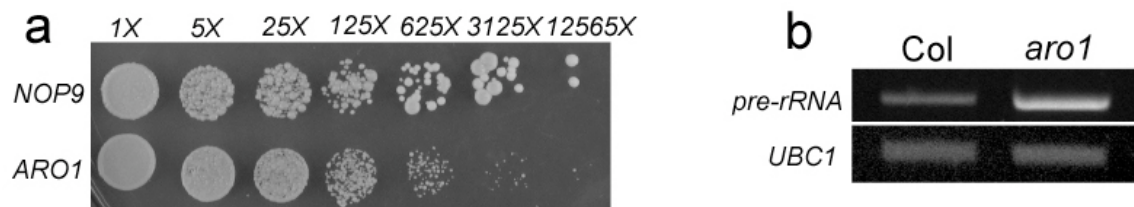


Figure 2-7 *ARO1* functions in 18S rRNA biosynthesis. (a) *ARO1* partially complements its yeast homolog *NOP9*. Haploid *nop9* mutant cells transformed with *NOP9* and *ARO1* are compared after being serially diluted and plated on magic medium [35]. Cells with *ARO1* form smaller colonies than those with native *NOP9*. Folds of dilution are indicated above each column. (b) Enrichment of unprocessed 35S pre-rRNA in *aro1-1* is revealed by semi-quantitative RT-PCR. *UBC1* serves as the loading control.

***aro1-1* displays defective cell division pattern in both leaves and roots**

aro1-1 mutant has fewer cells in the mesophyll and shorter cell division zone in the root, suggesting a reduced activity of cell proliferation. So we looked at the patterns of cell division in both wild type and *aro1-1* using the reporter gene *cycB1::β-glucuronidase* (GUS) with the destruction box [39]. GUS staining showed that the number of the division competent cells was significantly reduced in both leaves and roots of *aro1-1* when plants were 2 days and 4 days after germination (Fig. 2-8 a-f). However, active cell division persisted much longer in the leaves of *aro1-1*

compared to wild type that displayed an obvious basipetal decrease in cell division resulting in the almost absence of GUS expression in leaves 7 days after germination (Fig. 2-8 g, h). Cell proliferation is a critical process in modulating organ growth. The initial inactive but later persistent cell division pattern suggests a delayed overall growth in *aro1-1*, which is consistent with the morphological phenotypes of the mutant.

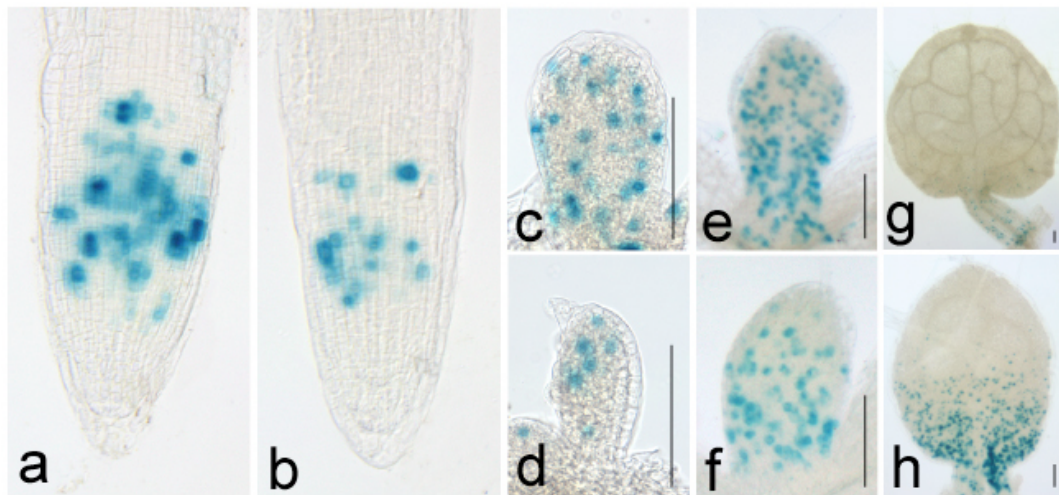


Figure 2-8 Cell division pattern is impaired in *aro1-1* mutant. CycB1: GUS-db expression in 2-day old Col (a) and *aro1-1* (b) roots, as well as the expression in developing leaves. (c),(e),(g) are leaf 2, 4 and 7 of Col and (d), (f), (h) are the corresponding leaves of *aro1-1*. GUS expression was highly reduced in roots and leaves of 2-day old *aro1-1* and kept being lower in leaves on the 4th day compared to Col. However, the GUS activity persists on the 7th day in *aro1-1* when the Col plants almost stopped producing the signal. Bar=100µm

Expression of *ARO1* in plants

ARO1 is differentially expressed in young seedlings, inflorescences, stems and roots as determined by RT-PCR. The relative abundance of *ARO1* mRNA revealed by two internal primers (in exon 6 and 8) is the highest in the seedlings and lowest in the stem with intermediate expression in the inflorescences and roots (Fig. 2-9a). The 5'

and 3' alternative splicing forms were also analyzed with RT-PCR. Both 5' transcripts showed the same pattern as described above. However, two splice forms at the 3' end accumulated the highest in the inflorescences followed by roots, stems and young seedlings. Only one mRNA had the same expression pattern as the 5' end (Fig. 2-9a). The spatial expression pattern of *ARO1* was studied with the whole-mount *in situ* hybridization. In shoots, *ARO1* mRNA was present throughout the vegetative meristem and young organ primordium (Fig. 2-9b). However, in roots, *ARO1* was highly expressed in the cell division zone and absent from the root meristem, which is consistent with its biological function (Fig. 2-9b).

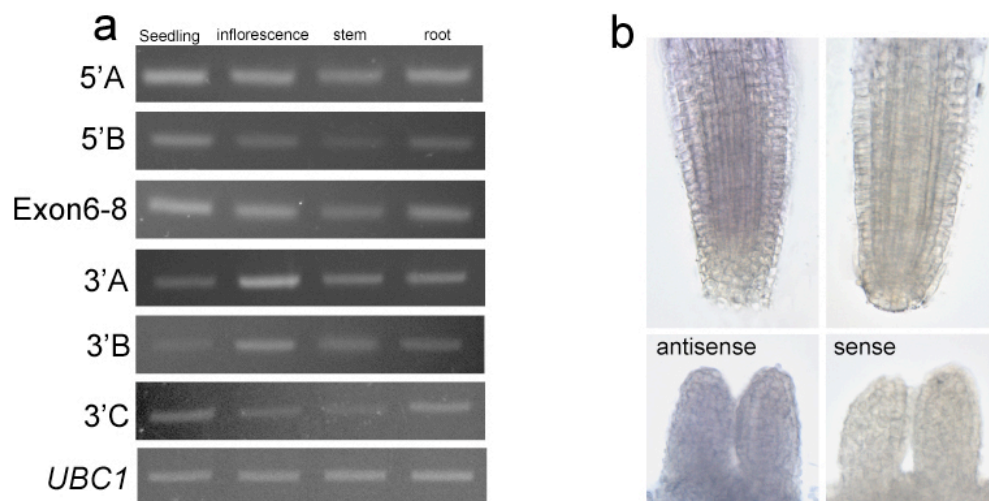


Figure 2-9 Expression pattern of *ARO1* in plants. (a) Accumulation of different splice variants of *ARO1* is revealed by RT-PCR in young seedlings, inflorescences, stems and roots. Two 5' (5'A and 5'B) and three 3' (3'A, 3'B and 3'C) splice forms were analyzed. The location of each splice junction is indicated in Fig. 2-6. An internal region flanking exon 6 and 8 were also amplified to evaluate the overall abundance of *ARO1* mRNA in these tissues. *UBC1* is the same loading control as in Fig. 2-7. (b) Spatial distribution of *ARO1* mRNA was analyzed by whole-mount *in situ* hybridization in both roots and shoots. *ARO1* is strongly expressed in the cell division zone of root and doesn't show polarized expression pattern in the leaf primordia. No hybridization signal was detected in the sense control.

***arol-1* mutant altered the expression timing of critical leaf polarity genes**

The function of *ARO1* in 18S rRNA biosynthesis and the universal localization of its mRNA imply that it unlikely regulates the tissue specific pattern of leaf polarity genes. In addition to the spatial distribution, expression timing is also an important parameter determining the genes' phenotypic output [40]. We then examined the expression of two critical polarity genes, *KAN1* and *AS2*, in time course by using the GUS reporter fused to their promoters. In 1-day old wild type seedlings, *pKAN1:GUS* was expressed in the meristem and abaxial side of young leaf primordia (Fig. 2-10a). GUS activity rapidly decreased in a basipetal fashion. In 5-day old plant, *pKAN1:GUS* was only detected on the petiole and the bottom of leaf (Fig. 2-10b, c). Compared to wild type, *aro1-1* plants showed a similar spatial pattern of *pKAN1:GUS* in the early stage of leaf development (Fig. 2-10d). However, GUS expression persisted much longer in *aro1-1* mutant. GUS activity was still present on the abaxial side of the leaf blade in 5-day old plants (Fig. 2-10e, f) and disappeared until 10 days after germination (data not shown). In contrast, *pAS2:GUS* displayed the same spatial and temporal pattern in both wild type and *aro1-1* seedlings. GUS stain was initially detected in the adaxial domain of leaves (Fig. 2-10 g, i). This expression pattern was maintained in both wild type and *aro1-1* plants on the 5th day after germination (Fig. 2-10h, j) and became undetectable until the 10th day (data not shown). These results indicate that the mutation in *ARO1* has distinct effects on the temporal expression pattern of different genes involved in leaf polarity.

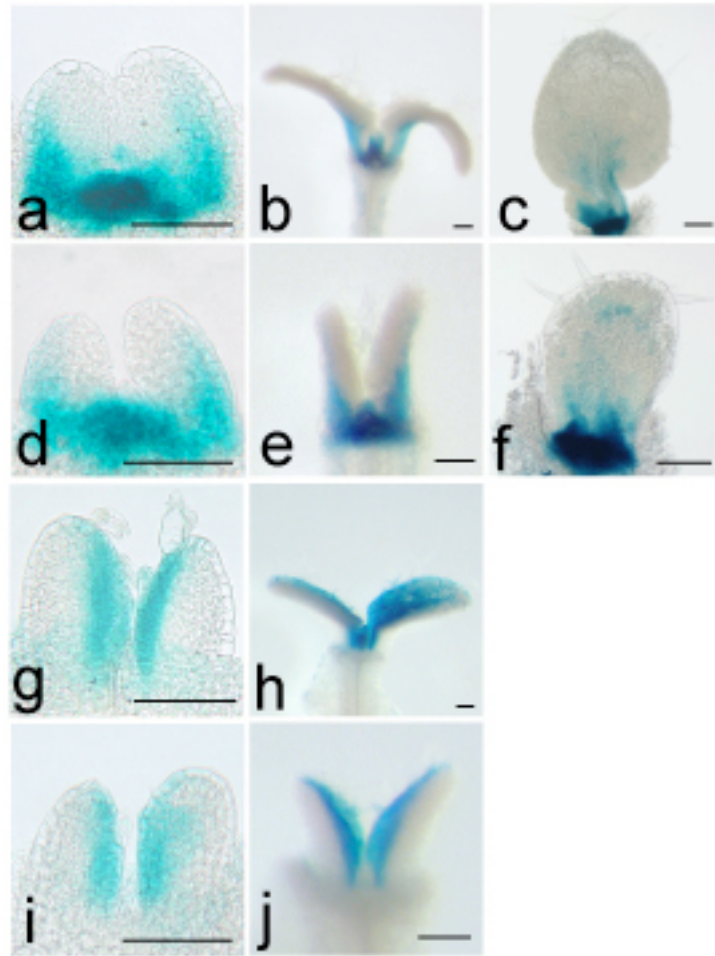


Figure 2-10 *aro1-1* affects temporal expression pattern of *KAN1* and *AS2*. The expression of *pKAN1:GUS* in 1-(**a**, **d**) and 5-day (**b**, **e**) plants after germination. In the early stage GUS stain showed the same pattern in Col (**a**) and *aro1-1*(**d**) and persisted longer in *aro1-1* until 5 days after germination (**e**) when the Col (**b**) has GUS activity restricted to the bottom of the leaf. (**c**) and (**f**) are the abaxial view of the leaf in (**b**) and (**e**), respectively. In contrast, *pAS2:GUS* displayed the same pattern in Col (**g**,**h**) and *aro1-1* (**i**, **j**) on both day1 (**g**,**i**) and day 5 (**h**,**j**) after germination. Bar=50 μ m in (**a**), (**d**), (**g**) and (**i**). Bar=100 μ m in (**b**), (**c**), (**e**), (**f**), (**h**) and (**j**).

Discussion

Defective cell proliferation is responsible for majority of the *aro1-1* mutant phenotypes

The major defect of *aro1-1* mutant at the cellular level is the reduced and prolonged cell proliferation pattern. This defect actually accounts for most of the morphological phenotypes of *aro1-1*. For example, the lower number of mesophyll cells in *aro1-1* is directly due to the impaired cell division, which can probably explain the pale green color of the mutant leaves. These mesophyll cells are also slightly bigger than those in wild type. This phenomenon is termed as “compensation”, a mechanism to coordinate the cell number and cell size in an organ [41]. Another consequence of the reduced cell division is the narrow and flat leaves, which is consistent with the result demonstrated by White that overexpressing a repressor of growth resulted in leaves with reduced curvature and blade expansion [42]. In addition, most root phenotypes, such as decreased length and shorter cell division zone, are all attributed to this reason. In conclusion, change of cell division pattern in *aro1-1* mutant greatly affected the morphology of the plant and retarded the overall growth rate leading to a slow-growing and late-maturing individual.

Function of *ARO1* in leaf polarity suggests a novel mechanism that links leaf growth and patterning

It has been well accepted that patterning directly affects growth in both animals and plants[1, 43]. However, the influence of growth on patterning seems to be largely undefined. Results of this study help to explain this aspect by providing novel

evidence that growth can strongly impact patterning through differential regulation of the expression timing of critical genes. We propose to group leaf polarity genes into two classes: the representative of the first class is *KAN*, whose expression is sensitive to the growth progress. In contrast, the gene expression of the second class is much more stable when growth is delayed and *AS2* is a typical example. Another difference between these two classes is that the second class is expressed longer in development than the first. Since leaf polarity is highly dependent on the antagonistic interactions between adaxial and abaxial promoting genes, the unmatched temporal pattern of *KAN1* and *AS2* implies another type of gene in the first class whose expression follows the early expressed *KAN* genes. Based on this hypothesis, we also divide the first class into early and late expressed genes. Furthermore, we tentatively pick up several candidate genes to fit in these two classes according to their functions and expression patterns. For example, on the adaxial side, HDZIPIII genes [3, 7, 44] are proposed to be the early genes, whose expression precedes the trans-acting RNA gene *TAS3* [45], a possible late genes in the class 1. Among the abaxial promoters, *AUXIN RESPONSE FACTOR 3* and *4* (*ARF3* and *4*) [46] are likely to be the late genes in the first class that follow the *KAN* gene in expression and *YABBY* genes are probably the best candidates for the second class genes [4] [47]. In *aro1-1* mutant, the expression timing of these genes are differentially altered, which may affect the regulatory network in the early stage of leaf development. Specifically, the reduced cell proliferation that prolongs the expression of early genes likely postpones the expression of late genes based on the theory “cell cycle dependent clock”, which

accounts for the phenomenon that cell cycle arrest can result in the failure of late gene expression in a regulatory cascade[48, 49]. In the *aro1-1* mutant, change of expression timing does not directly affect the antagonism of adaxial and abaxial genes in the development, so the defects in leaf polarity are relatively mild. However, altered temporal pattern may reduce the complexity of genes in the network during the early stage, which is a critical period for establishing and maintaining dorsiventral asymmetry. As the consequence, if one important polarity gene is lost, especially the genes expressed in the early stage including the early genes in class I and genes in class II, it will have a significant impact on the leaf morphogenesis. This hypothesis also suggests that mutants of late genes in class I have relatively subtle effects when *ARO1* is compromised, which is consistent with our observation that *ZIPPY2*, *ZIPPY3* and *RNA-DEPENDENT RNA POLYMERASE 6 (RDR6)*, genes involved in ta-siRNA function[45, 50, 51] are additive to *ARO1* when combined (data not shown).

In conclusion, this temporal regulatory mechanism provides a novel view for the interplay of growth and pattern formation. In order to further study this aspect, explicitly demonstrating the expression timing of these candidate genes in both wild type and *aro1-1* should be carried out in the first place. In addition, local expression of growth enhancers or repressors, followed by examining the expression pattern of important genes and investigating the possible targets interacting with these growth regulators, will aid us in more deeply understanding this process. We hope results from these studies can not only explain this fundamental relationship, but also help to generate novel tools in agriculture and horticulture to develop new plants with better

yield and better architecture.

Materials and methods

Plant materials: wild type, *aro1*, *kan1-11* and *kan2-5* plants used in this study were in the Columbia (Col) background. *as2-2* is in the an background. *as1-1* (CS3374) and *rev* (CS3826) were obtained from the Arabidopsis stock center. The *kan2-5* allele was described in the first chapter. All the plants were grown at 22°C under long day (16 hour) illumination. Double mutants *aro1 as2-2*, *aro1 as1-1* and *aro1 rev* were generated by initially crossing two parental lines followed by backcrossing the F1 with both parents. The progeny of the backcross was selected for parental phenotypes. These selected plants were self-pollinated and the double mutants were identified from the next generation by scoring different phenotypes. All the double mutants described in the results showed the same phenotype in both of the final generations from the reciprocal backcrosses and occupied around a quarter of the population, eliminating the interaction of different backgrounds in these genetic crosses. In order to make *aro1 kan1-11 kan2-5* triple mutant, *aro1* was first pollinated with *kan1 kan2*. The F1 then was crossed again by *kan1 kan2*. The progeny was planted out and the individuals displaying the *aro1* phenotype were genotyped for lesions in *kan1-11* and *kan2-5*. *aro1*-like plants homozygous for *kan1-11* and heterozygous for *kan2-5* were kept. In the next generation, the triple mutants were screened by their unique phenotype and about 1/4 ratio in the population.

Anatomical analysis: Petioles of 21-day old plants were fixed in 2% glutaraldehyde

in 25mM sodium phosphate buffer (pH 6.8) with 0.1% triton X-100 over night at 4°C. Samples were washed for 3 times in the same sodium phosphate buffer and dehydrated through an ethanol series. Ethanol was gradually replaced by histoclear in a progression of 2:1, 1:1 and 1:2 mixtures and finally pure histoclear. Paraffin chips were added in the histoclear in 1:1 ratio and incubated in 60 °C overnight. The samples were infiltrated by 100% paraffin 6 times for 8 hours each in 60 °C and finally embedded in wax blocks. 6µm sections were made on a Jung Biocut microtome and stained with 0.1% toluidine blue.

Molecular identification of *ARO1*: *ARO1* was cloned by a map-based approach. *aro1* mutants were first crossed with *L. er* plants. The F2 generation segregating the *aro1* phenotype was used as the mapping population, in which 929 mutant plants were identified. Genomic DNA was isolated from these mutants and applied in the mapping strategy by utilizing InDel and cleaved-amplified polymorphic sequence (CAPS) markers based on the Cereon *L. er*/Col SNP database. These molecular markers localized *ARO1* at the bottom of Chromosome I, in an approximate 17 kb region containing 13 genes. This region lies in the overlap of two BACs T9N14 and T10D10. Sequencing 6 candidate genes revealed a G-to-A change that disrupts the intron splicing in At1g72320. In order to confirm the molecular identity of *ARO1*, a 6.7kb genomic DNA fragment containing the entire *ARO1* gene was released from the BAC T10D10 by restriction digestion with SalI and Acc65I (Fermentas, Hanover, MD) followed by electrophoresis separation and gel purification. The purified fragment was cloned in the binary vector pCAMBIA1300 and transformed into *aro1* mutant

using the floral dip method[52]. A parallel transformation was also performed with the empty vector as a control. The T1 transgenic plants were selected on 1/2 MS medium containing 30mg/L Hygromycin. In addition, a SAIL T-DNA line was also identified with *Aro1*⁻. The T-DNA was verified to insert in At1g72320 by using three-primer PCR with the following primer set: 1G20.f (5'-agactaatgctgaaacaagatgag-3'), 1G20.r (5'-ccaaagtagtaatacaagaaacagc-3') and SAIL.LB1 (5'-gccttttcagaaatggataaatagccttgcttcc-3'). The genomic sequence flanking the T-DNA was amplified and sequenced.

5' and 3' RACE: 5' and 3'RACE were performed according to the manufacturer's protocol (Applied Biosystems, Foster City, CA). In 5'RACE, two primers RA2r (5'-tgaagtctctggatcaatctctttcc-3') and RA1r (5'-cggttaccccttatggctcttcc-3') served as outer and inner gene specific primers, while 3'RACE utilized pE5.f (5'-ctggtgagatgactggaaagaatcggc-3') and pE7.f (5'-gacagagagctgctgagatcg-3') as outer and inner gene specific primers, respectively.

Genetic complementation in yeast: Yeast magic marker *nop9* strain (BY4743) was obtained as a heterozygous diploid knock-out (open biosystems, Huntsville, AL). *ARO1* full-length cDNA was amplified from the BAC clone U09300 with primers GATEARO1N.f (5'-atggtttctgttggttctaaatcattg-3') and GATEARO1N.r (5'-acgtctcaaattctcattttatttgaatgccg-3'). The PCR product was cloned into the pCR8 vector (Invitrogen, Eugene, OR) and subcloned into the yeast expression vector BG1805 (a gift from Dr. Beth Grayhack) containing the GAL1 promoter and URA3 marker by GATEWAY cloning strategy (Invitrogen, Eugene, OR). The resulting

plasmid BG1805-*ARO1*, as well as the wild type *NOP9* gene in the same vector (BG1805-*NOP9*) that was commercially purchased (open biosystems, Huntsville, AL), was transformed into the *nop9*/+ diploid strain. An empty vector was also transformed separately as a control. The transformed cells were sporulated and spread on the magic medium[35] to select haploid cells that survived in the absence of uracine. The transformants were further confirmed by several sets of primers described as follows: NOP9A (5'-gttttcaaacttgctaggtgtatc-3') and NOP9B (5'-ccagttcttctctatctagcacacc3') were used to prove the knock-out of *NOP9* gene in the yeast genome, whereas NOP9A and kanB (5'-ctgcagcgaggagccgtaat-3') functioned to detect the *kanMX* insertion that disrupts *NOP9*. The second pair BNOP9.f (5'-caaaccttcaaataacgaatcaa3'-) and BNOP9.r (5'-agactcttcttgctggatgtgctc-3') confirmed the presence of BG1805-*NOP9* in the haploid cell and the third pair BARO1.f (5'-gcgaagcgatgattttgatctat-3') and BARO1.r (5'-cttctacgcattcccttattct-3') served as a similar tool for the detection of BG1805-*ARO1*.

Haploid cells containing either *NOP9* or *ARO1* were inoculated in the liquid magic medium and grown in 30 °C until OD600 reached 0.6. The culture was serially diluted with 5 times each dilution in sterile water and spotted on the solid magic medium. The plates were incubated in 30 °C for two days and the size and the number of colonies was compared.

RT-PCR: 2 µg total RNA extracted from 10-day old seedlings using TRIzol Reagent (Invitrogen, Eugene, OR) was treated with DNase I (Fermentas, Hanover, MD) then reverse transcribed with 200 units of Superscript III (Invitrogen Eugene, OR). 1µl of a

10-fold dilution was used as template for PCR. In the expression analysis of *ARO1*, primers pE8.f (5'-gcatcctcaaagggtttaacat-3') and pE8.r (5'-cggttacccttatggctcttcc-3'), as well as pE9.f (5'-gcatcctcaaagggtttaacat-3') and pE9.r (5'-cggttacccttatggctcttcc-3'), were used for the two 5' splice variants. The PCR condition is 95°C for 30s, 53°C for 30s, and 72°C for 30 s for 30 cycles. For examining the 3' alternative splicing, primers pE2.f (5'-gcgtcaccgagaaaaacatgc-3'), pE2.r (5'-gccaggagatgaaaggagagtc-3'), together with pE3.f (5'-gcgtcaccgagaaaaacatgc-3'), pE3.r (5'-cacagagatgaggaaaatacagcttga-3') and pE12.f (5'-tgaagcaacagataaaccaaaactagc-3'), pE12.r (5'-tggatgctgtaagctttgctactg-3') were utilized to recognize 3 different splice forms. The PCR condition of all the primers is 95°C for 30s, 57°C for 30s, and 72°C for 30 s for 30 cycles. In addition, an internal pair of primers targeting exon6 and 8, pE11.f (5'-tgaagcaacagataaaccaaaactagc-3') and pE11.r (5'-tggatgctgtaagctttgctactg-3'), were also applied to evaluate the overall expression pattern of all the transcripts. The PCR condition of this pair is 95°C for 30s, 56°C for 30s, and 72°C for 30 s for 30 cycles.

In the experiment to quantitate the unprocessed pre-rRNA in both Col and *aro1-1* plants, the 35S pre-RNA was specifically reconginized by primers U1 (5'-cgtaacgaagatgttcttggc-3') and U2 (5'-atgcgtcccttcataagtc-3'), and primer pair UBC.f (5'-tcaagaggttcagcaaga-3') and UBC.r (5'-ctttgctcaacaacatcacg-3') were employed to amplify an ubiquitin conjugating enzyme gene as the loading control. The PCR condition is 94°C for 15 s, 52°C for 15 s, and 72°C for 30 s for 33 cycles. The DNA band intensity was measured by using KODAK Molecular Imaging

Software 4.0 (Eastman KODAK Company, Rochester, NY). Bands were normalized using Gaussian curve with background subtraction. Mean intensities and standard errors were calculated from at least three independent experiments.

Histology: Transgenic plants containing *pKANI-GUS* and *pAS2-GUS* were constructed as described in the chapter I. GUS staining was performed according to [53] with modifications. Plants were fixed in 80% acetone in -20°C for 20min, then stained with 2mM X-Gluc in 1X GUS buffer (9mM potassium ferrocyanide and potassium ferricyanide) overnight in 30°C. After removing the chlorophyll with ethanol series, the first two leaves were dissected from the shoot and observed under either compound microscope or stereomicroscope.

Whole mount *in situ* hybridization: The whole mount *in situ* was conducted as previously described [54]. using 3- day old plants. In order to make the *ARO1* probe, the *ARO1* cDNA were cloned into pCR8 vector (Invitrogen, Eugene, OR) as described above, but in both forward and reverse orientations. Antisense and sense probes were transcribed with T7 polymerase following the linearization of the plasmid.

References

1. Day, S.J., and Lawrence, P.A. (2000). Measuring dimensions: the regulation of size and shape. *Development* 127, 2977-2987.
2. Kidner, C.A., and Timmermans, M.C. (2007). Mixing and matching pathways in leaf polarity. *Curr Opin Plant Biol* 10, 13-20.
3. Emery, J.F., Floyd, S.K., Alvarez, J., Eshed, Y., Hawker, N.P., Izhaki, A., Baum, S.F., and Bowman, J.L. (2003). Radial patterning of Arabidopsis shoots by class III HD-ZIP and KANADI genes. *Curr Biol* 13, 1768-1774.
4. Eshed, Y., Izhaki, A., Baum, S.F., Floyd, S.K., and Bowman, J.L. (2004). Asymmetric leaf development and blade expansion in Arabidopsis are mediated by KANADI and YABBY activities. *Development* 131, 2997-3006.
5. Kerstetter, R.A., Bollman, K., Taylor, R.A., Bombli, K., and Poethig, R.S. (2001). KANADI regulates organ polarity in Arabidopsis. *Nature* 411, 706-709.
6. McConnell, J.R., and Barton, M.K. (1998). Leaf polarity and meristem formation in Arabidopsis. *Development* 125, 2935-2942.
7. McConnell, J.R., Emery, J., Eshed, Y., Bao, N., Bowman, J., and Barton, M.K. (2001). Role of PHABULOSA and PHAVOLUTA in determining radial patterning in shoots. *Nature* 411, 709-713.
8. Waites, R., and Hudson, A. (1995). *phantastica*: A gene required for dorsoventrality in leaves of *Antirrhinum majus*. *Development* 121, 2143-2154.
9. Waites, R., Selvadurai, H.R., Oliver, I.R., and Hudson, A. (1998). The PHANTASTICA gene encodes a MYB transcription factor involved in growth and dorsoventrality of lateral organs in *Antirrhinum*. *Cell* 93, 779-789.
10. Towers, M.I., Ito, M., Roberts, G., and Doonan, J.H. (2003). Developmental control of the cell cycle. *Cell biology international* 27, 283-285.
11. Iwakawa, H., Iwasaki, M., Kojima, S., Ueno, Y., Soma, T., Tanaka, H., Semiarti, E., Machida, Y., and Machida, C. (2007). Expression of the ASYMMETRIC LEAVES2 gene in the adaxial domain of Arabidopsis leaves represses cell proliferation in this domain and is critical for the development of properly expanded leaves. *Plant J* 51, 173-184.
12. Pinon, V., Etchells, J.P., Rossignol, P., Collier, S.A., Arroyo, J.M., Martienssen, R.A., and Byrne, M.E. (2008). Three PIGGYBACK genes that specifically influence leaf patterning encode ribosomal proteins. *Development* 135, 1315-1324.
13. Yao, Y., Ling, Q., Wang, H., and Huang, H. (2008). Ribosomal proteins promote leaf adaxial identity. *Development* 135, 1325-1334.
14. Mata, J., Marguerat, S., and Bähler, J. (2005). Post-transcriptional control of gene expression: a genome-wide perspective. *Trends Biochem Sci* 30, 506-514.
15. Eshed, Y., Baum, S.F., Perea, J.V., and Bowman, J.L. (2001). Establishment of polarity in lateral organs of plants. *Curr Biol* 11, 1251-1260.
16. Otsuga, D., DeGuzman, B., Prigge, M.J., Drews, G.N., and Clark, S.E. (2001). REVOLUTA regulates meristem initiation at lateral positions. *Plant J* 25, 223-236.
17. Talbert, P.B., Adler, H.T., Parks, D.W., and Comai, L. (1995). The REVOLUTA gene is necessary for apical meristem development and for limiting cell divisions in the leaves and stems of *Arabidopsis thaliana*. *Development* 121, 2723-2735.

18. Xu, L., Yang, L., Pi, L., Liu, Q., Ling, Q., Wang, H., Poethig, R.S., and Huang, H. (2006). Genetic interaction between the AS1-AS2 and RDR6-SGS3-AGO7 pathways for leaf morphogenesis. *Plant Cell Physiol* 47, 853-863.
19. Tsukaya, H., and Uchimiya, H. (1997). Genetic analyses of the formation of the serrated margin of leaf blades in *Arabidopsis*: combination of a mutational analysis of leaf morphogenesis with the characterization of a specific marker gene expressed in hydathodes and stipules. *Mol Gen Genet* 256, 231-238.
20. Byrne, M.E., Barley, R., Curtis, M., Arroyo, J.M., Dunham, M., Hudson, A., and Martienssen, R.A. (2000). Asymmetric leaves1 mediates leaf patterning and stem cell function in *Arabidopsis*. *Nature* 408, 967-971.
21. Ori, N., Eshed, Y., Chuck, G., Bowman, J.L., and Hake, S. (2000). Mechanisms that control knox gene expression in the *Arabidopsis* shoot. *Development* 127, 5523-5532.
22. Semiarti, E., Ueno, Y., Tsukaya, H., Iwakawa, H., Machida, C., and Machida, Y. (2001). The ASYMMETRIC LEAVES2 gene of *Arabidopsis thaliana* regulates formation of a symmetric lamina, establishment of venation and repression of meristem-related homeobox genes in leaves. *Development* 128, 1771-1783.
23. Sun, Y., Zhou, Q., Zhang, W., Fu, Y., and Huang, H. (2002). ASYMMETRIC LEAVES1, an *Arabidopsis* gene that is involved in the control of cell differentiation in leaves. *Planta* 214, 694-702.
24. Ha, C.M., Jun, J.H., Nam, H.G., and Fletcher, J.C. (2007). BLADE-ON-PETIOLE 1 and 2 control *Arabidopsis* lateral organ fate through regulation of LOB domain and adaxial-abaxial polarity genes. *Plant Cell* 19, 1809-1825.
25. Wickens, M., Bernstein, D.S., Kimble, J., and Parker, R. (2002). A PUF family portrait: 3'UTR regulation as a way of life. *Trends Genet* 18, 150-157.
26. Murata, Y., and Wharton, R.P. (1995). Binding of pumilio to maternal hunchback mRNA is required for posterior patterning in *Drosophila* embryos. *Cell* 80, 747-756.
27. Forbes, A., and Lehmann, R. (1998). Nanos and Pumilio have critical roles in the development and function of *Drosophila* germline stem cells. *Development* 125, 679-690.
28. Lin, H., and Spradling, A.C. (1997). A novel group of pumilio mutations affects the asymmetric division of germline stem cells in the *Drosophila* ovary. *Development* 124, 2463-2476.
29. Wang, X., Zamore, P.D., and Hall, T.M. (2001). Crystal structure of a Pumilio homology domain. *Mol Cell* 7, 855-865.
30. White, E.K., Moore-Jarrett, T., and Ruley, H.E. (2001). PUM2, a novel murine puf protein, and its consensus RNA-binding site. *Rna* 7, 1855-1866.
31. Zamore, P.D., Bartel, D.P., Lehmann, R., and Williamson, J.R. (1999). The PUMILIO-RNA interaction: a single RNA-binding domain monomer recognizes a bipartite target sequence. *Biochemistry* 38, 596-604.
32. Sonoda, J., and Wharton, R.P. (1999). Recruitment of Nanos to hunchback mRNA by Pumilio. *Genes Dev* 13, 2704-2712.
33. Sonoda, J., and Wharton, R.P. (2001). *Drosophila* Brain Tumor is a translational repressor. *Genes Dev* 15, 762-773.
34. Thomson, E., Rappsilber, J., and Tollervey, D. (2007). Nop9 is an RNA binding protein present in pre-40S ribosomes and required for 18S rRNA synthesis in yeast. *Rna* 13,

- 2165-2174.
35. Pan, X., Yuan, D.S., Xiang, D., Wang, X., Sookhai-Mahadeo, S., Bader, J.S., Hieter, P., Spencer, F., and Boeke, J.D. (2004). A robust toolkit for functional profiling of the yeast genome. *Mol Cell* 16, 487-496.
 36. Venema, J., and Tollervey, D. (1999). Ribosome synthesis in *Saccharomyces cerevisiae*. *Annu Rev Genet* 33, 261-311.
 37. Saez-Vasquez, J., Caparros-Ruiz, D., Barneche, F., and Echeverria, M. (2004). A plant snoRNP complex containing snoRNAs, fibrillarin, and nucleolin-like proteins is competent for both rRNA gene binding and pre-rRNA processing in vitro. *Mol Cell Biol* 24, 7284-7297.
 38. Shi, D.Q., Liu, J., Xiang, Y.H., Ye, D., Sundaresan, V., and Yang, W.C. (2005). SLOW WALKER1, essential for gametogenesis in *Arabidopsis*, encodes a WD40 protein involved in 18S ribosomal RNA biogenesis. *Plant Cell* 17, 2340-2354.
 39. Harrar, Y., Bellec, Y., Bellini, C., and Faure, J.D. (2003). Hormonal control of cell proliferation requires PASTICCINO genes. *Plant Physiol* 132, 1217-1227.
 40. Fishman, G.I. (1998). Timing is everything in life: conditional transgene expression in the cardiovascular system. *Circulation research* 82, 837-844.
 41. Ferjani, A., Horiguchi, G., Yano, S., and Tsukaya, H. (2007). Analysis of leaf development in *fugu* mutants of *Arabidopsis* reveals three compensation modes that modulate cell expansion in determinate organs. *Plant Physiol* 144, 988-999.
 42. White, D.W. (2006). PEAPOD regulates lamina size and curvature in *Arabidopsis*. *Proc Natl Acad Sci U S A* 103, 13238-13243.
 43. Fleming, A.J. (2006). The co-ordination of cell division, differentiation and morphogenesis in the shoot apical meristem: a perspective. *J Exp Bot* 57, 25-32.
 44. Prigge, M.J., Otsuga, D., Alonso, J.M., Ecker, J.R., Drews, G.N., and Clark, S.E. (2005). Class III homeodomain-leucine zipper gene family members have overlapping, antagonistic, and distinct roles in *Arabidopsis* development. *Plant Cell* 17, 61-76.
 45. Garcia, D., Collier, S.A., Byrne, M.E., and Martienssen, R.A. (2006). Specification of leaf polarity in *Arabidopsis* via the trans-acting siRNA pathway. *Curr Biol* 16, 933-938.
 46. Pekker, I., Alvarez, J.P., and Eshed, Y. (2005). Auxin response factors mediate *Arabidopsis* organ asymmetry via modulation of KANADI activity. *Plant Cell* 17, 2899-2910.
 47. Siegfried, K.R., Eshed, Y., Baum, S.F., Otsuga, D., Drews, G.N., and Bowman, J.L. (1999). Members of the YABBY gene family specify abaxial cell fate in *Arabidopsis*. *Development* 126, 4117-4128.
 48. Isshiki, T., Pearson, B., Holbrook, S., and Doe, C.Q. (2001). *Drosophila* neuroblasts sequentially express transcription factors which specify the temporal identity of their neuronal progeny. *Cell* 106, 511-521.
 49. Weigmann, K., and Lehner, C.F. (1995). Cell fate specification by even-skipped expression in the *Drosophila* nervous system is coupled to cell cycle progression. *Development* 121, 3713-3721.
 50. Hunter, C., Willmann, M.R., Wu, G., Yoshikawa, M., de la Luz Gutierrez-Nava, M., and Poethig, S.R. (2006). Trans-acting siRNA-mediated repression of ETTIN and ARF4 regulates heteroblasty in *Arabidopsis*. *Development* 133, 2973-2981.

51. Yoshikawa, M., Peragine, A., Park, M.Y., and Poethig, R.S. (2005). A pathway for the biogenesis of trans-acting siRNAs in Arabidopsis. *Genes Dev* 19, 2164-2175.
52. Clough, S.J., and Bent, A.F. (1998). Floral dip: a simplified method for Agrobacterium-mediated transformation of Arabidopsis thaliana. *Plant Journal* 16, 735-743.
53. Senecoff, J.F., McKinney, E.C., and Meagher, R.B. (1996). De novo purine synthesis in Arabidopsis thaliana. II. The PUR7 gene encoding 5'-phosphoribosyl-4-(N-succinocarboxamide)-5-aminoimidazole synthetase is expressed in rapidly dividing tissues. *Plant Physiol* 112, 905-917.
54. Hejatko, J., Blilou, I., Brewer, P.B., Friml, J., Scheres, B., and Benkova, E. (2006). In situ hybridization technique for mRNA detection in whole mount Arabidopsis samples. *Nature protocols* 1, 1939-1946.

Chapter 3

A novel selected and amplified binding-sequence (SAAB) approach identified the DNA-binding motif of KANADI1 in *Arabidopsis*

The technique of SAAB is an important approach to study the DNA-binding activity of transcription factors [1]. We describe a novel SAAB method based on the electrophoretic mobility shift assay (EMSA) and PCR-assisted oligonucleotide selection to characterize the DNA-binding specificity of a plant transcription factor KANADI1 (KAN1). This strategy provides a clean, quick and reliable way to identify consensus sequence for DNA-protein interaction.

The DNA-binding domain (DBD) is a common structural feature of transcription factors. [2]. Studying the DNA binding specificity and capacity of the binding domain is essential for elucidating the function of a transcription factor. As a prevailing approach for this purpose, SAAB has been extensively applied in both animal and plant systems. Currently, there are two major types of SAAB. One is EMSA-based random oligonucleotide selection[3, 4],the other is affinity purification-based selection [5, 6]. Both of them utilize oligonucleotides containing random central sequences. These random oligos are incubated with the protein of interest. Oligos bound to the protein are isolated and amplified by PCR. The PCR products are reiteratively re-bound to the protein and re-amplified until the nonspecific-binding oligos no longer contribute a significant fraction. In the final step, PCR products (putative protein-binding oligos) are sequenced to identify the binding site of protein.

The difference between these two methods is the strategy for random oligonucleotide selection. In the former method, DNA-protein complex is recognized by a retarded DNA band in EMSA. Oligos interacting with the protein are isolated from this band. In the latter, DNA-protein complex is pulled down by a ligand immobilized to a solid support (usually sepharose beads). The complex is released from the ligand and protein-binding oligos can be extracted from the elute. Compared to EMSA-based selection, affinity purification-based strategy saves time and labor by avoiding electrophoresis and membrane-blotting in the selection process. It is also much safer without radioactive reactions. However, as a trade for speed and safety, it is potentially less specific due to the non-specific binding of the beads to target DNA. Moreover, this method lacks visible detection of DNA-protein interaction by EMSA, which makes it more vulnerable to random errors during selection. Based on these factors, researchers are seeking alternative techniques to circumvent the disadvantages of both methods. For this purpose, we applied the following strategy in our study to identify the DNA-binding property of KAN1 *in vitro*, and tried to compromise the limiting factors of both methods and provide a more efficient way for SAAB.

In this strategy, we firstly expressed and purified KAN1 DBD protein (a truncated KAN1 protein containing the putative DBD) in *Escherichia.coli* cells because the full-length KAN1 protein proved toxic (data not shown) in bacteria. In order to construct the plasmid incorporating the DNA of KAN1 DBD, PCR was performed on *KAN1* cDNA with two primers, 5'-attcggatccaagatgccgacaaagcgaagc-3' and 5'-aagcgaattccttgtagtggtcttaacagttcg-3'. PCR conditions were 94°C for 20s, 54°C for

20s, 72°C for 15s for 34 cycles. PCR product was digested by BamH1 and EcoR1 and cloned into *E. coli* vector pGEX-2TK (Amersham Biosciences, Piscataway, NJ) where the coding region of KAN1 DBD was fused with a glutathione S-transferase (GST) tag. Plasmid construct pGEX-DBD was transformed into *E.coli* BL21 (DE3) strain. Expression of KAN DBD was induced by 0.1mM IPTG in the transformed cell culture. After IPTG induction, *E.coli* cells were collected and lysed with sonication. After centrifuge, the soluble fraction of cell lysate was utilized for purification using MicroSpin GST Purification Module (Amersham Biosciences, Piscataway, NJ). KAN1 DBD purification was performed according to the manufacture's instruction. This purified protein was analyzed with SDS-PAGE eletrophoresis. A single protein band with proper molecular weight was detected in the gel after Coomassie Blue (Bio-rad, Hercules, CA) staining (data not shown). Before SAAB, proteins were dialyzed in the buffer containing 20mM Tris-HCl, pH 8.0 and 80mM KCl to remove reduced glutathione and treated with 0.07 U DNase I (Fermentas, Hanover, MD) on ice for 1 hour to remove any contaminating *E. coli* DNA followed by EDTA addition to 2 mM to inactivate DNaseI. Pretreated proteins were applied to the *in vitro* DNA binding site selection described in Protocol 1. This protocol was adapted from a random oligo-selection strategy by Hosoda, et.al. [5]

Protocol1 *in vitro* DNA binding site selection of KAN1 DBD

1. Random oligonucleotides synthesis. A mixture of 54-base oligonucleotides in which the middle 16 bases are composed of random sequences with each of the 4 nucleotides at equal molar concentration was synthesized (IDT, Coralville, IA). These

oligos were converted into dsDNA by extending from a primer 5'-cgacgctctgactcgagg-3' binding to their 3'- ends using Klenow fragment (Fermentas, Hanover, MD).

2. DNA and protein interaction. The dsDNA (0.5nmol) was incubated with purified KAN DBD protein (50 pmol) in dialysis buffer for 1 hour at 4°C.

3. EMSA. The mixture of DNA and protein was loaded to 9% native polyacrylamide gel in 0.5× Tris-borate-EDTA (TBE) buffer at 4°C. Two separate gels were performed simultaneously. One gel was stained with 1×SYBR Safe™ (Invitrogen, Eugene, OR) for 30 minutes and viewed under 306nm UV transilluminator equipped in The KODAK Gel Logic 200 Imaging System (Eastman KODAK Company, Rochester, NY) with 535nm WB50 filter to visualize DNA in the shifted DNA-protein complex. The other gel was stained with E-Zinc™ reversible stain kit (Pierce, Rockford, IL) following the procedure provided by the manufacturer and viewed under white light epi-illuminator in the same device described above to visualize protein in the complex. Gel images were captured using KODAK molecular imaging software (version 4.0) (Eastman KODAK Company, Rochester, NY).

4. Isolation of DNA interacting with KAN DBD. The shifted DNA-protein complex in EMSA was excised from the gel and DNA in the complex was purified with phenol/chloroform extraction followed by NaOAc/ethanol precipitation.

5. PCR. Purified DNA was subjected to PCR amplification using a pair of primers binding to the ends of 54-oligos (5'-gctgagtctgaacaagcttg-3' and 5'-cgacgctctgactcgagg-3'). The PCR condition was 94°C for 15s, 54°C for 15s, 72°C

for 15s for 15 cycles. PCR products were precipitated by NaOAc/ethanol method and used in the subsequent selections as described above.

6. Repeat of selection for 5 additional cycles. In two parallel samples, DNA from SYBR Safe™ staining was always used in selection with SYBR Safe™ and the same with E-Zinc™ stain.

7. Cloning of KAN DBD-binding DNA and data analysis. After 6 cycles of selection, the resulting DNA fragments were cloned into pGEM-T Easy (Promega, Madison, WI) and sequenced. Sequence comparison and motif identification utilized web implementations of MEME [7](<http://meme.nbcr.net/meme/intro.html>) and the Gibbs Motif Sampler [8] (<http://bayesweb.wadsworth.org/gibbs/gibbs.html>).

Sequence analysis identified a 6 bp motif GNATA(A/T). This motif was found at least once in each of 50 oligonucleotides and 28 oligonucleotides contained a second binding site (10). The probability matrix for the alignment is shown in Table 3-1. This consensus sequence was subsequently confirmed by gel-shift assay in which KAN1 DBD exhibited higher affinity to this core-binding site than to mutant variants (Huang et al., 2008). Furthermore, statistical analysis of promoter sequences in putative *in vivo* KAN1 targets showed significant enrichment of this motif compared to other unrelated genes (10). These results indicate the biological significance of this *in vitro* binding site for the function of KAN1 in plants.

Table 3-1

	A	C	G	T
1	0	0	78	0
2	48	11	11	8
3	78	0	0	0
4	0	0	0	78
5	62	0	7	9
6	32	0	0	46

Table 3-1:Alignment of oligonucleotides identified in SAAB. The first column displays the position of each nucleotide in the binding motif. In the subsequent columns, the number in each cell shows the actual number of different base pair (A, C, G or T) identified in that position.

In this strategy, we applied two independent methods to detect the DNA-protein complex in EMSA. In both SYBR SafeTM and E-ZincTM staining, a shifted band relative to free DNA or free protein was observed with the same migration distance to the bottom of loading well (Fig. 3-1). Moreover, the KAN1 DBD-binding oligos identified in both methods are strictly consistent. These results suggest that these two staining strategies can serve as two parallel replicates. Although double stain of DNA and protein with non-radioactive dyes is not a novel approach in EMSA, such as the EMSA kit E33075 (Invitrogen, Eugene, OR), applying this strategy to DNA-binding site selection hasn't been reported so far. The SYBR SafeTM stain for DNA has low mutagenicity, which makes it much safer than autoradiography and ethidium bromide (EtBr) stain (<http://probes.invitrogen.com/media/publications/494.pdf>)

Furthermore, it provides greater sensitivity than EtBr and the abundance of DNA

bound to protein can be quantitated. The E-ZincTM stain is a reversible stain technique for protein. The formation of zinc hydroxide on the gel surface produces a semiopaque background which makes protein bands transparent in the gel [9]. The addition of imidazole significantly increases its sensitivity to the level equivalent to silver stain (0.25ng). E-ZincTM stain is rapid (only 15minutes) compared to Coomassie stain and silver stain and there is no requirement for fixation before staining. So all the molecules (DNA and protein) remain active after elution from the gel, which makes it feasible to isolate DNA from the retarded band and use it for subsequent binding to KAN1 DBD protein in our approach.

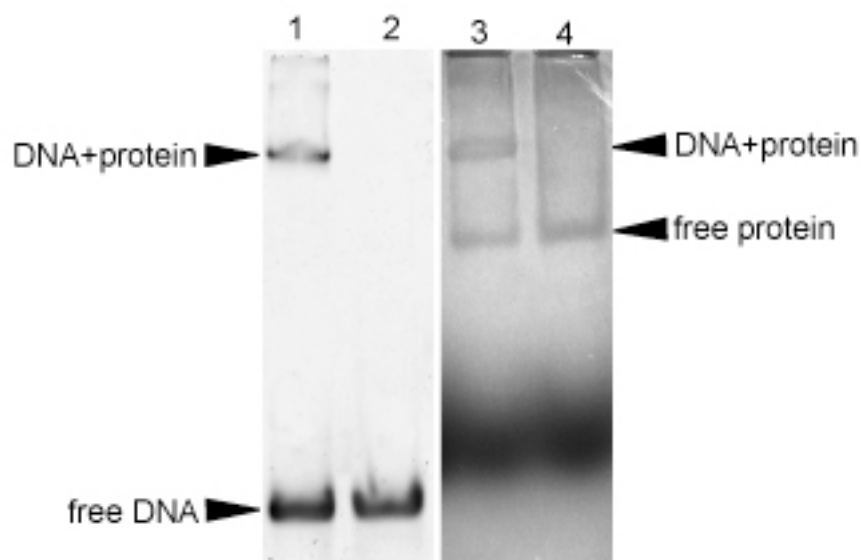


Figure 3-1. EMSA in the oligonucleotide selection step of SAAB. Two parallel staining methods were applied to the samples run in the same gel for the same amount of time. DNA and KAN1 protein mixture (Lane 1), as well as the free DNA (Lane 2) was stained with SYBR SafeTM to visualize the DNA in the gel, whereas the protein detection was also performed on another sample of DNA+KAN1 (Lane 3) and the KAN1 protein (Lane 4) as a replicate. Note that the shifted DNA and protein complex in two different stains migrated the same distance to the bottom of the loading well.

SYBR SafeTM and E-ZincTM utilize two distinct mechanisms to detect DNA and protein interaction. Combination of these two methods provides a reliable pool of

protein-targeting oligos with high specificity. This strategy is more rapid than traditional EMSA-based selection and provides a clean experimental condition by avoiding hazardous reagents. All these features indicate the potential of this modified SAAB to be broadly applicable to identify target sequence of any DNA-binding protein that can be expressed and purified *in vitro*.

References

1. Blackwell, T.K., and Weintraub, H. (1990). Differences and similarities in DNA-binding preferences of MyoD and E2A protein complexes revealed by binding site selection. *Science* 250, 1104-1110.
2. Riechmann, J.L., Heard, J., Martin, G., Reuber, L., Jiang, C., Keddie, J., Adam, L., Pineda, O., Ratcliffe, O.J., Samaha, R.R., et al. (2000). Arabidopsis transcription factors: genome-wide comparative analysis among eukaryotes. *Science* 290, 2105-2110.
3. Tang, W., and Perry, S.E. (2003). Binding site selection for the plant MADS domain protein AGL15: an in vitro and in vivo study. *J Biol Chem* 278, 28154-28159.
4. Viola, I.L., and Gonzalez, D.H. (2006). Interaction of the BELL-like protein ATH1 with DNA: role of homeodomain residue 54 in specifying the different binding properties of BELL and KNOX proteins. *Biol Chem* 387, 31-40.
5. Hosoda, K., Imamura, A., Katoh, E., Hatta, T., Tachiki, M., Yamada, H., Mizuno, T., and Yamazaki, T. (2002). Molecular structure of the GARP family of plant Myb-related DNA binding motifs of the Arabidopsis response regulators. *Plant Cell* 14, 2015-2029.
6. Ghosh, T.K., Packham, E.A., Bonser, A.J., Robinson, T.E., Cross, S.J., and Brook, J.D. (2001). Characterization of the TBX5 binding site and analysis of mutations that cause Holt-Oram syndrome. *Human molecular genetics* 10, 1983-1994.
7. Bailey, T.L., Williams, N., Misleh, C., and Li, W.W. (2006). MEME: discovering and analyzing DNA and protein sequence motifs. *Nucleic Acids Res* 34, W369-373.
8. Thompson, W., Rouchka, E.C., and Lawrence, C.E. (2003). Gibbs Recursive Sampler: finding transcription factor binding sites. *Nucleic Acids Res* 31, 3580-3585.
9. Ortiz, M.L., Calero, M., Fernandez Patron, C., Patron, C.F., Castellanos, L., and Mendez, E. (1992). Imidazole-SDS-Zn reverse staining of proteins in gels containing or not SDS and microsequence of individual unmodified electroblotted proteins. *FEBS Lett* 296, 300-304.
10. Huang, T., Harrar, Y., Lin, C., and Kerstetter, R. A. (2008). KANADI1 acts as a transcriptional repressor of genes involved in auxin responses. submitted

Appendices

Introduction

The appendices are the two manuscripts I submitted and published.

Appendix1 describes the *in vitro* and *in vivo* identification of KAN1 targets. In this manuscript, I demonstrate that KAN1 recognizes the 6 base pair motif GNATA(A/T) *in vitro* and directly regulates genes implicated in auxin responses and gibberellin metabolism *in vivo*. These results indicate important roles of KAN and its interaction with phytohormones in leaf morphogenesis.

Appendix 2 investigates in detail a specific target of KAN1, *AS2*. KAN1 is found to directly bind *AS2* promoter and represses its transcription in abaxial domain of leaves. Disruption of KAN1 binding by a mutation in the *AS2* promoter causes ectopic expression of *AS2* in the abaxial region and results in an adaxialized leaf phenotype. *AS2* is an important transcription factor specifying adaxial identity. This manuscript demonstrates that the interplay of key transcription regulators is critical for establishing leaf polarity.

The second manuscript has been published in *PNAS* in Oct. 2008. The first manuscript has also been submitted for review.

Appendix 1

KANADI1 acts as a transcriptional repressor of genes involved in auxin responses

The formation of leaves and other lateral organs in plants depends on the proper specification of adaxial-abaxial (dorsal-ventral) polarity. Although transcriptional regulators of adaxial-abaxial polarity have been identified (1-6), their targets and the regulatory circuitry by which they operate remain unknown. *KANADI1* (*KAN1*), a member of the GARP family of transcription factors, is a key regulator of abaxial identity and leaf growth in *Arabidopsis* (3, 5, 6). Here, we demonstrate that the Myb-like domain in KAN1 binds the 6 base pair motif GNATA(A/T). In addition, we report that KAN1 acts primarily as a transcriptional repressor and directly regulates genes implicated in auxin responses (*IAA2*, *PIN4*, *FLS2*, and *HAT2*) and gibberellin (GA) metabolism (*AtGA2ox6*). These results are consistent with evidence indicating that auxin transport is disrupted in *kan* mutants (7), and suggest that KAN1 regulates leaf polarity and leaf expansion by modulating responses to auxin and GA.

Genetic studies in *Arabidopsis* indicate that *KANADI* genes (*KAN1* to *KAN4*) have over-lapping functions in the promotion of abaxial fate in lateral organs and peripheral identity in the hypocotyl and stem (3, 5-11). Mutations in any single gene

have relatively mild effects on shoot morphology (3, 8, 11). However, plants lacking several of these genes exhibit conspicuous defects in embryos, lateral organs and vascular patterning that can be attributed to the loss of abaxial or peripheral identity. For example, *kan1 kan2* double mutants have reduced blade expansion and form ectopic leaf-like outgrowths on the abaxial blade surface (5) (Suppl. Fig. A1-2), whereas *kan1 kan2 kan3* triple mutants have almost no blade expansion, and produce nearly unifacial, adaxialized leaves with radialized stem vasculature (6). Mutations in *kan4/aberrant test shape* only produce defects in the polarity and growth of ovule integuments, but in combination with *kan1 kan2* cause significant changes in auxin distribution and produce major defects in embryo patterning (7, 11). Ectopic expression of individual *KAN* genes causes profound abaxialization of lateral organs, disrupted vascular patterning, and a loss of central-peripheral asymmetry in the embryo (3, 5, 6, 9). These complementary loss- and gain-of-function phenotypes indicate that abaxial fate depends on the level and pattern of *KAN* gene expression during organogenesis.

Although other members of the GARP family have been shown to function as transcription factors (12-14), the biochemical function of KAN proteins has not been investigated. To determine if KAN1 binds to DNA, we performed oligonucleotide selection experiments using purified KAN1 protein. The full-length KAN1 protein proved toxic when expressed in *E. coli* (not shown), so we instead generated a recombinant protein consisting of the predicted KAN1 DNA-binding domain (KAN1bd) fused to glutathione-S-transferase (GST). KAN1bd-GST was affinity

purified, and used for EMSA-based PCR-assisted oligonucleotide selection. This experiment produced 50 non-redundant oligonucleotide sequences that contained one or more instances of the partly degenerate 6 bp motif GNATA(T/A), which we termed the KANADI box (KBX) (Fig. A1-1, Supp. Fig. A1-1). To clarify the contributions of individual bases of KBX to KAN1 binding, we performed EMSA with double-stranded oligonucleotides bearing point mutations throughout this sequence. Nucleotides at the first, third, fourth, and sixth positions were critical for high affinity binding *in vitro* (Fig. A1-1). KAN1bd-GST bound equally well to the 6 bp consensus sequence GAATAA and to an 8 bp palindrome, GAATATTC, that appeared in six of the fifty selected sequences (Fig. A1-1, Suppl. Fig. A1-1). In contrast, the protein showed little affinity for the consensus binding site (AGATT) of the GARP protein ARR10 (13) (Fig. A1-1). These results demonstrate that the KAN1 GARP domain selectively binds DNA, and define a novel binding site for this member of the GARP family of transcription factors.

Transgenic plants that constitutively express *KAN1* usually fail to produce a shoot apical meristem and die as seedlings (3, 5). In order to characterize the effects of ectopic KAN1 expression later in shoot development, we produced an inducible form of this protein by fusing the regulatory domain of the rat glucocorticoid receptor (GR) to the C-terminal end of KAN1 (15). Transgenic plants expressing *KAN1-GR* under the regulation of the *CaMV 35S* promoter grew slightly slower than normal, but were otherwise morphologically normal (Fig. A1-2, Suppl. Fig. A1-2). In contrast, *35S:KAN1-GR* (*KAN-GR*) seedlings grown on media containing 1 mM DEX were

striking similar to *35S:KAN1* plants (3, 5, 16); in addition to having narrow cotyledons, the first true leaves of these plants emerged as small, radialized, peg-like structures, and no subsequent leaves were formed (Fig. A1-2, Suppl. Fig. A1-2). These plants also displayed defects in root gravitropism and root hair production (Suppl. Fig. A1-3). In contrast, soil-grown *KAN-GR* plants treated with DEX every other day had relatively mild developmental defects that resembled those seen in *asymmetric leaves 1 (as1)* and *asymmetric leaves 2 (as2)* mutants (17) (Fig. A1-2, Suppl. Fig. A1-2).

To identify *KAN1* target (*KANT*) genes that regulate leaf polarity, we performed a microarray analysis of gene expression in mock- and DEX-treated *KAN-GR* seedlings using the Affymetrix ATH1 GeneChip and RNA isolated from 9-day-old seedlings following 4-hour mock or DEX treatments. After removing loci whose expression was affected by DEX in wild-type controls, we identified 222 loci that displayed at least a 1.8 fold difference ($p < 0.005$, Suppl. Table A1-1) in mock- and DEX-treated *KAN-GR* plants. Of these, 133 loci were down-regulated and 89 were up-regulated. The number of KBX sites in the promoters of these genes was compared to their frequency in all promoters. The sequence GNATA(A/T) or its complement occurs on average 6 times in the upstream 1000 bp of the 31,407 annotated Arabidopsis genes (TAIR 6.0), but appeared an average of 7 times in the promoters of the 222 responsive loci ($p < 0.005$, Table A1). When up- and down-regulated promoters were examined independently, it became apparent that the down-regulated genes possessed, on average, 8 KBX sequences ($p < 0.005$) whereas up-regulated

genes were not significantly different from the genome average (Table A1). This correlation indicates that KAN-GR may function primarily as a transcriptional repressor.

To identify potential direct targets of KAN-GR, microarray analyses were performed in the presence of cycloheximide (CHX), a potent inhibitor of protein synthesis (18, 19). Genes directly regulated by KAN-GR are expected to be insensitive to CHX because protein synthesis is not required for the effect of DEX on KAN-GR activity (19). CHX treatment had a dramatic effect on global gene expression; nearly 1/3 of the transcripts in wild-type seedlings were affected by a 4 hour exposure to CHX (not shown). Genes that showed a significant expression difference ($p < 0.005$) in DEX+CHX vs. mock+CHX seedlings which was in the same direction as in the DEX- vs. mock-treated seedlings were considered to be “direct” targets of KAN-GR. Genes that were differentially expressed in DEX but not DEX+CHX-treated seedlings were considered to be “indirect” targets of KAN-GR. Using these parameters, a majority (61.7%, 82 of 133) of down-regulated loci appeared to be direct targets of KAN-GR, whereas only a minority (24.7%, 22 of 89) of up-regulated genes was in this category (Suppl. Table A1-1). This result also suggests that activated KAN-GR primarily functions as a repressor. Semi-quantitative RT-PCR on independently isolated RNA samples confirmed the microarray results for more than 80% of the 34 down-regulated “direct” target genes tested (Suppl. Fig. A1-4). We also re-examined the expression of the Aux/IAA transcriptional regulator *IAA2* by RT-PCR because KAN genes have been implicated in auxin distribution (7)

and response (10), and *IAA2* expression is sensitive to CHX (20). In contrast to the results of the microarray analysis, we found that *IAA2* was repressed by DEX in the presence of CHX, suggesting that it too is a direct target of KAN-GR (Suppl. Figs. A1-4 & 5). Morphological defects caused by *KAN* overexpression were shown to depend on the function of two specific *AUXIN RESPONSE FACTORS*, *ETTIN/ARF3* and *ARF4* (10). Post-translational regulation of ARF4 activity by IAA2 suggested a possible mechanism linking the effects of *KAN* and *ARF* genes in specifying abaxial fate. In order to determine if *IAA2* is misregulated in *kan1* mutants, we examined *IAA2* expression by quantitative RT-PCR and found that *IAA2* was up-regulated in *kan1* and further up-regulated in *kan1 kan2* mutant seedlings (Suppl. Fig. A1-5). This result indicates that *IAA2* mRNA has a reciprocal relationship with the level of KAN activity, which would be consistent with KAN1 repression of *IAA2*.

To test whether KAN1 binds directly to the promoters of these putative *KANT* genes, we performed chromatin immunoprecipitation (ChIP) assays on *KAN-GR* seedlings using an anti-GR antibody. Because DEX treatment promotes the translocation of GR fusion proteins to the nucleus (21), chromatin fragments bound by KAN-GR are expected to be enriched in DEX-treated relative to mock-treated samples. We were particularly intrigued by the fact that many putative *KANT* genes are transcription factors, or have been implicated in phytohormone signaling or biosynthesis, and therefore chose to focus on these genes. Promoter fragments of *IAA2* and eleven *KANT* genes that we examined were enriched in DEX-treated *KAN-GR* samples (Fig. A1-3), although enrichment was dependent on the specific

fragment tested; for example, only one of two KBX-containing regions of the *HAT2* promoter (*HAT2b*) appeared to be associated with KAN-GR (Fig. A1-3). This result suggests that KBX alone is not sufficient for KAN1 binding. ChIP experiments performed with wild-type plants did not reveal detectable differences between mock- and DEX-treated samples, confirming that the DEX-dependent enrichment of these fragments in *KAN-GR* plants depends on KAN-GR (Suppl. Fig.A1-6). We conclude that most of the genes identified as repressed by DEX both in the presence and absence of CHX in the microarray analysis are direct targets of KAN-GR.

Among these confirmed *KANT* genes are *PIN-FORMED 4 (PIN4)*, an auxin efflux carrier (22), *IAA2*, a negative regulator of AUXIN RESPONSE FACTORS (23), *HAT2*, a homeobox gene that is rapidly and specifically induced by auxin and promotes auxin responses (24), and *FLS2*, a protein which mediates flagellin-induced expression of miR393a, a miRNA that targets the auxin receptor *TIR1* (25). Other phytohormone-related *KANT* genes include the gibberellin catabolism gene *GIBBERELLIN-2 OXIDASE 6 (GA2ox6)* (26) and *BRASSINOSTEROID ENHANCED EXPRESSION 1 (BEE1)*, a bHLH transcription factor that mediates early responses to brassinosteroids (27). Another target of interest is *RADIALIS-LIKE 2 (RL2)*, a putative Myb transcription factor closely related to an *Antirrhinum* gene required for dorsal-ventral asymmetry during flower development (28).

The identity of these *KANI* target genes, and the profound developmental defects associated with either the loss or inappropriate expression of *KANI* and related genes reveal the central role that this gene family plays in the regulation of

plant morphogenesis and growth. We propose that KAN1 may function to enhance auxin accumulation, sensitivity, and signaling on the abaxial side of the initiating leaf primordium, leading to asymmetric changes in gene expression and growth. Specially, we propose that a low concentration of auxin on the adaxial side of the early leaf primordium and higher concentration on the abaxial side leads to changes in gene expression critical for establishing the asymmetry of the primordium. This model is consistent with observations that the auxin efflux protein PIN1 reverses its polarity on the adaxial side of a leaf primordium very early in leaf initiation, thereby depleting this region of auxin (29). This model is also consistent with epidermal ablation studies indicating that adaxial fate depends on continuity between the leaf primordium and the shoot meristem (30). While such experiments have traditionally been interpreted to indicate a “signal” from the meristem is required for adaxial identity, it is plausible that ablation prevents the depletion of auxin from the adaxial side of the primordium, resulting in its abaxialization.

METHODS SUMMARY

Plant materials and treatments: All plants used in this study were in the Columbia (Col) background and were grown at 22°C under long day (16 hour) illumination. The *kan2-5* and *kan2-6* alleles were identified in an EMS mutagenized population homozygous for *kan1-11*. DNA sequencing of PCR products from genomic DNA of the mutant plants revealed that *kan2-5* carries the same nucleotide lesion as *kan2-1* (5) resulting in a stop codon in the first exon and the *kan2-6* allele carries a G to A change

in the 5' splice site of the second intron. The *KAN-GR* construct (31) was transformed into Col plants using the floral dip method (32) and transformants were selected using hygromycin B. A line homozygous for the *KAN-GR* T-DNA that was phenotypically normal in the absence of DEX and showed a strong and consistent response on DEX containing media was selected for all subsequent experiments. For continuous DEX treatments, seeds homozygous for *KAN-GR* were germinated on media containing 1/2X MS salts and 0.8% agar supplemented either with 10 mM DEX or 0.05% ethanol for mock treatment. For intermittent treatment, soil-grown seedlings were painted every second day either with 10 mM DEX or mock (0.05% ethanol) plus 0.015% Silwet L-77. For RNA and chromatin isolation, 9 day old seedlings were grown on 1/2X MS basal medium without sucrose before being submerged for 4 hours with gentle agitation in liquid 1/2X MS plus 1% sucrose containing one or more of the following: 0.05% ethanol (mock), 10 mM DEX, and 10 mM cycloheximide (CHX).

Plasmid Construction: The putative DNA binding domain of KAN1 was amplified from the cDNA clone (3) using the following primers and cycling conditions: 5'-ATTCggatCcAAGATGCCGACAAAGCGAAGC-3' and 5'-AAGCgaattcCTTGTTAGTGGTCTTAACAGTTTCG-3' (lowercase letters represent mismatched bases), 94°C for 20s, 54°C for 20s, 72°C for 15s for 34 cycles. Amplified DNA and the vector pGEX-2TK (Amersham Biosciences, Piscataway, NJ) were digested with BamHI and EcoRI and recombined such that the amino acids 210-280 of KAN1 were fused in-frame with glutathione S-transferase (GST) to form

pGEX-KAN1bd.

Purification of KAN1bd protein: *E.coli* BL21 (DE3) cells carrying pGEX-KAN1bd were grown at 37°C in LB medium to OD₆₀₀ between 0.6-0.8 and harvested 2.5 hours after protein expression was induced with 0.1 mM IPTG. Cell pellets were resuspended and lysed by sonication in 1X PBS at 4°C then centrifuged at 12,000xg for 30 minutes to pellet debris. Soluble recombinant protein was purified using MicroSpin GST Purification Modules (Amersham Biosciences, Piscataway, NJ) according to the manufacturer's instructions. Purified KAN1bd protein was subsequently dialyzed against 20 mM Tris-HCl, pH 8.0 and 80 mM KCl to remove reduced glutathione. Proteins were prepared for EMSA by treating with 0.07 U/ml DNase I (Fermentas, Hanover, MD) on ice for 1 hour to remove contaminating *E. coli* DNA and DNase I was inactivated with 2 mM EDTA.

Electrophoretic mobility shift assay (EMSA): Complementary 54-bp oligonucleotides (Suppl. Table A1-2) containing a KBX or its variants were synthesized (IDT, Coralville, IA), annealed, and 2 pmol of DNA was incubated with 10 pmol of purified protein for 1 hour at 4°C. DNA-protein complexes were resolved on a 9% native polyacrylamide gels in TBE buffer at 4°C and stained with SYBR SafeTM (Invitrogen Corp., Eugene, OR). The fluorescence intensity of each DNA fragment was measured using KODAK Molecular Imaging Software 4.0 (Eastman KODAK Company, Rochester, NY). Bands were normalized using Gaussian curve with background subtraction. Mean fluorescence intensities and standard errors were calculated from at least three independent EMSA experiments.

Microarray analysis: After DEX- or mock treatments, seedlings were frozen in liquid nitrogen. Total RNA was extracted from tissue ground with mortar and pestle using TRIzol Reagent (Invitrogen) followed by subsequent purification using RNeasy Plant Mini Kit (Qiagen). For each genotype and treatment, two independently obtained RNA extracts from plants grown and treated at different times (biological replicates) were labeled and hybridized to ATH1 microarrays at the Transcriptional Profiling Shared Resource of the Cancer Institute of New Jersey (New Brunswick, NJ) with Affymetrix reagents and protocols. Analysis was performed using the Affymetrix Microarray Suite v5 with a median target intensity of 150. Only significant ($p < 0.005$) n -fold changes of at least 1.8 in DEX- versus mock-treated *KAN-GR* samples were reported in Suppl. TableA1-1, although smaller changes were sometimes significant.

ChIP analysis: 9-day-old DEX- or mock-treated *KAN-GR* and wild-type seedlings were harvested, washed with deionized water and crosslinked with 1% formaldehyde. Crosslinking was quenched with 0.125M glycine. Procedures for nuclear extracts and immunoprecipitation were adapted (33) with following modifications: Conditions for sonication of nuclear extracts were empirically determined to obtain an average DNA fragment size of 600bp. Sonication was performed on ice with 4 pulses of 12 seconds with 1 minute pauses at power setting 6 (40% duty cycle, 20% input; Heat System-Ultrasonics, Farmingdale, NY). After chromatin shearing, 10 μ l anti-GR P-20 (Santa Cruz Biotechnology, Santa Cruz, CA) was added to each sample to immunoprecipitate KAN-GR proteins. After reversing crosslinks, DNA was purified by phenol:chloroform extraction, ethanol precipitated, and resuspended in 50 ml TE.

1µl of immunoprecipitated DNA was used in semi-quantitative ChIP PCR. Input DNA was diluted 120 times to achieve PCR product band intensities comparable to ChIP samples. Primers recognizing different regions in the promoters and the control gene RPL4D can be found in Suppl. Table A1-4. PCR conditions were as follows: 33 cycles, 94°C for 30s, 56°C for 30s, and 72°C for 30s. DNA band intensity was measured using the Gaussian Curve method with background subtraction with Molecular Imaging Software 4.0 (Eastman KODAK Company, Rochester, NY). The abundance ratio of promoter fragments in DEX- versus mock-treated ChIP and input samples were normalized by dividing by the ratio of the negative-control gene RPL4D in DEX- or mock-treated samples. The enrichment of each gene in DEX- versus mock-treated samples results from dividing normalized DEX- to mock-treated ChIP ratios by the DEX- to mock-treated input ratios.

Acknowledgements We thank D. Wagner for pBS-GR, G. O. Romero for qPCR analysis on *IAA2*, Curtis Krier and Hao Liu at the Transcriptional Profiling Shared Resource of the Cancer Institute of New Jersey for microarray services. This work was supported by grants from the National Science Foundation (IBN-0343179 to R.A.K.) and Charles and Johanna Busch Foundation to R.A.K., Y.H. and T.H.

Author information. The authors declare no competing financial interests. Correspondence and requests for materials should be addressed to R.A.K (randallk@waksman.rutgers.edu).

References

1. Waites, R., Selvadurai, H. R., Oliver, I. R., & Hudson, A. (1998) The PHANTASTICA gene encodes a MYB transcription factor involved in growth and dorsoventrality of lateral organs in *Antirrhinum*. *Cell* 93, 779-789.
2. Siegfried, K. R., Eshed, Y., Baum, S. F., Otsuga, D., Drews, G. N., & Bowman, J. L. (1999) Members of the YABBY gene family specify abaxial cell fate in *Arabidopsis*. *Development* 126, 4117-4128.
3. Kerstetter, R. A., Bollman, K., Taylor, R. A., Bomblied, K., & Poethig, R. S. (2001) KANADI regulates organ polarity in *Arabidopsis*. *Nature* 411, 706-709.
4. McConnell, J. R., Emery, J., Eshed, Y., Bao, N., Bowman, J., & Barton, M. K. (2001) Role of PHABULOSA and PHAVOLUTA in determining radial patterning in shoots. *Nature* 411, 709-713.
5. Eshed, Y., Baum, S. F., Perea, J. V., & Bowman, J. L. (2001) Establishment of polarity in lateral organs of plants. *Curr Biol* 11, 1251-1260.
6. Eshed, Y., Izhaki, A., Baum, S. F., Floyd, S. K., & Bowman, J. L. (2004) Asymmetric leaf development and blade expansion in *Arabidopsis* are mediated by KANADI and YABBY activities. *Development* 131, 2997-3006.
7. Izhaki, A. & Bowman, J. L. (2007) KANADI and class III HD-Zip gene families regulate embryo patterning and modulate auxin flow during embryogenesis in *Arabidopsis*. *Plant Cell* 19, 495-508.
8. Eshed, Y., Baum, S. F., & Bowman, J. L. (1999) Distinct mechanisms promote polarity establishment in carpels of *Arabidopsis*. *Cell* 99, 199-209.
9. Emery, J. F., Floyd, S. K., Alvarez, J., Eshed, Y., Hawker, N. P., Izhaki, A., Baum, S. F., & Bowman, J. L. (2003) Radial patterning of *Arabidopsis* shoots by class III HD-ZIP and KANADI genes. *Curr Biol* 13, 1768-1774.
10. Pekker, I., Alvarez, J. P., & Eshed, Y. (2005) Auxin response factors mediate *Arabidopsis* organ asymmetry via modulation of KANADI activity. *Plant Cell* 17, 2899-2910.
11. McAbee, J. M., Hill, T. A., Skinner, D. J., Izhaki, A., Hauser, B. A., Meister, R. J., Venugopala Reddy, G., Meyerowitz, E. M., Bowman, J. L., & Gasser, C. S. (2006) ABERRANT TESTA SHAPE encodes a KANADI family member, linking polarity determination to separation and growth of *Arabidopsis* ovule integuments. *Plant J* 46, 522-531.
12. Sakai, H., Aoyama, T., & Oka, A. (2000) *Arabidopsis* ARR1 and ARR2 response regulators operate as transcriptional activators. *Plant J* 24, 703-711.
13. Hosoda, K., Imamura, A., Katoh, E., Hatta, T., Tachiki, M., Yamada, H., Mizuno, T., & Yamazaki, T. (2002) Molecular structure of the GARP family of plant Myb-related DNA binding motifs of the *Arabidopsis* response regulators. *Plant Cell* 14, 2015-2029.
14. Imamura, A., Kiba, T., Tajima, Y., Yamashino, T., & Mizuno, T. (2003) In vivo and in

- vitro characterization of the ARR11 response regulator implicated in the His-to-Asp phosphorelay signal transduction in *Arabidopsis thaliana*. *Plant Cell Physiol* 44, 122-131.
15. Wagner, D., Sablowski, R. W., & Meyerowitz, E. M. (1999) Transcriptional activation of APETALA1 by LEAFY. *Science* 285, 582-584.
 16. Hawker, N. P. & Bowman, J. L. (2004) Roles for Class III HD-Zip and KANADI genes in *Arabidopsis* root development. *Plant Physiol* 135, 2261-2270.
 17. Serrano-Cartagena, J., Robles, P., Ponce, M. R., & Micol, J. L. (1999) Genetic analysis of leaf form mutants from the *Arabidopsis* Information Service collection. *Mol Gen Genet* 261, 725-739.
 18. Abel, S., Nguyen, M. D., & Theologis, A. (1995) The PS-IAA4/5-like family of early auxin-inducible mRNAs in *Arabidopsis thaliana*. *J Mol Biol* 251, 533-549.
 19. Sablowski, R. W. M. & Meyerowitz, E. M. (1998) A homolog of NO APICAL MERISTEM is an immediate target of the floral homeotic genes APETALA3/PISTILLATA. *Cell* 92, 93-103.
 20. Abel, S., Oeller, P. W., & Theologis, A. (1994) Early auxin-induced genes encode short-lived nuclear proteins. *Proc Natl Acad Sci U S A* 91, 326-330.
 21. Pratt, W. B., Galigniana, M. D., Morishima, Y., & Murphy, P. J. (2004) Role of molecular chaperones in steroid receptor action. *Essays in biochemistry* 40, 41-58.
 22. Friml, J., Benkova, E., Blilou, I., Wisniewska, J., Hamann, T., Ljung, K., Woody, S., Sandberg, G., Scheres, B., Jurgens, G., et al. (2002) AtPIN4 mediates sink-driven auxin gradients and root patterning in *Arabidopsis*. *Cell* 108, 661-673.
 23. Rogg, L. E. & Bartel, B. (2001) Auxin signaling: derepression through regulated proteolysis. *Dev Cell* 1, 595-604.
 24. Sawa, S., Ohgishi, M., Goda, H., Higuchi, K., Shimada, Y., Yoshida, S., & Koshiba, T. (2002) The HAT2 gene, a member of the HD-Zip gene family, isolated as an auxin inducible gene by DNA microarray screening, affects auxin response in *Arabidopsis*. *Plant J* 32, 1011-1022.
 25. Navarro, L., Dunoyer, P., Jay, F., Arnold, B., Dharmasiri, N., Estelle, M., Voinnet, O., & Jones, J. D. (2006) A plant miRNA contributes to antibacterial resistance by repressing auxin signaling. *Science* 312, 436-439.
 26. Wang, H., Caruso, L. V., Downie, A. B., & Perry, S. E. (2004) The embryo MADS domain protein AGAMOUS-Like 15 directly regulates expression of a gene encoding an enzyme involved in gibberellin metabolism. *Plant Cell* 16, 1206-1219.
 27. Friedrichsen, D. M., Nemhauser, J., Muramitsu, T., Maloof, J. N., Alonso, J., Ecker, J. R., Furuya, M., & Chory, J. (2002) Three redundant brassinosteroid early response genes encode putative bHLH transcription factors required for normal growth. *Genetics* 162, 1445-1456.
 28. Baxter, C. E., Costa, M. M., & Coen, E. S. (2007) Diversification and co-option of RAD-like genes in the evolution of floral asymmetry. *Plant J* 52, 105-113.

29. Heisler, M. G., Ohno, C., Das, P., Sieber, P., Reddy, G. V., Long, J. A., & Meyerowitz, E. M. (2005) Patterns of auxin transport and gene expression during primordium development revealed by live imaging of the *Arabidopsis* inflorescence meristem. *Curr Biol* 15, 1899-1911.
30. Reinhardt, D., Frenz, M., Mandel, T., & Kuhlemeier, C. (2005) Microsurgical and laser ablation analysis of leaf positioning and dorsoventral patterning in tomato. *Development* 132, 15-26.
31. Wu, G., Lin, W.-c., Huang, T., Poethig, R. S., Springer, P. S., & Kerstetter, R. A. KANADII regulates abaxial-abaxial polarity in *Arabidopsis* by repressing the transcription of *ASYMMETRIC LEAVES 2*. *Proc Natl Acad Sci U S A*. 105: 16392-7
32. Clough, S. J. & Bent, A. F. (1998) Floral dip: a simplified method for *Agrobacterium*-mediated transformation of *Arabidopsis thaliana*. *Plant Journal* 16, 735-743.
33. Gendrel, A. V., Lippman, Z., Yordan, C., Colot, V., & Martienssen, R. A. (2002) Dependence of heterochromatic histone H3 methylation patterns on the *Arabidopsis* gene DDM1. *Science* 297, 1871-1873.
34. Toufighi, K., Brady, S. M., Austin, R., Ly, E., & Provart, N. J. (2005) The Botany Array Resource: e-Northern, Expression Angling, and promoter analyses. *Plant J* 43, 153-163.

Table A1: Enrichment of KBX sites in KAN-responsive promoters

	Loci (Promoters ^a)	GNATA(A/T) sites	Mean (\pm st. dev)	p value ^b
Nuclear genes	(31,128)	180,827	5.8 ± 2.9	
DEX responsive genes	222 (231)	1644	7.1 ± 3.1	9×10^{-12}
Repressed	133 (137)	1059	7.7 ± 3.0	1×10^{-14}
Direct targets	82 (84)	646	7.7 ± 2.9	3×10^{-9}
Indirect targets	38 (39)	287	7.4 ± 3.0	5×10^{-4}
Induced	89 (94)	585	6.2 ± 3.0	0.087
Direct targets	22 (23)	122	5.3 ± 2.4	0.206
Indirect targets	61 (64)	421	6.6 ± 3.1	0.019

^aPromoters (upstream 1,000 bp) of differentially expressed genes were analyzed for the occurrence of KAN1 binding sites using Promomer (34) (<http://bbc.botany.utoronto.ca/>). Some array element loci recognize more than one expressed sequence. The number of promoters represented is indicated in parentheses.

^bStudent's t-Test with 2-tailed distribution

FIGURES

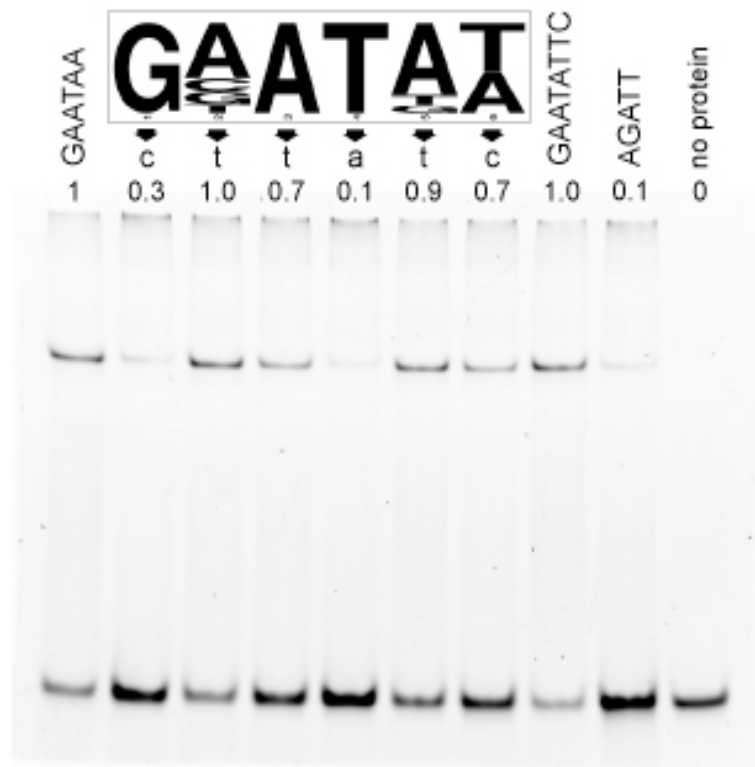


Figure A1-1: EMSA reveals KAN1 DNA-binding characteristics *in vitro*. The *in vitro* KAN1 DNA binding site (KBX, boxed) was identified using affinity purified KAN1db-GST protein in EMSA-based oligonucleotide selection (Suppl. Fig. A1-1). The height of each nucleotide letter is proportional to its representation. Effects of mutating individual sites within the consensus DNA binding site are shown immediately below each position in the consensus KBX site. The mean fraction of bound DNA in three independent replicates was calculated relative to the consensus (GAATAA, lane 1), which was arbitrarily set to 1.0. EMSA of KAN1db-GST bound to a perfect palindrome of KBX (GAATATT, lane 8) was similar to that of that of a single site. The KAN1db-GST showed little affinity for the consensus binding site for the GARP protein ARR10 (AGATT, lane 9) (13).

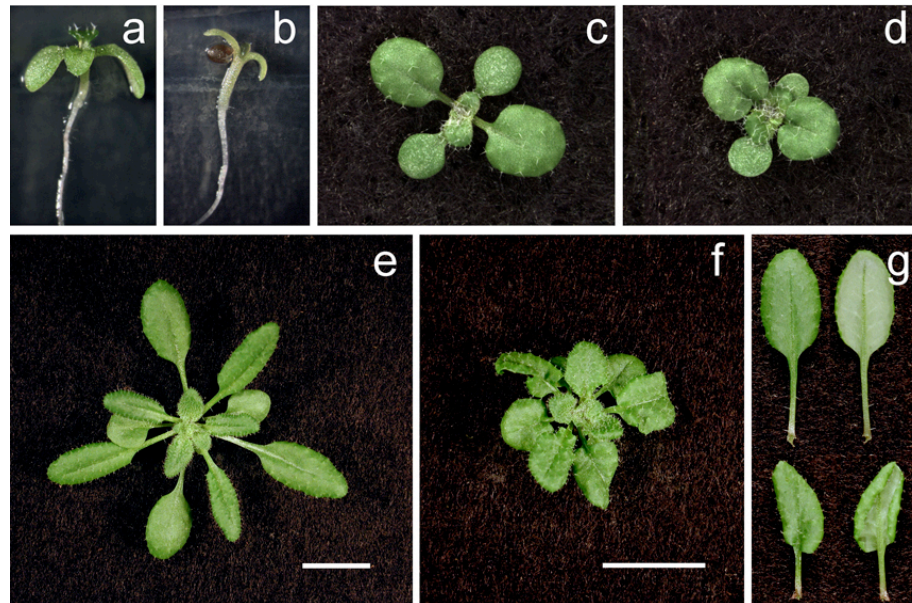


Figure A1-2: Post-translational activation of KAN-GR produces defects in leaf polarity and meristem function. Continuous exposure of *KAN-GR* seedlings to 10 μ M DEX (b) on media for 9 days led to loss of cotyledon blade expansion, formation of partially radialized leaf primordia, and inhibition of further shoot meristem activity consistent with strong *KAN1* overexpression (3, 5). Mock-treated *KAN-GR* seedlings (a) resembled mock- or DEX- treated Col seedlings (Suppl. Fig.A1-2). In contrast, soil grown *KAN-GR* seedlings exposed every other day to 10 μ M DEX (d, and f) displayed reduced petiole and blade expansion with strong epinasty leading to leaves with an asymmetric appearance (g, bottom) that was not evident in mock-treated plants (c, e, and g top). Plants were photographed at 14 (c & d) and 29 days old (e, f, g).

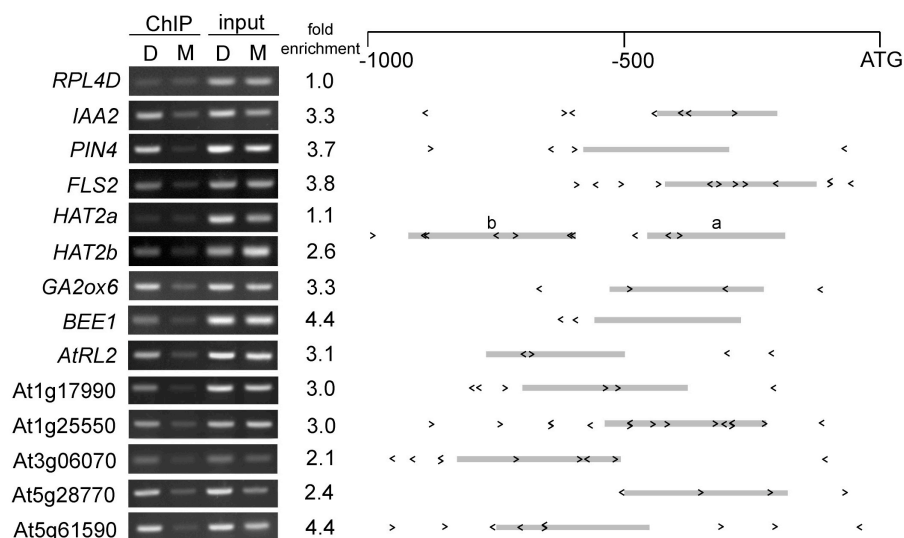


Figure A1-3: Chromatin immunoprecipitation confirms DEX-dependent association of KAN-GR with the promoters of *KANT* genes. Chromatin immunoprecipitation (ChIP) was performed on 9 day old transgenic Arabidopsis

seedlings using antibodies specific for GR. Immunoprecipitated genomic DNA from mock (M) and DEX (D) treated KAN-GR and wild-type control seedlings (Suppl. Fig. A1-6) was amplified with primers specific for the indicated promoters. Fold enrichment was calculated by normalizing PCR product intensities to a negative control, the *RIBOSOMAL PROTEIN L4D (RPL4D)* coding region, followed by calculating the ratio DEX IP/input to mock IP/input. The mean of at least two independent IP experiments with technical replicates is reported as fold-enrichment. Schematics of the gene promoters are shown with the positions and orientations of KBX sites indicated by < or > and the amplified region represented by a grey bar.

SUPPLEMENTARY INFORMATION

SUPPLEMENTARY METHODS

PCR-Assisted *in vitro* DNA binding site selection: KAN1bd DNA binding site selection was performed essentially as described (13). A mixture of 54-base oligonucleotides was synthesized (IDT, Coralville, IA) with the central 16 bases consisting of random sequences. Oligonucleotides were converted into dsDNA using Klenow fragment (Fermentas, Hanover, MD) and primer BSSr (Suppl. Table 2). 2 nmol of dsDNA was incubated with 20 pmol of purified protein in dialysis buffer for 1 hour at 4°C. Sample buffer (2% SDS, 10% glycerol, 60 mM Tris, 5% β-mercaptoethanol and 0.01% bromophenol blue, pH 6.8) was added and the protein/DNA mixture was separated on two identical 9% native polyacrylamide gels in 0.5X Tris-borate-EDTA (TBE) buffer at 4°C for 120 volt hours. One gel was stained with SYBR SafeTM (Invitrogen, Eugene, OR) to visualize DNA in the DNA-protein complex and the other gel was stained with E-ZincTM reversible stain kit (Pierce, Rockford, IL) to visualize protein in the complex. A single band that was retarded relative to free DNA or free protein was excised from the gel and DNA was purified by phenol:chloroform extraction then amplified using primers BSSf and BSSr

(Suppl. Table A1-2). PCR products were precipitated and used in subsequent rounds of oligonucleotide selection. SYBR SafeTM and E-ZincTM visualized EMSA selections were performed independently. After 6 cycles of selection, the resulting DNAs were cloned into pGEM-T Easy (Promega, Madison, WI) and sequenced. Sequence comparison and motif identification were performed using web implementations of MEME (S1) (<http://meme.nbcr.net/meme/intro.html>) and the Gibbs Motif Sampler (S2) (<http://bayesweb.wadsworth.org/gibbs/gibbs.html>).

Reverse transcription PCR: 2 µg total RNA was treated with DNaseI (Fermentas, Hanover, MD) then reverse transcribed into first-strand cDNA using iScript (BioRad, Hercules, CA) in 20 µl reactions. 1 µl of a 10-fold dilution was used as template for PCR. The number of cycles for each primer set was determined empirically. PCRs were repeated at least thrice with independent cDNA synthesis reactions. Quantitative PCR was performed on a Rotor-Gene 3000 (Corbett Life Science, Sydney, Australia) with IQ SYBR Green Supermix (BioRad, Hercules, CA).

SUPPLEMENTARY REFERENCES

- S1. Bailey, T. L., Williams, N., Misleh, C., & Li, W. W. (2006) MEME: discovering and analyzing DNA and protein sequence motifs. *Nucleic Acids Res* **34**, W369-373.
- S2. Thompson, W., Rouchka, E. C., & Lawrence, C. E. (2003) Gibbs Recursive Sampler: finding transcription factor binding sites. *Nucleic Acids Res* **31**, 3580-3585.

SUPPLEMENTAL TABLES

Suppl. Table A1-2: Primers for Oligonucleotide Selection and EMSA

Oligo Name	Sequence (forward strand)
BSSlong	gctgagtctgaacaagcttgNNNNNNNNNNNNNNNNNNcctcgagtcagagcgctcg
BSSr	cgacgctctgactcgagg
BSSf	gctgagtctgaacaagcttg
GS13	gctgagtctgaacaagcttgGGAATAAAAACGTGCCcctcgagtcagagcgctcg
GS15	gctgagtctgaacaagcttgGcAATAAAAACGTGCCcctcgagtcagagcgctcg
GS17	gctgagtctgaacaagcttgGGtATAAAAACGTGCCcctcgagtcagagcgctcg
GS18	gctgagtctgaacaagcttgGGAAtTAAAAACGTGCCcctcgagtcagagcgctcg
GS19	gctgagtctgaacaagcttgGGAaAaaaaACGTGCCcctcgagtcagagcgctcg
GS20	gctgagtctgaacaagcttgGGAATtAAAACGTGCCcctcgagtcagagcgctcg
GS28	gctgagtctgaacaagcttgGGAATAgAAACGTGCCcctcgagtcagagcgctcg
GS21	gctgagtctgaacaagcttgGGAATATTCACGTGCCcctcgagtcagagcgctcg
GS35 (ARR10 binding site)	gctgagtctgaacaagcttgCAATCTAAAACGTGCCcctcgagtcagagcgctcg
GS14	gctgagtctgaacaagcttgGtAATAAAAACGTGCCcctcgagtcagagcgctcg
GS16	gctgagtctgaacaagcttgGaAATAAAAACGTGCCcctcgagtcagagcgctcg
GS29	gctgagtctgaacaagcttgGGAATAcAAACGTGCCcctcgagtcagagcgctcg
GS32	gctgagtctgaacaagcttgGGAATcAAAACGTGCCcctcgagtcagagcgctcg
GS33	gctgagtctgaacaagcttgGGAATgAAAACGTGCCcctcgagtcagagcgctcg

Suppl. Table A1-3: Primers for RT-PCR

Gene	forward	reverse
At1g02400	gtttcggagaacattctgacctca	gccgacatacgtggcttctttg
At1g04240	gaggctgggattaccgggaaca	catccaacaatctgagccttcgag
At1g11210	aggagccggaggtgtgtatgaa	caacggaagcgttgacttgttc
At1g17990	tcccgccattgtcaacgactttag	tgcaaatggcgagagtctgattcc
At1g18400	tgcccgatgttataaggctatgg	ctgcatggaatcaactgcatctgc
At1g21830	cagcctccctaagatattcgcttg	ttgcgcatctaagcgatgact
At1g21910	cctacttcacgacgctctcgt	catcgagcatcgctcgcgagt
At1g22570	cgtggtcgggaactgcctctatac	gaccctctcgctattacctcctcg
At1g23480	ccctgagctccaagttcctaaatgg	cgtcctgcctctagtaacccgatg
At1g24530	atcttctcactcagcgacgtaacc	acggcgagacaagttacaggaagac
At1g25550	tcaccggagtacaccgcgattc	actgccgttggttgatttcacc
At1g35350	ccgcttcttctcctcatggttcta	agtgccttgccctcgttggaagtc
At1g51805	ggagagtcacgtgtgttcgttc	gggtgcacggctcacgtttaagttg
At1g52290	acccgcggttagagaatgattttg	ttcgatctcctgcgttgatcgttg
At1g53870	cggagcaagagaggttcacgatt	cttgattgcgaaaactgatccacga

At1g76520	gcacttgtgatcgggctcattactc	gcaaccaagacgccgataataactgg
At2g01420	ccggtacgggtgtttcaactaaacc	ggcgcatatgtgtccgtgtgt
At2g21650	gcacaatgttgctagagctgttg	ttgcttctgtctactgcagctt
At2g39380	agatgaacacaacaaccacgcagt	ttgcagcgtagcttctgagtttg
At3g04210	tgcctgaatgagttggcactga	ccatcccaactaagtcgctgaaatc
At3g06070	tctcttccagggtttgttcagagg	gggataaaggaaaccgatgaatctcc
At3g19850	gggggtttacgatgtggatttggga	tctcgggatgatagtttcggatgag
At3g22420	gacgtgtaggctaacggcattgg	gccgtctcaaaccgggaagtaaatgt
At3g23030	gcaatggcgtagagaaagtaaac	gtcaaaactccgatccgaatcaaacc
At4g17460	tccgcagttctcgaagacactttc	ccgccgattctcttccgttaatttc
At4g18010	ttatggattgccggaagatttggg	ttgtggccggaagttaagtgtgag
At4g30270	aaccgccaatttccacattactca	cctcatcggtgttcttggaaac
At5g02760	gaatcagggccgcttacattcaac	cctaccctcggacgcaaactct
At5g11000	atccagaagcagaggaggttgtg	cgaatcgaagacgacgaagaact
At5g14120	ccgagctcgtgtcagggacta	gggccatccgtacgcaaagaatatg
At5g20250	gcgattgtttgtcgtgatcct	ctcgtgctcacggattttgagtg
At5g28770	tactggtcggtaaatggaatgacg	tgctcatcattggtgtagcttggga
At5g46330	ctcacgtaagcgattttggaactgc	ctcacgtaagcgattttggaactgc
At5g47370	agactcccatggaacaaacattcg	ctctcccgtaatggtgcttga
At5g59080	aaacatgggtcacaagctcaacgta	gggttctgtccattagcgtcgtc
At5g61590	tgatattgatgctgcaagggtta	ttgttctccttgaggtgtgga
At5g62280	ggtctgctgagaatgctactaaagc	gcgattagtgcacgagtagtgcg
At5g62570	tggaaagcatctagcaggcatca	cacgggaagcgtatagattgttaag
ubc/At5g25760	ctgagccggacagtctcttaactg	cggcgaggcgtgtatacatttgg

Suppl. Table A1-4: Primers for Chromatin Immunoprecipitation

Gene	left primer	right primer
<i>RPL4D/At5g02870</i>	tgtgtttgtcattactgtgctatgc	ataaagctggcggttcgagt
<i>IAA2/At3g23030</i>	cgggtcggccgatagaat	tcggaagcatgaaaggcaag
<i>PIN4/At2g01420</i>	aacgggtccaacagtggcttg	gttttctggaggacgtgga
<i>FLS2/At5g46330</i>	cgtcaaaaactaaatcggaaa	agggatcatgtcacggatgt
<i>HAT2a/At5g47370</i>	ttggccatcttattgttttggga	tggtaatgaagaagagaggggatt
<i>HAT2b/At5g47370</i>	tgttttgtaccaaccactccaatta	tggataacgcaatttgcactactt
<i>GA2ox6/At1g02400</i>	ggttaggcaagaatgttgacaataaa	catcctacaaatcgcgtaagggtg
<i>BEE1/At1g18400</i>	gcattggccatttgaagtt	tggtcgtgggttcattagg
<i>AtRL2/At2g21650</i>	ttgatattggtttcatggcagaga	acgtgctcgcggaaaattac
<i>At1g17990</i>	gaaatggggtgagacagagatgat	aagacgtgcacaaatgcttaagggt
<i>At1g25550</i>	ttttctggttacatatcttgattccaa	cggattttacttgggaaagggttag
<i>At3g06070</i>	ttttaatggatgcgaatgcaaat	ggaattcctaactacttatccaatga
<i>At5g28770</i>	cgttgtaactgtaggcgaatctca	taatggccccgacaagagtc
<i>At5g61590</i>	caagacaacctacaagacaagca	cacaaacaaaacaaaaagacttg

SUPPLEMENTARY FIGURES

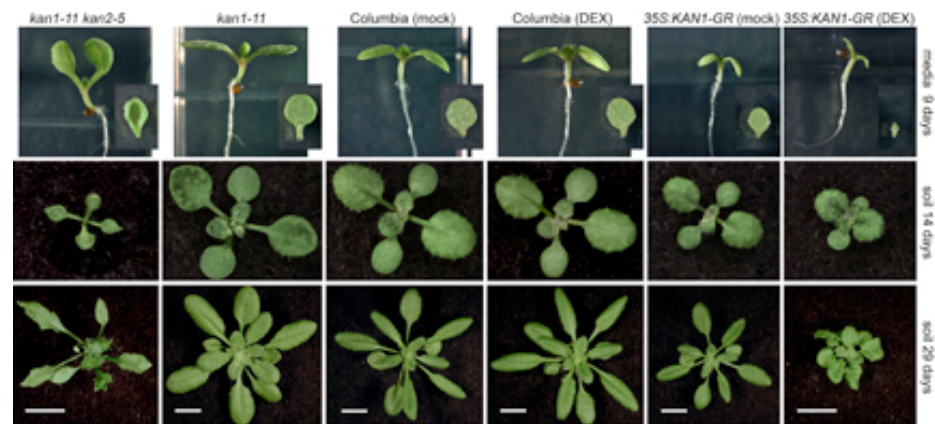
```

s61 - gctgagtcctgaacaagcttgACGGTGGGAATATTCcctcgagtcagagcgctcg
s11 +      cgacgctctgactcgaggGAATATTCGCTAGCcaagcttggttcagactcagc
s51 -      gctgagtcctgaacaagcttgAGGAATATTCGTCGCCcctcgagtcagagcgctcg
z41 +      gctgagtcctgaacaagcttgGGAATATTCCTCACAGCctcgagtcagagcgctcg
z32 -      gctgagtcctgaacaagcttgGCGGAATATTCGTGACCcctcgagtcagagcgctcg
s12 +      cgacgctctgactcgaggGGGGAATATTCGTGCGcaagcttggttcagactcagc
z40 +      cgacgctctgactcgaggGAATATACCTGCCCTcaagcttggttcagactcagc
s62 -      gctgagtcctgaacaagcttgGGGAGGAATATACGGCCcctcgagtcagagcgctcg
s59 +      cgacgctctgactcgaggGGCGAATATACCTACcaagcttggttcagactcagc
z38 +      gctgagtcctgaacaagcttgGAGTACCGAATATACcctcgagtcagagcgctcg
s16 +      cgacgctctgactcgaggGGGAATATGCGTACCcaagcttggttcagactcagc
z83 -      gctgagtcctgaacaagcttgATTAGACGGAATATGCcctcgagtcagagcgctcg
s20 +      gctgagtcctgaacaagcttgCCCTCACGAATATGCcctcgagtcagagcgctcg
s47 -      gctgagtcctgaacaagcttgACA GAATATGCCCTTCcctcgagtcagagcgctcg
z82 +      gctgagtcctgaacaagcttgGGGAATATCCATCGcctcgagtcagagcgctcg
z34 -      gctgagtcctgaacaagcttgTTTAGCGAATATCCCCcctcgagtcagagcgctcg
s9 -      gctgagtcctgaacaagcttgACCGCAGAATATCCCCcctcgagtcagagcgctcg
z27 -      gctgagtcctgaacaagcttgGTAAGGAATAATCTGcctcgagtcagagcgctcg
z77 -      gctgagtcctgaacaagcttgAGAATAATCCCGATAcctcgagtcagagcgctcg
z29 -      cgacgctctgactcgaggGGAATAATTATGCTGcaagcttggttcagactcagc
z24 -      cgacgctctgactcgaggGCACGAATAATTCTCTcaagcttggttcagactcagc
s58 +      gctgagtcctgaacaagcttgGGGAATAATGAGTCCcctcgagtcagagcgctcg
z36 +      cgacgctctgactcgaggCGAATAATGCACTATGcaagcttggttcagactcagc
s14 -      gctgagtcctgaacaagcttgCCAGAGAATAATGCCcctcgagtcagagcgctcg
s46 -      gctgagtcctgaacaagcttgGAATAGGGAATAACCGcctcgagtcagagcgctcg
s3 -      gctgagtcctgaacaagcttgAAGAATAACCCAGTGCcctcgagtcagagcgctcg
s17 -      gctgagtcctgaacaagcttgGAATAAACGTAACCGCCcctcgagtcagagcgctcg
z42 -      cgacgctctgactcgaggGGAATAAACGTACTAAcaagcttggttcagactcagc
s6 -      gctgagtcctgaacaagcttgAGGAATAAACACGGGCcctcgagtcagagcgctcg
s49 -      gctgagtcctgaacaagcttgGGAATAAAAACGTGCCcctcgagtcagagcgctcg
z33 -      gctgagtcctgaacaagcttgTGCGAGAATAAGTCGCcctcgagtcagagcgctcg
z39 +      gctgagtcctgaacaagcttgAGAATATCAGCTGTACcctcgagtcagagcgctcg
s60 +      cgacgctctgactcgaggGGGATAATCCGTCCGTcaagcttggttcagactcagc
s52 -      cgacgctctgactcgaggGGGATAATCTGTGTACaagcttggttcagactcagc
s63 +      cgacgctctgactcgaggGGATATCCGTGGTGTcaagcttggttcagactcagc
s5 -      cgacgctctgactcgaggGGATAATTCGGACCCcaagcttggttcagactcagc
s44 +      cgacgctctgactcgaggCCGGATATCGGAATGTcaagcttggttcagactcagc
z81 -      gctgagtcctgaacaagcttgGCGATAATACAGAATAcctcgagtcagagcgctcg
s22 -      cgacgctctgactcgaggGCGATAATTACCGTCCcaagcttggttcagactcagc
z26 +      tgacgctctgactcgaggCGCATATAATTATACcaagcttggttcagactcagc
s21 -      gctgagtcctgaacaagcttgACAACGCATAAAGGGCcctcgagtcagagcgctcg
z30 +      cgacgctctgactcgaggCAAGTATATTATGGTACaagcttggttcagactcagc
z75 -      cgacgctctgactcgaggGGAATGTCTTCCAGTcaagcttggttcagactcagc
s15 -      cgacgctctgactcgaggCGGAATGTCTTCTGCaagcttggttcagactcagc
s43 -      gctgagtcctgaacaagcttgAAGAATGTCTCGGGCcctcgagtcagagcgctcg
z28 +      gctgagtcctgaacaagcttgAAAGAATGTGCGCAGGcctcgagtcagagcgctcg
s8 -      cgacgctctgactcgaggGGACAATCGAATGTGAcagcttggttcagactcagc
z25 -      cgacgctctgactcgaggGGAATGATATAGCGGAcagcttggttcagactcagc
z37 -      gctgagtcctgaacaagcttgGGAATTAAATATGTCCGcctcgagtcagagcgctcg
s18 +      gctgagtcctgaacaagcttgGTATTACTCAATTCCCcctcgagtcagagcgctcg
consensus      Gnatdw

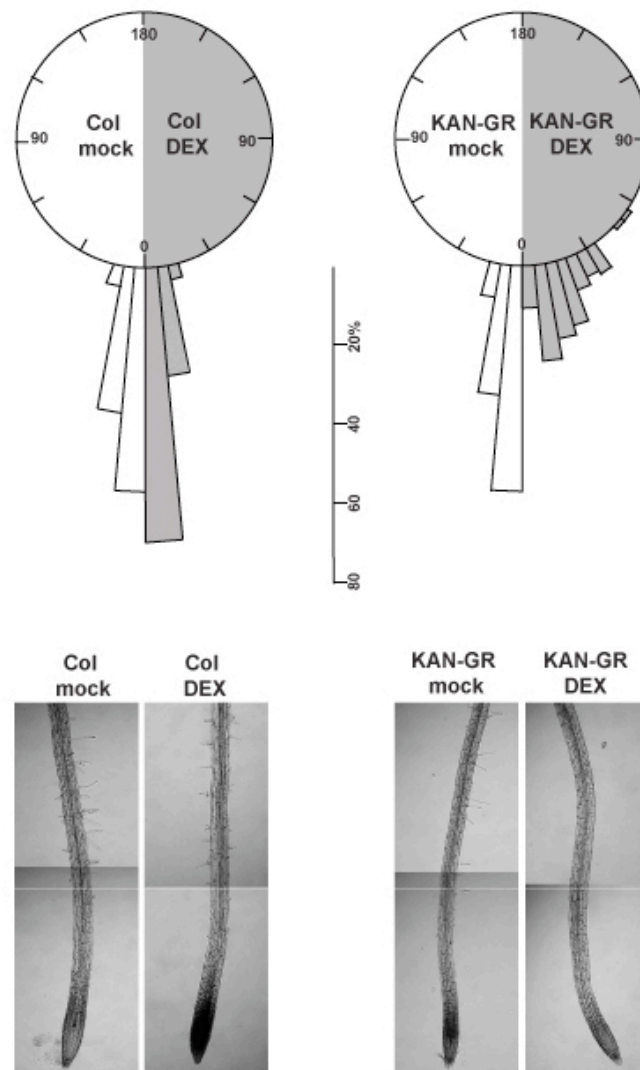
```

Supplementary Figure A1-1: Alignment of 50 sequences obtained from PCR-assisted binding site selection. The DNA sequences of fifty unique clones derived from two independent PCR-assisted binding site selection experiments were

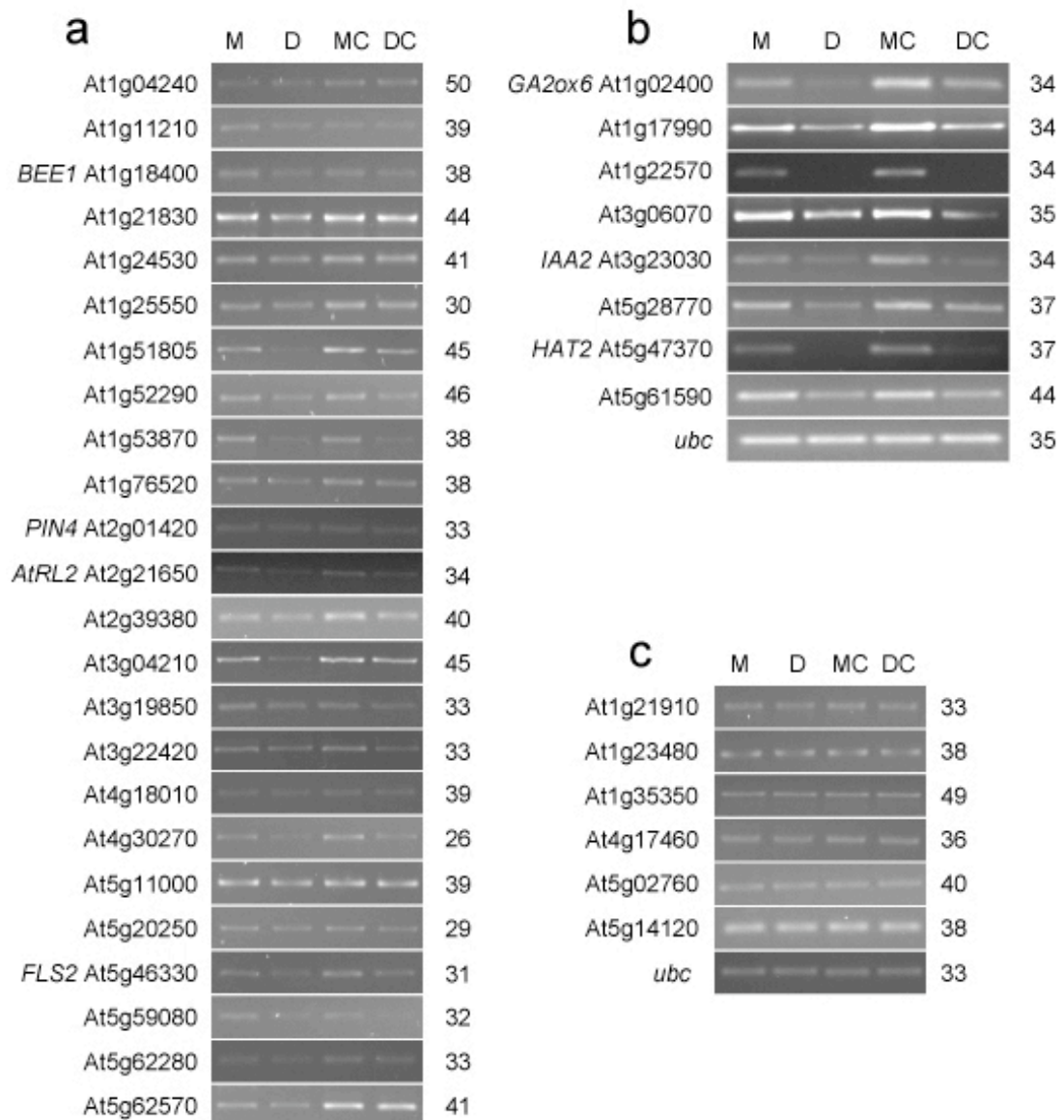
manually aligned to identify the consensus DNA binding site. Each oligonucleotide contained at least one instance of GNATDW (where N is any nucleotide, D is A, G, or T, and W is A or T) and 28 oligonucleotides contained a second potential binding site. S indicates clones from DNA EMSA selection, Z indicates clones from protein EMSA selection; + & - the clone orientation. Consensus GAATAW sites are red and complementary (often overlapping) WTATTC sites are orange except where they overlap with red nucleotides.



Supplementary Figure A1-2: Table of phenotypes in loss of function mutants and post-translationally activated *KAN-GR* plants. Top row, *kan1-11*, *kan1-11 kan2-5*, wild-type (Col), and *KAN-GR* seeds were germinated and grown for 9 days on media containing mock or DEX supplementation (as indicated). Cotyledons (inset photos, first row) of *kan1-11 kan2-5* are strongly cupped and DEX-treated *KAN1-GR* cotyledons are narrow and pointed in contrast to Col or mock-treated *KAN-GR* seedlings that form normal cotyledons and first leaves. Intermittent DEX application has different effects on morphogenesis of soil-grown *KAN-GR* plants than continuous exposure in media. Whole 14-day old (second row) and 29-day old (third row) rosettes display effects of loss of *kan* function and ectopic expression of *KAN-GR*. Soil-grown DEX-treated *KAN-GR* plants formed leaves with short petioles and asymmetric leaf blades, which were not observed in mock-treated plants. (Bar = 1 cm)

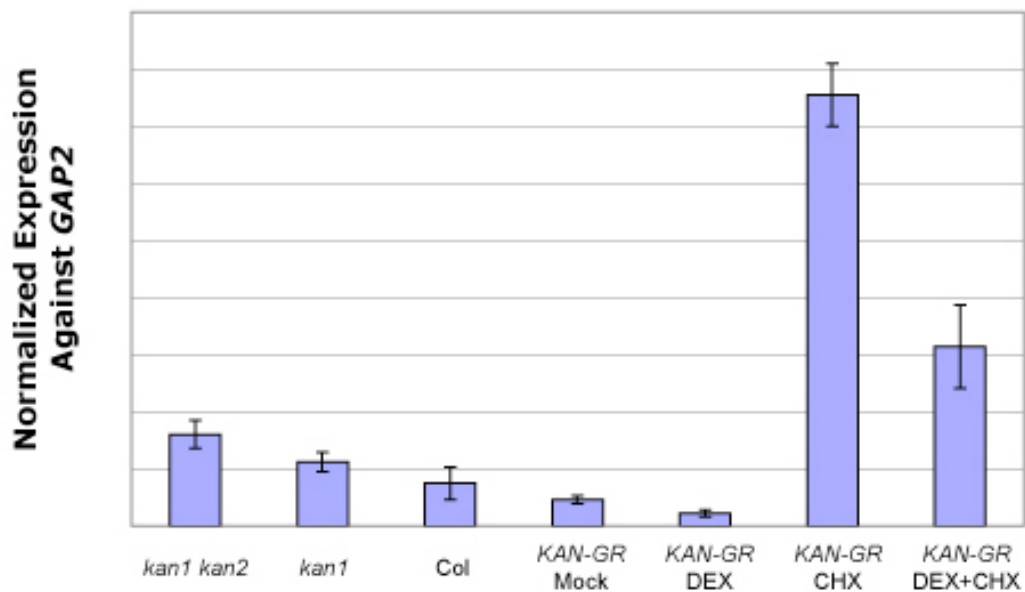


Supplementary Figure A1-3: DEX and mock-treated *KAN-GR* plants display defects in root development. Roots were analyzed on 5 day old seedlings grown on vertically oriented media with DEX or mock supplementation. 72 plants were examined in each combination of genotype and treatment. The angle of root growth relative to gravity was measured with Image J. Angles were allocated to 5° bins and with length of each bar indicating the fraction of plants within that bin (upper panel). Root angles diverged more in DEX-treated *KAN-GR* seedlings than mock-treated seedlings (upper panel right) indicating potential defects in sensing or responding to gravity. No differences were detected between mock- and DEX-treated Col roots. Root hair formation was also affected by DEX-treatment. DEX-treated *KAN-GR* seedlings failed to produce root hairs, which was not observed in mock-treated (lower right panels) or wild-type seedlings (lower left panels). Surprisingly, DEX influenced Col root hair formation; the number and length of hairs was slightly reduced in DEX- compared to mock-treated Col roots (lower left panels).

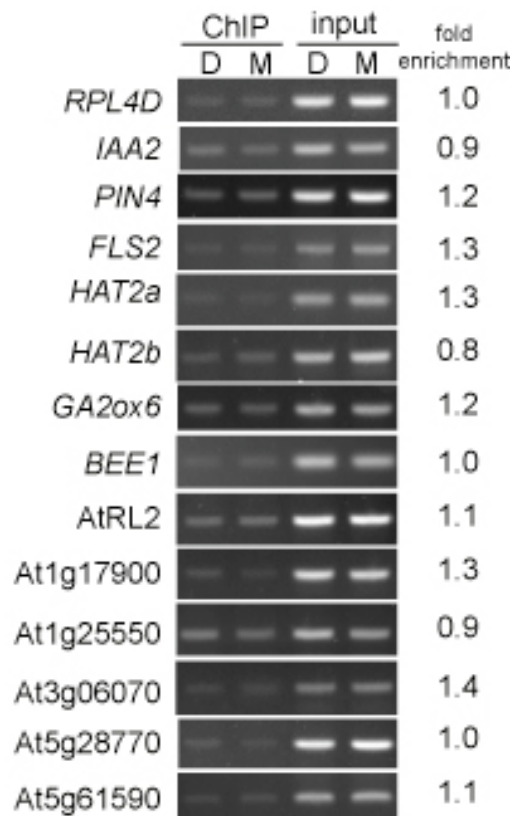


Supplementary Figure A1-4: Expression of candidate KAN1 target genes was confirmed using semi-quantitative PCR. Semi-quantitative reverse-transcription PCR was used to confirm microarray results for select candidate *KANT* genes. Most putative *KANT* genes displayed reduced expression in DEX (D) and DEX+CHX (DC) compared to mock (M) and mock+CHX (MC) treated seedlings (a and b). A few genes showed no detectable expression differences (c) in RT-PCR and may represent false discovery. For each template-primer combination, the number of PCR cycles was determined empirically and shown to the right of each gel image. At least two biological replicates and two technical replicates were performed and a single representative gel image is shown.

IAA2 Expression



Supplementary Figure A1-5: *IAA2* expression is up-regulated in loss-of-function *kan* mutants and down-regulated in posttranslationally activated *KAN-GR*. Quantitative RT-PCR was used to assay expression levels of *IAA2* in the following genotypes: *kan1-11 kan2-5*, *kan1-11*, wild-type (Col), and *KAN-GR* treated with mock- or DEX in the absence and presence of CHX. Results were normalized to GAP2 with the results of *KAN-GR* mock arbitrarily set to 1.



Supplementary Figure A1-6: Chromatin immunoprecipitation experiments on mock- and DEX-treated Col seedlings reveal no enrichment. ChIP was performed on Col seedlings lacking the *KAN-GR* transgene as a control for potential non-specific immunoprecipitation effects. None of the promoter fragments tested showed enrichment in DEX- versus mock-treated Col samples indicating that enrichment depends on the *KAN-GR* transgene. Fold enrichment was calculated as in Fig. 3.

This manuscript has been submitted. The title is “KANADI1 acts as a transcriptional repressor that links genes involved in auxin responses with adaxial-abaxial polarity” and the authors are Tengbo Huang, Yaël Harrar, Changfa Lin and Randall A. Kerstetter.

Author contributions: R.A.K conceived and designed the experiments, made the constructs, generated transgenic lines. T.H. & Y.H. characterized the transgenic plants, Y.H. performed the microarray experiments. C.L. performed RT-PCR to confirm expression results. T.H. performed the oligonucleotide selection and ChIP experiments. R.A.K analyzed the data and wrote the paper.

Appendix 2

KANADI1 regulates abaxial-abaxial polarity in *Arabidopsis* by repressing the transcription of *ASYMMETRIC LEAVES2*

Introduction

Adaxial-abaxial polarity in plants is specified by interactions between genes that individually specify either adaxial or abaxial identity (1, 2). In *Arabidopsis*, adaxial identity is specified by class III homeodomain leucine zipper (HD-ZIP III) transcription factors (3, 4), the LOB domain transcription factor AS2 (5, 6), and the trans-acting siRNA tasiARF (7), whereas abaxial identity is specified by KANADI (KAN) (8, 9), YABBY (YAB) (10, 11), AUXIN RESPONSE FACTOR (ARF) (12) and LITTLE ZIPPER (ZPR) (13) transcription factors, and by the miRNAs miR165/miR166 (14, 15). Genetic analysis indicates that many of these genes interact antagonistically: loss-of-function mutations in adaxial genes typically produce an abaxialized phenotype that is accompanied by the expanded expression of abaxial genes, whereas loss-of-function mutations in abaxial genes produce an adaxialized phenotype that is associated with the expanded expression of adaxial genes; mutations or transgenes that produce ubiquitous expression of these genes have a phenotype opposite to that of the loss-of-function mutations. miR165/166 and tasiARF repress the expression of their targets--respectively, *HD-ZIP III* genes and *ARF3/ETTIN*--by directing the cleavage of the transcripts of these genes (14, 16). The molecular basis

for the antagonistic interactions between other adaxial and abaxial regulators is unknown.

KAN1, *KAN2* and *KAN3* are members of the GARP family of transcription factors and act redundantly to promote abaxial identity in both lateral organs and the shoot axis.

These genes are expressed in abaxial cells of lateral organs and peripheral cells of the hypocotyl and stem (9, 17). Loss-of-function mutations in individual genes have

relatively weak effects on organ polarity (9, 18), but *kan1 kan2* (8) and *kan1 kan2 kan3* (17) mutants are strongly adaxialized and resemble plants ectopically expressing the HD-ZIPIII genes *PHB*, *PHV* and *REV* (3, 15), or the LOB gene *AS2* (5, 6).

Consistent with this observation, *PHB* is abaxially expressed in *kan1 kan2 kan3* triple mutants (17). The effect of *kan* on the expression of *AS2* has not been examined.

Here we show that *KAN1* promotes abaxial identity by directly repressing the transcription of *AS2* in abaxial tissue. Specifically, we demonstrate that *KAN1* binds to a site in the promoter of *AS2*, and that a single nucleotide mutation in this site interferes with *KAN1* binding and produces an adaxialized phenotype that is associated with the inappropriate expression of *AS2* in abaxial tissue. These results indicate that *KAN1* acts as a transcriptional repressor, and provide the first evidence for a direct interaction between transcription factors involved in the specification of adaxial-abaxial polarity. In addition, we show that *AS2* represses the expression of *KAN1* in adaxial tissue, suggesting that these transcription factors may interact in a mutually repressive fashion.

Results and Discussion

To identify genes involved in the specification of adaxial-abaxial polarity, we took advantage of the observation that adaxialized mutants often have flat or upwardly curled leaves. Screens for EMS-induced mutations with this leaf phenotype identified a dominant mutation that was mapped to a region on chromosome 1 containing *AS2*. Because this new mutation had a phenotype that strongly resembled transgenic plants that ectopically express *AS2* (5, 6, 19) we immediately focused on this gene. Sequencing of the region surrounding *AS2* revealed a G-to-A substitution 1484 bp upstream of the *AS2* ATG (Fig. A2-1A). Existing ESTs and cDNAs (www.arabidopsis.org) and the results of 5' RACE (data not shown) indicate that *AS2* has multiple transcription start sites. The mutation, which we refer to as *as2-5D*, is located in the first intron of one of these transcripts, but is in the promoter of most of the transcripts produced from this locus (Fig. A2-1A). To confirm that this mutation is responsible for the *as2-5D* phenotype, wild-type (*pAS2*) and *as2-5D* (*pas2-5D*) genomic sequences extending from the 3' end of the upstream gene to the transcription stop site of *AS2* (Fig. A2-1A) were transformed into wild-type plants and *as2-1* loss-of-function mutants (Fig. A2-1B). 97% (N=422) of *as2-1* plants transformed with the wild-type genomic sequence had a wild-type phenotype, indicating that this sequence contains all of the regulatory information necessary for *AS2* function. Interestingly, introduction of the *AS2* sequence into a wild-type background did not produce an *AS2* gain-of-function phenotype, demonstrating that additional copies of this locus are insufficient to direct ectopic adaxial development.

In contrast, 99% (N=572) of *as2-1* plants and 97% (N=570) of wild-type plants transformed with the *as2-5D* genomic construct exhibited the dominant cupped leaf phenotype (Fig. A2-1B). These results demonstrate that the *as2-5D* phenotype is attributable to the G-to-A mutation in the *AS2* promoter sequence and that this mutation is a gain-of-function mutation.

Plants homozygous or heterozygous for *as2-5D* produced erect, cupped-up cotyledons, which remained cupped throughout their development (Fig. A2-2A, B). The true leaves of mutant plants were strongly up-rolled early in development, but became flatter as they expanded and at maturity were quite similar to wild-type leaves (Fig. A2-2A -C). *as2-5D* also affected the polarity of the mesophyll in the leaf blade (Fig. A2-2D). In wild-type leaves the adaxial layer of the mesophyll is occupied by round, densely packed cells, whereas the middle and lower (abaxial) mesophyll layers consist of irregularly shaped, loosely packed cells. In *as2-5D* leaves, cells in the adaxial mesophyll had more intercellular air space than normal, whereas cells in the abaxial layers of the mesophyll were more regular in shape and more densely arrayed than in wild-type leaves. Thus, *as2-5D* reduces the polarity of the mesophyll by affecting the differentiation of both adaxial and abaxial tissue. *as2-5D* plants also exhibited a slight reduction in the size of leaves and floral organs, and had flowers and siliques that pointed downward (Fig. A2-2C). In contrast to other adaxializing mutations, *as2-5D* did not affect the production of trichomes on the abaxial surface of the lamina; wild-type plants first produced abaxial trichomes on leaf 6.2 ± 0.2 (N=10), and *as2-5D/+* plants were not significantly different (6.4 ± 0.2 ; N=10).

To examine the effect of the *as2-5D* mutation on the expression of *AS2*, we generated promoter-reporter constructs containing wild-type or mutated *AS2* regulatory sequences fused to β -glucuronidase (*GUS*). Constructs containing the wild-type *AS2* promoter (*pAS2:GUS*), the *as2-5D* promoter (*pas2-5D:GUS*), and an *AS2* promoter in which the second G in the GAATAAGAATAA repeat was mutated (*pAS2m:GUS*) were introduced into plants. Consistent with the distribution of *AS2* mRNA observed by *in situ* hybridization (19, 20), *pAS2:GUS* embryos and seedlings displayed GUS activity exclusively in the adaxial domain of cotyledons and leaf primordia (Fig. A2-3A, D), and this same pattern was observed in plants transformed with *pAS2m:GUS* (Fig. A2-3C, F). In contrast, plants transformed with *pas2-5D:GUS* expressed *GUS* throughout the cotyledons, leaf primordia and the hypocotyl (Fig. A2-3B, E). These results suggest that *as2-5D* interferes with the binding of a factor that represses the transcription of *AS2* in abaxial tissue and the hypocotyl. The fact that *as2-5D* affects the repeated sequence GAATAA suggests that this sequence may be particularly important for the binding of this factor. However, because a mutation in the second G in the GAATAAGAATAA repeat had no effect on *AS2* expression, the identity of this binding site remains unclear.

The phenotypic similarity between *as2-5D* and loss-of-function mutations of *KAN1* (9) suggested that *KAN1* might correspond to this negative regulator. To test this hypothesis, we examined the expression of *AS2* and several other polarity genes in plants transformed with *35S: KAN1-GR*, a construct that constitutively expresses a dexamethasone (DEX)-inducible form of KAN1. Semi-quantitative RT-PCR

analysis of *35S:KAN-GR* plants grown on media with and without DEX, revealed that DEX reduced the amount of *AS2* mRNA, but had no effect on the expression of *AS1*, *FIL1* or *YAB3* (Fig. A2-4A). We then tested if KAN1 binds directly to the *AS2* promoter by examining the chromatin fragments that immunoprecipitate with KAN1-GR in DEX- and mock-treated *35S:KAN1-GR* seedlings. A 300 bp region surrounding the site of *as2-5D* mutation and two adjacent 300 bp regions were amplified by PCR from immunoprecipitated material. KAN1 binding (as judged by enrichment following chromatin immunoprecipitation) was only detected for the fragment containing the *as2-5D* mutation (Fig. A2-4B). No enrichment was observed in *35S:KAN1-GR* plants homozygous for *as2-5D*, demonstrating that the *as2-5D* mutation prevents or greatly reduces the binding of KAN1 to this site. Consistent with this result, we found that *as2-5D* suppresses the morphological defects produced by DEX treatment of *35S:KAN1-GR* plants. Nine-day-old *KAN-GR* seedlings treated with DEX have unexpanded leaves and cotyledons (Fig. A2-4C) and have poorly gravitropic roots (Suppl. Fig. A2-1), whereas DEX-treated *as2-5D* *KAN-GR* seedlings closely resemble untreated *as2-d* *KAN-GR* plants and display no defect in root gravitropism. These results indicate that *AS2* is directly repressed by KAN1 via the site that is mutated in *as2-5D*.

If the effect of *as2-5D* on the pattern of *AS2* expression is attributable to a defect in KAN1 binding, loss of *KAN1* activity should have the same effect on *AS2* expression as *as2-5D*. To test this hypothesis, we examined the effect of loss-of-function mutants of *KAN1* and *KAN2* on the expression of *pAS2:GUS* in embryos and

8-day-old seedlings. Similar results were obtained with mutations isolated in the Landsberg *erecta* (*kan1-2*, *kan2-1*) and Columbia (*kan1-11*, *kan2-5*) genetic backgrounds. Consistent with their subtle morphological phenotype, mutations in *KAN2* had no apparent effect on *pAS2:GUS* expression (data not shown). In contrast, mutations in *KAN1* little or no effect on the expression of *pAS2:GUS* in cotyledons (Fig A2-3H), but caused this reporter to be expressed on both the adaxial and abaxial sides of leaf primordia (Fig. A2-3K). Plants mutant for both *KAN1* and *KAN2* expressed *pAS2:GUS* ubiquitously in cotyledons (Fig. A2-3I), leaf primordia (Fig. A2-3L), and the hypocotyl. These results indicate that *KAN1* and *KAN2* redundantly repress *AS2* in the abaxial domain of cotyledons and the hypocotyl, and that *KAN1* has a non-redundant function in the repression of *AS2* in leaf primordia. The observation that loss of *KAN1* and *KAN2* has essentially the same effect on the expression of *pAS2:GUS* (Fig. A2-3I, L) as *pas2-5D:GUS* (Fig. A2-3 B, E) suggests that both of these proteins act via the site that is mutated in *as2-5D*.

To determine if mis-expression of *AS2* in the *KAN1* expression domain accounts for the phenotype of *as2-5D*, we generated plants expressing *AS2* under the control of the *KAN1* promoter. Plants transformed with *pKAN1:AS2* were nearly indistinguishable from *as2-5D*. In addition to possessing cupped cotyledons and leaves, they displayed the downward-pointing flowers characteristic of this mutation (Fig. A2-5). This result demonstrates that the phenotype of *as2-5D* is indeed a consequence of the misexpression of *AS2* in the *KAN1* expression domain, and along with the results described above, supports the conclusion that the expression domain of *AS2* is

defined by KAN1 and other abaxially-expressed KAN genes. The floral phenotype of *as2-5D* and *pKAN1:AS2* is strikingly similar to the phenotype of loss-of-function mutations in the *KNOX* gene *BREVIPEDICELUS (BP)* (21, 22). Because *AS2* represses *BP* (5), this floral phenotype is likely due to the repression of *BP* in the abaxial region of the pedicel by the inappropriate expression of *AS2* in this domain.

kan1 kan2 double mutants have a very severe adaxialized phenotype with many features that are not observed in *as2-5D* plants. To determine if the ectopic expression of *AS2* contributes to this phenotype, we generated a *kan1-12 kan2-4 as2-1* triple mutant. Consistent with previous studies results (23, 24), we found that triple mutants had nearly the same phenotype as *kan1 kan2*, although their leaf blades were shorter and more irregular than *kan1 kan2* (Suppl. Fig. A2-2). The observation that the *as2-1* mutation is unable to ameliorate this adaxialized phenotype indicates that KAN1 and KAN2 have other targets that have significant roles in leaf polarity. Possible candidates include *LBD* genes that are closely related to *AS2*, such as *LBD36/ASL1*. Over-expression of *ASL1* produces a phenotype that is similar to that of *as2-5D*, suggesting that *AS2* and *ASL1* have overlapping functions (25, 26). If *AS2* and *ASL1* contribute redundantly to the *kan1 kan2* phenotype, loss-of-function mutations in only one of these mutations may have little or no effect on this phenotype. In addition to *AS2*, KAN1 appears to directly regulate the transcription of at least a dozen genes in *Arabidopsis*, several of which are involved in auxin and gibberellin metabolism and response (Huang T, Harrar Y, Lin C, & Kerstetter RA,

unpublished results). It is likely that some of these genes also contribute to the phenotype of *kan1 kan2* double mutants.

Plants transformed with *35S:AS2* have reduced levels of *KAN1* and *KAN2* mRNA and have a leaf phenotype reminiscent of the *kan1 kan2* double mutant whereas *as2-1* mutants have elevated levels of *KAN2* (5, 20). These observations suggest that *AS2* and *KAN* genes may mutually repress each other's transcription. To test this hypothesis, we examined the effect of *as2-1* and *as2-5D* on the expression of the *KAN1* reporter *pKAN1:GUS*. In wild-type plants, *pKAN1:GUS* expression was restricted to the abaxial side of young leaf primordia and disappeared quickly as the leaf expanded (Fig. A2-6A). In *as2-1*, *pKAN1:GUS* expression extended to the adaxial side of young leaf primordia and persisted late in leaf development (Fig. A2-6C). *as2-5D* had the opposite effect; in *as2-5D* plants, *pKAN1:GUS* expression was excluded from leaf primordia and restricted to a smaller region of the shoot apex than in wild type plants (Fig. A2-6B). Thus, *AS2* directly or indirectly represses *KAN1* expression. Repression of *KAN* genes by *AS2* is further supported by the phenotype of plants doubly mutant for *kan1-11* and *as2-5D* (Fig. A2-6D-G). Leaves of double mutant plants display abaxial outgrowths that are a characteristic feature of *kan1 kan2* double mutants but are not present in either *kan1* or *as2-5D* single mutants; that is, *kan-11 as2-5D* plants resemble *kan1 kan2* double mutants (Fig. A2-6F, G). A reasonable interpretation of this result is that *as2-5D* represses *KAN2* as well as *KAN1*.

These results provide strong evidence that the spatial expression patterns of *AS2* and *KAN1* are specified by mutual repression, and that *AS2* is a direct target of KAN1. We do not have evidence that KAN2 also binds to the *AS2* promoter. However, this seems likely because of the similarity of these proteins, and the observation that the expression of *pAS2:GUS* in a *kan1 kan2* background is essentially identical to the expression pattern of *pas2-5D:GUS*; single *kan1* mutations have a much less significant effect on *pAS2:GUS* expression. The result is surprising because it suggests that KAN1 and KAN2 regulate *AS2* entirely via the site that is mutated in *pas2-5D*. Multiple binding sites are usually required to confer regulation by a specific transcription factor, and we are unaware of another case in which a single nucleotide mutation in a plant promoter has such a profound effect on gene expression.

Although it is clear that KAN1 and KAN2 play a major role in the regulation of *AS2*, these factors probably do not act alone. In particular, the observation that mutations of *ARF3/ETT* are capable of suppressing the floral phenotype of *AP3:KAN1* suggests that *ARF3/ETT* cooperates with KAN1 and KAN2 to promote abaxial identity (12). This result is interesting in light of the observation that over-expression of *ARF3* produces a phenotype nearly indistinguishable from that of *as2-1* (27). This latter result is consistent with experimental evidence indicating that *ARF3* acts as transcriptional repressor (28), and suggests that *ARF3/ETT* may work with KAN1 and KAN2 to repress *AS2* transcription in some tissues. Defining the functional relationships between KAN family members and these and other major regulators of adaxial-abaxial polarity is an important goal for future research.

Methods and Materials

Genetic stocks and growth conditions

Seeds of the Col ecotype were mutagenized by suspending in 0.4% ethyl methane sulphonate (EMS) at room temperature for 10 hours, and then rinsed 5 times with water. Bulk M2 progeny of mutagenized seeds were screened for defects in leaf expansion. Phenotypic characterization was carried out on the progeny of the second backcross of *as2-5D* to wild-type Col.

Unless otherwise noted, all mutants stocks were in a Col background. *kan2-4* (SALK_095643) and *as2-1* seed were obtained from the Arabidopsis Biological Resource Center; the *as2-1* stock was crossed to Col two times before analysis. *kan1-2* and *kan2-1* were obtained from John Bowman (Monash University), and are in *Ler*. *kan1-11* and *-12* have been previously described (9). The lesion in *kan2-5* is identical to that in *kan2-1* (8) but was independently isolated in Col. Seeds were sown on Metromix 360 (Sun-Gro) and kept at 4°C for 2 days before transfer to growth chambers. Plants were grown in 96-well flats under continuous fluorescent light (100 $\mu\text{E}/\text{minute}/\text{m}^2$; Sylvania VHO) at 22°C. Abaxial trichomes were scored with a stereomicroscope 2-3 weeks after planting.

as2-5D was mapped in the F2 progeny of a cross to *Ler*. 179 wild-type plants in the F2 were used to map the mutation to a site between the BACs F5I14 and F12P19 on chromosome 1.

Transgenic plants

The *AS2* ORF and the entire 5' intergenic region were PCR-amplified from wild-type and *as2-5D* genomic DNA using the 5' primer

5'-CGCGGATCCAATTTTGGTTAATGATCGGTGAGAG-3', which incorporates a *Bam*HI site, and the 3' primer

5'-CGCATGCCATGGATCAATTAAGAGAGCAAGTCCATAAA-3', which

incorporates an *Nco*I site, and the products were cloned into pCAMBIA3301. These clones were transformed into wild-type and *as2-1* plants to confirm the identity of the *as2-5D* mutation. To examine the effect of this mutation on gene expression, the

wild-type *AS2* promoter sequence was amplified from wild-type genomic DNA using primers pAS2-F: 5'-GGATCCTGGTAGCTAGCGTTGTTGACA-3' and pAS2-R:

5'-GGATCCGTGAACGTTTGCGAATTTTGTG-3', which contained introduced

*Bam*HI sites, and the resulting PCR products were cloned into the binary vector

pCB308 (29) generating a translational fusion to the *GUS* gene in the pAS2:*GUS*

construct. The *pas2-5D:GUS* and pAS2-*m:GUS* constructs were generated using

site-directed mutagenesis, by amplification of the pAS2:*GUS* template with primers containing introduced mutations: *pas2-5D*-F:

5'-CCCTAGACAAAAAAATAAGAATAAAAAGAGC-3' and *pas2-5D*-R:

5'-GCTCTTTTATTCTTATTTTTTTGTCTAGGG-3' or pAS2-*m*-F:

5'-CCCTAGACAAAAAGAATAAAAATAAAAAGAGC-3', and pAS2-*m*-R:

5'-GCTCTTTTATTTTTATTCTTTTTGTCTAGGG-3' with *PfuTurbo* DNA

polymerase (Stratagene, La Jolla, CA). The PCR products were digested with *Dpn*I

to restrict the parental DNA template and dsDNA containing the introduced mutation was transformed into TOP10 *E. coli* cells (Invitrogen, Carlsbad, CA). The p35S:*KAN1-GR* construct was produced as follows: the p35S:*KAN1-mGFP5* plasmid (9) was digested with *Bgl*II and partially digested with *Nhe*I to remove the fragment encoding *mGFP5*. In its place, a DNA fragment was ligated that encoded amino acids 508-795 of the rat glucocorticoid receptor isolated from pBS-GR (a gift from Doris Wagner) by digestion with *Bam*HI and *Xba*I. In order to generate p*KAN1:GUS*, a 7.7 kb *Bgl*II fragment from P1 clone MQK4 was ligated into the *Bam*HI site of pCambia2300 (www.cambia.org). A 3.5 kb *Xba*I fragment carrying the *KAN1* promoter was subcloned into pBI101.2 to generate a translational fusion between the first 8 amino acids of the KAN1 coding region and GUS. The resulting constructs were sequenced to confirm their integrity and introduced into Arabidopsis plants using the floral dip method. To generate the p*KAN1:AS2* construct, the *KAN1* promoter was amplified from genomic DNA using the primers pKAN1-F: 5'-ACTAGTAAGACCAACACAAACAAATTACC-3' and pKAN1-R: 5'-CCATGGAATTAAAGAAACCTTTCTCTTGCT-3', which contained introduced *Spe*I and *Nco*I restriction sites, respectively. The amplified promoter fragment was fused to the *AS2* coding sequence and an *OCS3'* terminator in pCB302.

Histology

GUS staining was conducted according to the method of Donnelly et al (30), with the exception that specimens were placed directly in the staining solution. Siliques

were opened along the valve margin with a needle and stained with GUS staining buffer. After staining, developing seeds were placed on a glass slide and the embryos were removed from the seed by applying gentle pressure with a needle.

RT-PCR and ChIP analysis

Semi-quantitative RT-PCR analysis of transcript levels in *35S:KAN1-GR* plants was performed as previously described (5). For ChIP analysis, approximately 200 surface-sterilized seeds of *as2-5D 35S:KAN1-GR*, *as2-5D*, *AS2 35S:KAN1-GR* or wild-type were sown on 1/2X MS media without sucrose. 9-day-old seedlings were treated with 10 μ M dexamethasone or mock solution for 4 hours. Seedlings were harvested, washed with deionized water and crosslinked with 1% formaldehyde. Crosslinking was quenched by adding 0.125M glycine. Nuclear extract preparation and immunoprecipitation procedures were adapted (31) with the following modifications: Sonication conditions for nuclear extracts were empirically determined to obtain an average DNA size of 600bp. Sonication was performed on ice at power setting 6 (40% duty cycle and 20% input) for 12 seconds repeated 4 times with 1-minute pauses between for *35S:KAN1-GR* and wild-type or 9 seconds repeated 4 times with 1-minute pauses between for *as2-5D 35S:KAN1-GR* and *as2-5D* samples. After chromatin shearing, 10 μ l anti-GR P-20 (Santa Cruz Biotechnology, Santa Cruz, CA) was added to immunoprecipitate KAN1-GR proteins. After reversing crosslinks, DNA was purified by phenol:chloroform extraction, ethanol precipitated, and resuspended in 50 ml TE. 1 μ l of immunoprecipitated DNA was used in ChIP PCR.

Input DNA was diluted 120 times to achieve comparable PCR product band intensities. Primers recognizing different regions in the promoter of *AS2* indicated in Fig. 3 were as follows: AS2A-F: 5'-TTTGACCGAAGAACTTTGAGGAC-3', AS2A-R: 5'-AACCCCTGGACCCTAGCATAGACT-3', AS2B-F: 5'-CGAAAAGCACCTTCATGTTACTCA-3', AS2B-R: 5'-AAGTTGCTCAATCTTTATTGTTGTCA-3', and AS2C-F: 5'-TTGACAATCGCTTAACCCAAAGTT-3', AS2C-R: 5'-GGCACCGTTTCTTAGATGCTTTAG-3'. Control primers were RPL4-F: TGTGTTTGTTCATTACTGTGCTATGC, RPL-R: 5'-ATAAAGCTGGCGGTTCGAGT-3' and IAA2-L: 5'-CGGGTCGGCCGATAGAAT-3', IAA2-R: 5'-TCGGAAGCATGAAAGGCAAG-3'. PCR conditions were 33 cycles of 94°C for 30s, 56°C (except AS2C which was 53°C) for 30s, and 72°C for 30s. ChIP analysis performed on wild-type and *as2-5D* seedlings lacking KAN1-GR displayed no detectable differences (not shown). DNA band intensity was measured using the Gaussian Curve method with background subtraction with Molecular Imaging Software 4.0 (Eastman KODAK Company, Rochester, NY). To compare the abundance of promoter fragments in DEX- versus mock-treated plants, band intensities were first normalized to the negative-control gene RPL4D. The band intensities of Dex- and mock-treated samples were then divided by the band intensities of the input samples, to obtain input-normalized values. The relative abundance of a fragment in DEX- versus mock-treated samples was calculated by

determining the ratio of these input-normalized values.

Acknowledgements

We thank Stewart Gillmor and Li Yang for helpful discussions. This work was supported by a DOE grant (DE-FG02-99ER20328) to R. S. P. and by National Science Foundation grants IBN-0318822 to P. S. and IBN-0343179 to R. A. K.

References

1. Bowman, JL, Eshed Y, & Baum SF (2002) Establishment of polarity in angiosperm lateral organs. *Trends Genet* 18, 134-141.
2. Kidner, CA & Timmermans MC (2007) Mixing and matching pathways in leaf polarity. *Curr Opin Plant Biol* 10, 13-20.
3. McConnell, JR, et al. (2001) Role of PHABULOSA and PHAVOLUTA in determining radial patterning in shoots. *Nature* 411, 709-713.
4. Prigge, MJ, et al. (2005) Class III homeodomain-leucine zipper gene family members have overlapping, antagonistic, and distinct roles in Arabidopsis development. *Plant Cell* 17, 61-76.
5. Lin, WC, Shuai B, & Springer PS (2003) The Arabidopsis LATERAL ORGAN BOUNDARIES-domain gene ASYMMETRIC LEAVES2 functions in the repression of KNOX gene expression and in adaxial-abaxial patterning. *Plant Cell* 15, 2241-2252.
6. Xu, L, et al. (2003) Novel as1 and as2 defects in leaf adaxial-abaxial polarity reveal the requirement for ASYMMETRIC LEAVES1 and 2 and ERECTA functions in specifying leaf adaxial identity. *Development* 130, 4097-4107.
7. Garcia, D, Collier SA, Byrne ME, & Martienssen RA (2006) Specification of leaf polarity in Arabidopsis via the trans-acting siRNA pathway. *Curr Biol* 16, 933-938.
8. Eshed, Y, Baum SF, Perea JV, & Bowman JL (2001) Establishment of polarity in lateral organs of plants. *Curr Biol* 11, 1251-1260.
9. Kerstetter, RA, Bollman K, Taylor RA, Bombliès K, & Poethig RS (2001) KANADI regulates organ polarity in Arabidopsis. *Nature* 411, 706-709.
10. Sawa, S, et al. (1999) FILAMENTOUS FLOWER, a meristem and organ identity gene of Arabidopsis, encodes a protein with a zinc finger and HMG-related domains. *Genes Dev* 13, 1079-1088.
11. Siegfried, KR, et al. (1999) Members of the YABBY gene family specify abaxial cell fate in Arabidopsis. *Development* 126, 4117-4128.
12. Pekker, I, Alvarez JP, & Eshed Y (2005) Auxin response factors mediate Arabidopsis organ asymmetry via modulation of KANADI activity. *Plant Cell* 17, 2899-2910.
13. Wenkel, S, Emery J, Hou BH, Evans MM, & Barton MK (2007) A feedback regulatory module formed by LITTLE ZIPPER and HD-ZIPIII Genes. *Plant Cell* 19, 3379-3390.
14. Mallory, AC, et al. (2004) MicroRNA control of PHABULOSA in leaf development: importance of pairing to the microRNA 5' region. *Embo J* 23, 3356-3364.
15. Emery, JF, et al. (2003) Radial patterning of Arabidopsis shoots by class III HD-ZIP and KANADI genes. *Curr Biol* 13, 1768-1774.
16. Allen, E, Xie Z, Gustafson AM, & Carrington JC (2005) microRNA-directed phasing during trans-acting siRNA biogenesis in plants. *Cell* 121, 207-221.
17. Eshed, Y, Izhaki A, Baum SF, Floyd SK, & Bowman JL (2004) Asymmetric leaf development and blade expansion in Arabidopsis are mediated by KANADI and YABBY activities. *Development* 131, 2997-3006.
18. Eshed, Y, Baum SF, & Bowman JL (1999) Distinct mechanisms promote polarity establishment in carpels of Arabidopsis. *Cell* 99, 199-209.

19. Iwakawa, H, et al. (2002) The ASYMMETRIC LEAVES2 gene of *Arabidopsis thaliana*, required for formation of a symmetric flat leaf lamina, encodes a member of a novel family of proteins characterized by cysteine repeats and a leucine zipper. *Plant Cell Physiol* 43, 467-478.
20. Iwakawa, H, et al. (2007) Expression of the ASYMMETRIC LEAVES2 gene in the adaxial domain of *Arabidopsis* leaves represses cell proliferation in this domain and is critical for the development of properly expanded leaves. *Plant J* 51, 173-184.
21. Douglas, SJ, Chuck G, Dengler RE, Pelecanda L, & Riggs CD (2002) KNAT1 and ERECTA regulate inflorescence architecture in *Arabidopsis*. *Plant Cell* 14, 547-558.
22. Venglat, SP, et al. (2002) The homeobox gene BREVIPEDICELLUS is a key regulator of inflorescence architecture in *Arabidopsis*. *Proc Natl Acad Sci U S A* 99, 4730-4735.
23. Ha, CM, Jun JH, Nam HG, & Fletcher JC (2007) BLADE-ON-PETIOLE1 and 2 control *Arabidopsis* lateral organ fate through regulation of LOB domain and adaxial-abaxial polarity genes. *Plant Cell* 19, 1809-1825.
24. Fu, Y, et al. (2007) Genetic interactions between leaf polarity-controlling genes and ASYMMETRIC LEAVES1 and 2 in *Arabidopsis* leaf patterning. *Plant Cell Physiol* 48, 724-735.
25. Chalfun-Junior, A, et al. (2005) ASYMMETRIC LEAVES2-LIKE1 gene, a member of the AS2/LOB family, controls proximal-distal patterning in *Arabidopsis* petals. *Plant Mol Biol* 57, 559-575.
26. Nakazawa, M, et al. (2003) Activation tagging, a novel tool to dissect the functions of a gene family. *Plant J* 34, 741-750.
27. Hunter, C, et al. (2006) Trans-acting siRNA-mediated repression of ETTIN and ARF4 regulates heteroblasty in *Arabidopsis*. *Development* 133, 2973-2981.
28. Tiwari, SB, Hagen G, & Guilfoyle TJ (2004) Aux/IAA proteins contain a potent transcriptional repression domain. *Plant Cell* 16, 533-543.
29. Xiang, C, Han P, Lutziger I, Wang K, & Oliver DJ (1999) A mini binary vector series for plant transformation. *Plant Mol Biol* 40, 711-717.
30. Donnelly, PM, Bonetta D, Tsukaya H, Dengler RE, & Dengler NG (1999) Cell cycling and cell enlargement in developing leaves of *Arabidopsis*. *Dev Biol* 215, 407-419.
31. Gendrel, AV, Lippman Z, Yordan C, Colot V, & Martienssen RA (2002) Dependence of heterochromatic histone H3 methylation patterns on the *Arabidopsis* gene DDM1. *Science* 297, 1871-1873.

FIGURES

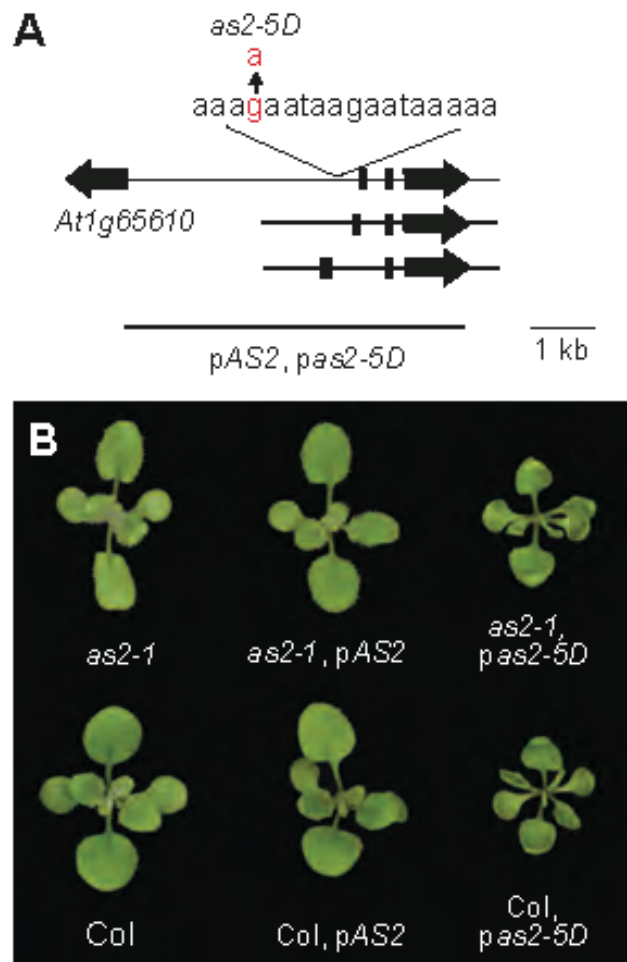


Figure A2-1. *as2-5D* affects a predicted KAN1 binding site. (A) *AS2* transcripts share exons 2 and 3, but have variable first exons. The location of the *as2-5D* mutation is indicated in red. (B) The phenotype of wild-type and *as2-1* plants transformed with wild-type (*pAS2*) and mutant (*pas2-5D*) genomic constructs.

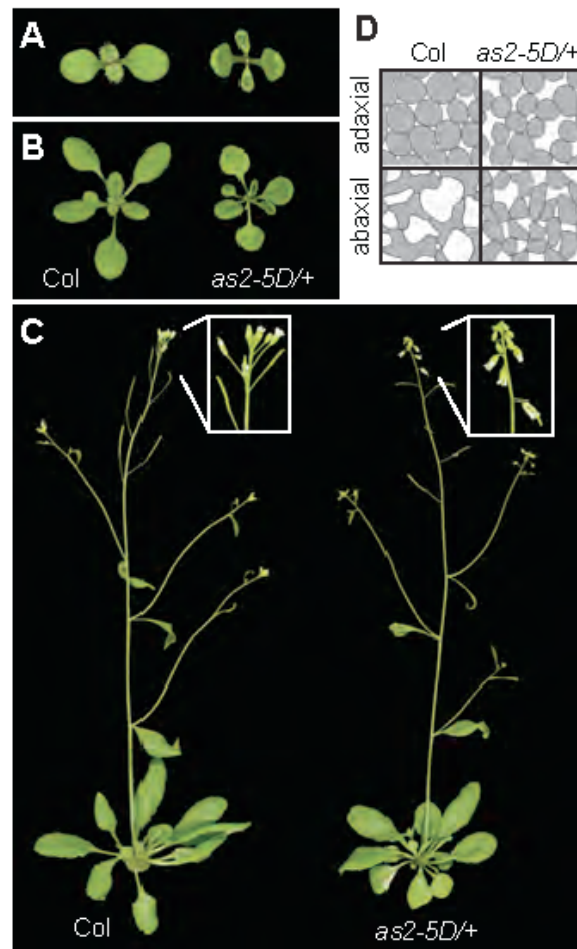


Figure A2-2. *as2-5D* has an adaxialized phenotype. (A) 8-day-old, (B) 21-day-old, and (C) mature wild-type Columbia and *as2-5D/+* plants. *as2-5D* causes immature leaves and cotyledons to curl upwards, and flowers and siliques to bend downwards. (D) Camera-lucida drawings of the adaxial and abaxial mesophyll of leaf 3 demonstrating the loss of tissue polarity in *as2-5D/+*.

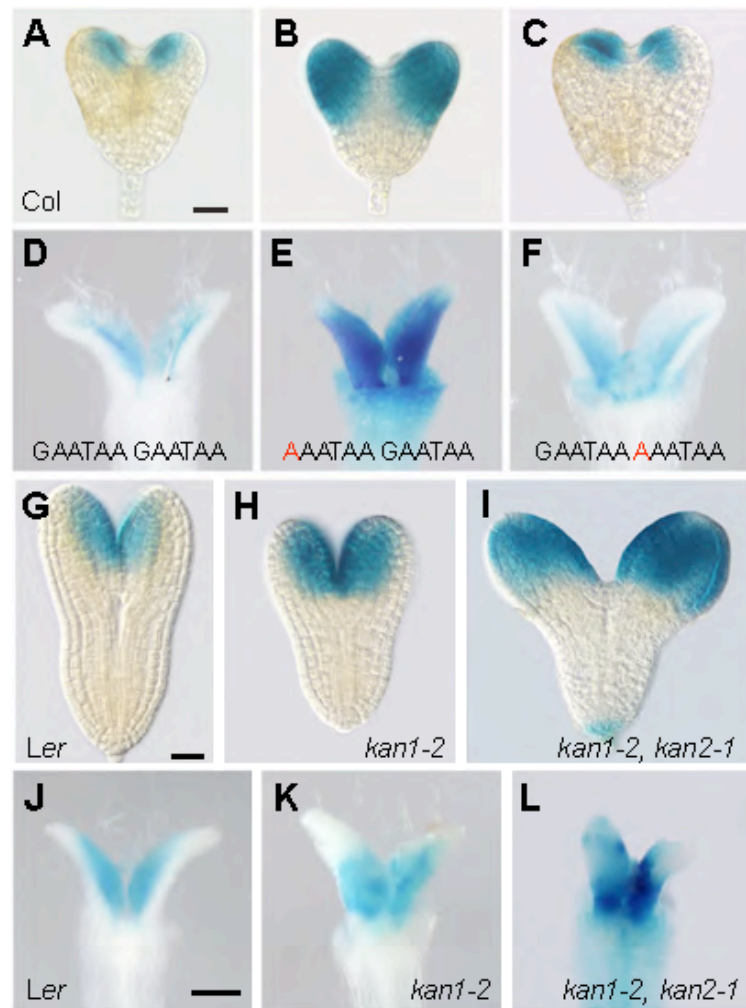


Figure A2-3. KAN1 and KAN2 determine the spatial expression pattern of *AS2*.

The expression pattern of *pAS2:GUS* (A, B), *pAS2-5D:GUS* (B, E) and *pAS2m:GUS* (C, F) in embryos (upper row), and the leaf primordia of 8 day-old Columbia seedlings (lower row). The sequence of the KAN1 binding site in each construct is shown, with the mutated nucleotide shown in red. The *as2-5D* mutation causes *AS2* to be expressed in the abaxial domains of cotyledons and leaves, and in the hypocotyl. The expression of *pAS2:GUS* in embryos and the first two leaf primordia of 8-day-old Landsberg erecta (*Ler*) (G, J), *kan1-2* (H, K)), and *kan1-2 kan2-1* (I, L) seedlings. The expression pattern of *pAS2:GUS* in *kan1 kan2* is similar to expression pattern of *pas2-5D:GUS*. Cotyledons were removed in D-F and J-L in order to reveal leaf primordia. Bar = 20 μm in A-C and G-I and 100 μm in D-F and J-L.

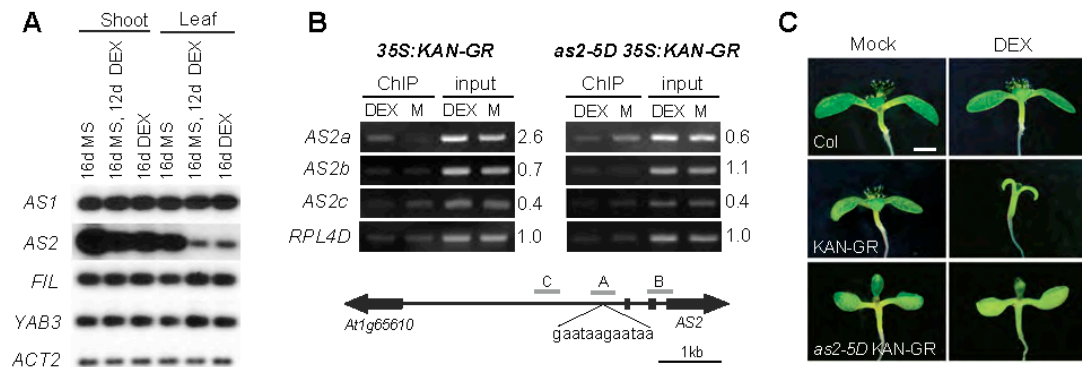


Figure A2-4. KAN1-GR represses AS2 directly. (A) RT-PCR analysis of AS1, AS2, FIL, and YAB3 transcripts in control and dexamethasone (DEX)-treated *35S:KAN-GR* plants; AS2 is repressed DEX-treated plants, primarily in leaves. (B) Chromatin immunoprecipitation (ChIP) assays performed on DEX- and mock (M)-treated *35S:KAN1-GR* and *35S:KAN1-GR as2-5D* seedlings (C) using antibodies specific for GR. Chromatin from three different regions 5' of AS2 (A, B, and C indicated by grey bars) were analyzed with semi-quantitative PCR prior to (input) and after ChIP. Fragment A contains the *as2-5D* point mutation. Average fold enrichment is indicated on the right of each image, and was calculated for three replicates in DEX versus mock samples after normalizing the band intensity to that of the control gene *RPL4D*. Note that *as2-5D* blocks the binding of KAN1-GR to the AS2 promoter, as well as the effect of KAN-GR on seedling morphology. Bar = 1 mm.

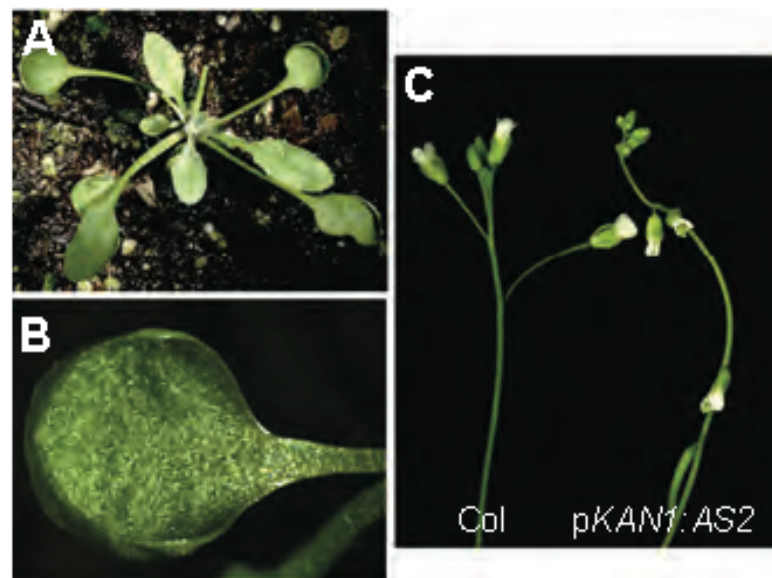


Figure A2-5. Transgenic plants expressing AS2 under the regulation of the KAN1 promoter resemble *as2-5D*. (A) Rosette of *pKAN1:AS2* plant. (B) Cotyledon of *pKAN1:AS2* showing cupped margin. (C) The flowers and siliques of *pKAN1:AS2* plants point downward.

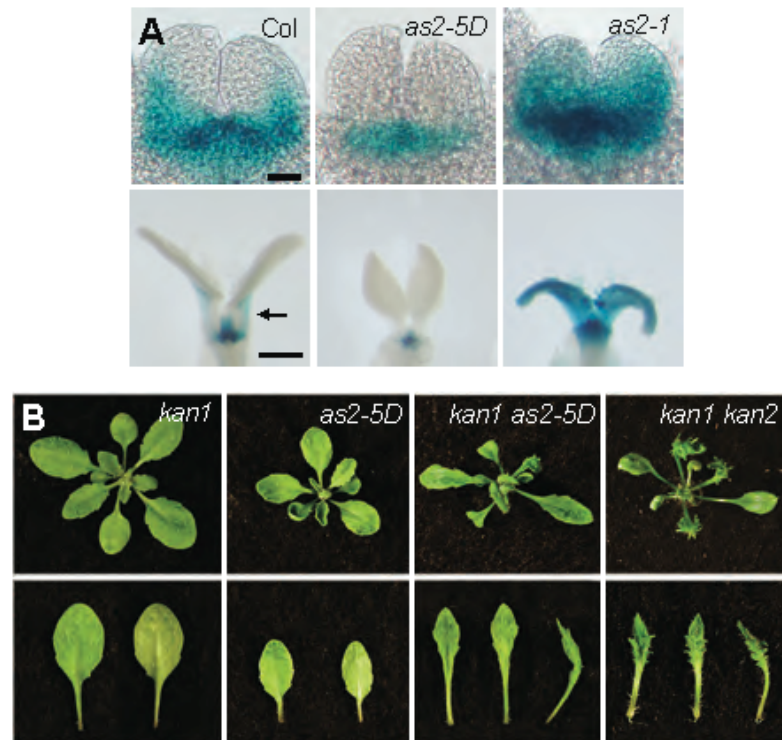
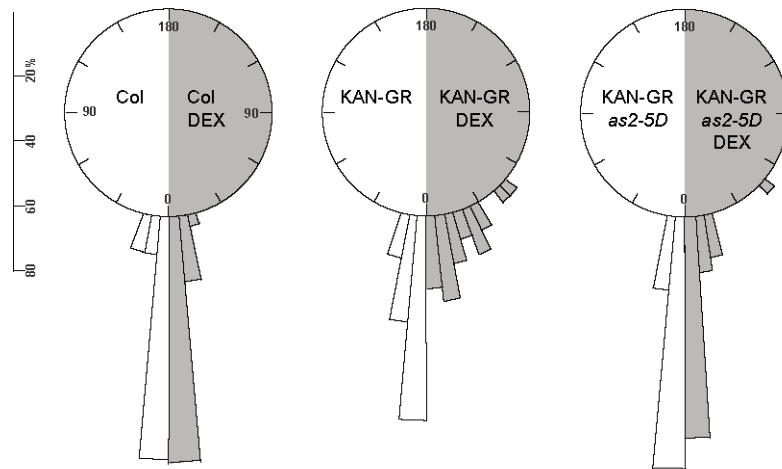
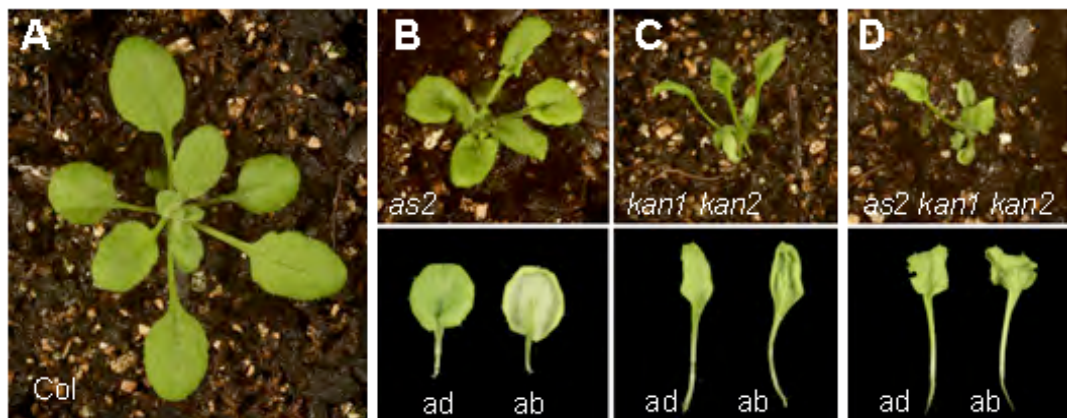


Figure A2-6 *AS2* represses *KAN1* and *KAN2*. (A) The expression of *pKAN1:GUS* in the leaf primordia of 5- (upper row) and 9-day-old (lower row) wild-type, *as2-5D* and *as2-1* seedlings. Cotyledons were removed to reveal the leaf primordia. Bar = 20 μm in upper row and 200 μm in lower row. The expression domain of *pKAN1:GUS* is reduced in *as2-5D* and expanded in *as2-1*. (B) The rosette (top row) and leaf five (bottom row) of 18-day-old wild type, *kan1-11*, *as2-5D*, *kan1-11 as2-5D*, and *kan1-11 kan2-5* plants. Adaxial, abaxial, and side views of the leaf are shown from left to right. The phenotype of *kan1-11 as2-5D* resembles that of *kan1-11 kan2-5*.

SUPPLEMENTARY FIGURES



Supplementary Figure A2-1. *as2-d* suppresses the effects of DEX on *35S:KAN-GR* seedlings. The angle of root growth deviation from vertical was determined in DEX- and mock-treated seedlings grown on vertically oriented media. Angles were assigned to bins of 5° and the length of each bar represents the percent of seedlings within that bin (N=27).



Supplementary Figure A2-2. *as2-1* does not rescue the mutant phenotype of *kan1 kan2*. (A) Wild-type Columbia. Seedlings (top row) and the first two leaves (bottom row) of *as2-1* (B) *kan1-12 kan2-4* (C) and *kan1-12 kan2-4 as2-1* (D).

This manuscript has been published in *PNAS* in Oct. 2008. The title is “KANDAI1 regulates adaxial-abaxial polarity in *Arabidopsis* by repressing the transcription of *ASYMMETRIC LEAVES2*”. The authors are Gang Wu, Wan-ching Lin, Tengbo Huang, R. S. Poethig, Patricia S. Springer, and Randall A. Kerstetter.

Author contributions: G.W., R.S.P., P.S.S., and R.A.K. designed research; G.W., W.-c.L., T.H., and R.S.P. performed research; G.W., W.-c.L., T.H., R.S.P., P.S.S., and R.A.K. analyzed data; and G.W. and R.S.P. wrote the paper.

***CURRICULUM VITAE* for Tengbo Huang**

EDUCATION

Rutgers, the State University of New Jersey, New Brunswick, NJ

2003-2008 Ph.D. in Plant Biology

Thesis Title: Transcriptional and Translational Regulation of Leaf Polarity

Beijing University, Beijing, China

2000-2003 M.S. in Plant Biology

Thesis Title: Programmed Cell Death in the Cold Treatment of Tobacco Pollens

Beijing University, Beijing, China

1996-2000 B.S. in Plant Biology

PUBLICATIONS

1. Tengbo Huang, Jeon J. Hong, Randall A. Kerstetter (2008), *ARO1* functions in translational regulation of leaf polarity. In preparation.
2. Tengbo Huang, Yaël Harrar, Changfa Lin, Randall A. Kerstetter (2008), KANADI1 acts as a transcriptional repressor that links genes involved in auxin responses with adaxial-abaxial polarity. Submitted.
3. Gang Wu, Wan-ching Lin, Tengbo Huang, R. S. Poethig, Patricia S. Springer, Randall A. Kerstetter (2008), KANDAI1 regulates adaxial-abaxial polarity in *Arabidopsis* by repressing the transcription of *ASYMMETRIC LEAVES2*. Proc Natl Acad Sci U S A. 105: 16392-7
4. Tengbo Huang and Ruilin You (2003) A Study on the Ultrastructural Changes in Tobacco Pollens during the Course of Cold Treatment. *Acta Scientiarum Naturalium Universitatis Pekinensis* 39:780-791.